Synthesis of Ultrahigh Surface Area Polymer Networks using Tetrahedral Monomers

Thesis submitted in accordance with the requirements of the University of Liverpool for the degree of Doctor in Philosophy

by

Ev Stöckel

November 2011

In stillem Gedenken an Oma Mietze und Anneliese,

und

für Paps, Mutti und Ray

Ohne euch hätte ich das nicht geschafft.

Acknowledgements

Firstly I would like to thank my supervisor, Andy Cooper, for giving me the opportunity to carry out this PhD project with him. I greatly appreciate the chance to carry the project out under your supervision.

Most of my appreciation is owed to Dave Adams without whom this thesis would not have happened and would be very badly written indeed. Thank you Dave for all the hours you spent discussing ideas and results with me. Also thank you ever so much for correcting this thesis so many times and making it coherent and more scientific. I am truly grateful to you for all your help.

I would also like to take this opportunity to thank the analytical and secretarial staff in the department and in the CMD without whose support some tasks would have been impossible to solve. So in no particular order thank you Rob C, Moya, Sean, Jean, Debbie, Nadeen, Sheila, Sandra, John G., 'Anne' Bell, Paul and everybody else.

Thanks also need to go to to my fellow Cooper Troopers past and present. Thank you Lyndsey, Tom H, Michael, Briggsy, Tommy M., Donocadh, Marc, JTAJ, JJ, Xiaofeng, Shan, Shijie, Rob D., Jamie, Ben and Andrea.

Special thanks are going to my friends throughout all those years who supported me through all the ups and downs a PhD comes with. Thank you Emma, Jacquie, Matt, Ollie, Neil, Michelle and Robin for always being there for me when it was needed.

Thanks also need to go to my friends back home. Danke Nadja, Robert, Caroline, Diana, André, Nicole, Lena und Frank. Auch wenn ihr es nicht glaubt, aber ohne euch wäre vieles um einiges schwieriger gewesen. Danke dass ihr mich nicht vergessen habt in den vielen Jahren.

En dernier mais pas le moindre, merci Caillou de ton soutien pour m'aider a continuer quand je pensais que je n'irai pas plus loin.

THANK YOU

Index

List of Figures

Chapter 1

Chapter 2

Chapter 3

Chapter 5

List of Tables

Abstract

Conjugated microporous polymers (CMPs) are a class of amorphous materials with pore sizes in the micropore range (< 2 nm). CMPs have potential advantages over inorganic and inorganic hybrid materials due to the use of only the lighter elements in the periodic table and their stability as well as having the diversity of organic synthesis not available to activated carbons. Due to their sorption properties CMPs find applications as gas storage materials. By tuning the chemistry and designing the monomers around the chemistry ultrahigh surface areas can be achieved. This way, novel materials with good gas storage capabilities for hydrogen, carbon dioxide, and methane can be synthesised.

Abbreviations

CMP	Conjugated Microporous Polymer
2D	two dimensional
3D	3 dimensional
SA_{BET}	Brunauer-Emmet-Teller Surface Area
SA_{Lang}	Langmuir Surface Area
COF	Covalent Organic Framework
DFT	Density Functional Theory
NL-DFT	Non-Local Density Functional Theory
DMF	N,N-Dimethylformamide
EOF	Element Organic Framework
FTIR	Fourier Transformed Infra-red Spectroscopy
GPC	Gel Permeation Chromatography
HCP	Hyper-Crosslinked Polymer
IUPAC	International Union of Pure and Applied Chemistry
MOF	Metal Organic Framework
MOP	Microporous Organic Polymer
NMR	Nuclear Magnetic Resonance
PIM	Polymer of Intrinsic Microporosity
PAE	Poly(arylene ethynylene)

SA	Surface Area
SEM	Scanning Electron Microscopy
ssNMR	Solid State Nuclear Magnetic Resonance
TGA	Thermo Gravimetric Analysis
ZIF	Zeolitic Imidazolate Framework

List of Publications

C.D. Wood, B. Tan, A. Trewin, H. Niu, D. Bradshaw, M.J. Rosseinsky,Y.Z. Khimyak, N.L. Campbell, R. Kirk, E. Stöckel, A.I. Cooper, *Hydrogen storage in microporous hypercrosslinked organic polymer networks, Chem. Mat*., **2007**, *19*, 2034-2048

C.D. Wood, B., E. Stöckel, M. Rosseinsky, D. Bradshaw, Y. Khimyak, H. Niu, A. Trewin, J. Jiang, F. Su, A. I. Cooper, *Abstracts of Papers of the American Chemical Society*, **2007,** 234

C. D. Wood, D. Bradshaw, E. Stöckel, B. Tan, A. Trewin, M. Rosseinsky, A.I. Cooper, *Abstracts of Papers of the American Chemical Society*, **2007,** 234

A.I. Cooper, J. Jiang, A. Trewin, F. Su, B. Tan, E. Stöckel, H. Niu, N. L. Campbell, A. Ganin, C. Dickinson, M. J. Rosseinsky, Y. Khimyak, C. D. Wood *Abstracts of Papers of the American Chemical Society*, **2007**, 234

A. I. Cooper, N. L. Campbell, J. X. Jiang, E. Stöckel, R. Dawson, S. Higgins, H. J. Niu, R. Clowes, *Abstracts of Papers of the American Chemical Society,* **2008**, 236

E. Stöckel, X. Wu, A. Trewin, C.D. Wood, R. Clowes, N.L. Campbell, J.T.A. Jones, Y.Z. Khimyak, D.J. Adams and A.I. Cooper, *High surface area amorphous microporous poly(aryleneethynylene) networks using tetrahedral carbon- and silicon-centred monomers, Chem. Commun*., **2009**, 212-214

J.R. Holst, E. Stöckel, D.J. Adams and A.I. Cooper, *High surface area networks from tetrahedral monomers: Metal catalyzed coupling, thermal polymerization and 'Click' chemistry, Macromolecules*, **2010**, *43*, 8531-8538

C. F. Martín, E. Stöckel, R. Clowes, D. J. Adams, A. I. Cooper, J. J. Pis, F. Rubiera, C. Pevida, *Hypercrosslinked organic polymer networks as potential adsorbents for pre-combustion CO_2 capture, J. Mater. Chem.,* **2011,** *21*, 5475-5483

R. Dawson, E. Stöckel, J.R. Holst, D.J. Adams and A.I. Cooper, *Microporous organic polymers for carbon dioxide capture*, *Energy Environ. Sci.*, **2011**, DOI: 10.1039/C1EE01971F

Chapter 1

General Introduction to Polymeric Materials and Gas Storage

1.1 Aims and Objectives

The aim of this project was to design, synthesise and characterise new conjugated microporous polymers[1] (CMPs), which have good gas storage characteristics[2]. Initially we focused on the storage of hydrogen gas for the possible application in hydrogen fuel cells.[3] This focus was expanded throughout the project to include the capture of methane gas[4] and carbon dioxide.[5] The syntheses discussed here are based on the hypothesis that the use of a tetrahedral monomer in the polymerisation process may increase the rigidity of the network and hence produce a well-defined pore structure. The polymers were synthesised by Sonogashira-Hagihara[6] and Yamamoto[7] cross-coupling reactions. The materials were designed for the purpose of novel gas storage properties by the increase of permanent surface areas.[8] The networks synthesised might be applied in hydrogen storage or methane storage, for example, for the use in hydrogen fuel cells, or carbon dioxide scrubbing, for example in post combustion.

The objectives of this project were (a) to design and (b) to synthesise novel CMPs, (c) to characterise the CMPs by gas sorption measurements and (d) to screen the materials for exceptional gas storage properties.

1.2 Microporous Materials

Although the focus in this thesis will be on conjugated microporous polymers and porous aromatic frameworks, there are more types of polymers which are permanently porous. This thesis will be mainly focused on microporous materials with pores smaller than 2 nm.

1.2.1 Definition

A porous material is a 'sponge-like' material usually consisting of interconnected pores. The skeletal portion of the material is called the 'matrix'. The skeletal material is usually a solid, but structures like foams are often also used as precursors for porous materials.[9] Porous materials are defined by IUPAC according to their pore sizes[10] and can be divided into three main groups:

- macroporous (pore sizes of larger than 50 nm),
- mesoporous (pore sizes between 2 nm and 50 nm) and
- microporous (pore sizes of less than 2 nm).

The focus for this work will be on microporous materials; that is, materials with pore sizes of less than 2 nm, although some microporous materials do exhibit some characteristics of mesoporous materials, as can be seen in later discussion. Microporosity can lead to materials with high surface areas[11] (> 1000 m^2/g). It also contributes to gas uptake at low pressures.[12] The characterisation of the materials synthesised here by gas sorption and Brunauer-Emmet-Teller (BET) surface area will be discussed in following chapters.

1.2.2 Types of Microporous Materials

Naturally occurring microporous materials include activated carbons[13] and zeolites.[14] The focus in this thesis will be on synthetically derived materials, and especially on materials that contain only carbon, hydrogen, and first row elements. These materials are known as microporous organic polymers (MOPs).

1.2.2.1 Activated Carbon, Silica Gel and Zeolites

Activated carbon[13] is a highly porous material. It usually consists of micro-crystallites with a graphite lattice. Activated carbon can be prepared as pellets or a powder. A disadvantage of activated carbon is that it tends to react with oxygen at temperatures over 300 °C. Activated carbons are used for the adsorption of organic substances[15] and non-polar adsorbates.[16] Activated carbons are also used for waste gas and wastewater treatment due to its selective sorption properties.[17]

Silica gel is the chemically inert, nontoxic, polar and thermally stable amorphous form of SiO_2.[18] It is synthesised by reacting sodium silicate with acetic acid, followed by after-treatment processes such as aging and pickling.[19] Pickling is the process of removing oxide impurities from the silicon wafer by dissolving the impurities in hydrofluoric acid. These treatments determine the pore sizes of the silica gel. Silica gel is therefore commercially available with various different pore sizes.

Zeolites[20] are naturally occurring or synthesised crystalline aluminosilicates with a repeating pore network. Zeolites release water at high temperatures. They are synthesised by hydrothermal synthesis of sodium aluminosilicate or a similar

silica source in an autoclave. This is followed by an ion exchange reaction with Na^+, Li^+, Ca^+, K^+, or NH_4^+ for example. Zeolite cages normally have a channel diameter of 2 Å to 9 Å. Zeolites are used in the drying process of air, in CO_2 removal from natural gas, in CO removal from reforming gas, in air separation, in catalytic cracking and in catalytic synthesis and reforming.[21]

1.2.2.2 Metal Organic Frameworks (MOFs) and Covalent Organic Frameworks (COFs)

The field of Metal Organic Frameworks (MOFs) has been highly active over the past 10 years. The first MOF with permanent porosity was discovered in 1999 by Omar Yaghi and his group.[22] More MOFs are being discovered frequently[23] with new characteristics and applications. Recently MOFs, were investigated and scaled-up by BASF to use as gas storage materials.[25]

MOFs are crystalline microporous materials consisting of metal centres or clusters linked by organic units. The linkers are similar to those used in organometallic complexes.[26] However, the linkers in MOFs contain at least two functionalities that cause the network formed to be 3 dimensional. Since MOFs are crystalline in nature, they can have very well-defined pore sizes and very high Langmuir surface areas of over 5000 m^2/g.[27] As MOFs can be designed easily,[28] due to their crystallinity, a series of networks has now been published with increasing strut lengths.[29] It is now also possible to model structures of possible MOFs first before synthesising them in the lab.[30] An example of three MOFs can be seen in Figure 1. MOF-5, IRMOF-6 and IRMOF-8 were synthesised by Yaghi's group and investigated for hydrogen storage capacities.[31]

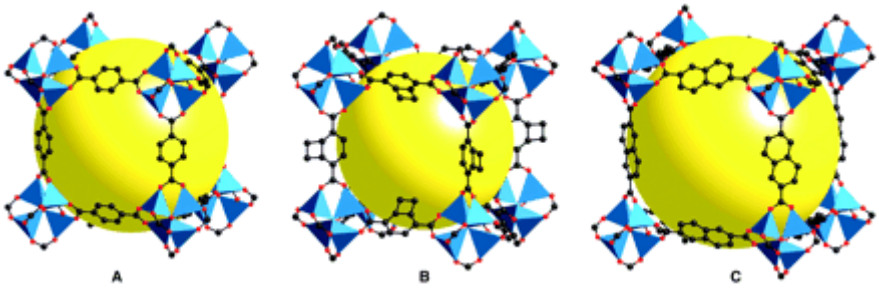

Figure 1: Single-crystal x-ray structures of MOF-5 (**A**), IRMOF-6 (**B**), and IRMOF-8 (**C**) illustrated for a single cube fragment of their respective cubic three-dimensional extended structure. On each of the corners is a cluster $[OZn_4(CO_2)_6]$ of an oxygen-centered Zn_4 tetrahedron that is bridged by six carboxylates of an organic linker (Zn, blue polyhedron; O, red spheres; C, black spheres). The large yellow spheres represent the largest sphere that would fit in the cavities without touching the van der Waals atoms of the frameworks. Hydrogen atoms have been omitted (Figure from reference 31)

Hydrogen storage is an important field of research and many MOF materials have high capacities.[32] MOF-5 (Figure 1, A) has a hydrogen uptake of 7.1 wt% at 77 K and 40 bar. This uptake can be increased to 10 wt% when increasing the pressure to 100 bar. These uptakes are very high. However, the storage pressures are high as well. At higher pressures, the material is 'forced' to adsorb the maximum amount of gas possible. Measurements at high pressures do not reflect the pressures the materials might need to be used at for everyday applications, and only show how much the material can adsorb if pushed to its limits. Moreover, the use of cryogenic temperatures (77K) is a disadvantage. In order to increase the uptake of hydrogen at lower pressures and higher temperatures, the spill-over technique was investigated.[33] The mechanism of spill-over is still debated, but it is thought to be caused by metal centres catalysing the dissociation of hydrogen onto the surface of the microporous material.[33, 34]

Covalent Organic Frameworks (COFs) are also crystalline materials but, contrary to MOFs, they do not have metal centres and comprise only of light elements such as boron, carbon, nitrogen, oxygen and hydrogen.[35] COFs were also first discovered in 2005 by Omar Yaghi and his group.[35] COFs contain strong boron –

oxygen bonds.[36] The first COFs to be published were named COF-1 and COF-5, and were synthesised by self-condensation of the corresponding boronic acids with the by-product of water (Figure 2).[35] COFs can exhibit high surface areas between 700 m^2/g and 1600 m^2/g (COF-1 and COF-5 respectively). Recently, COFs with surface areas as high as 3600 m^2/g were synthesised by Yaghi's group by the self-condensation reaction of a tetrahedral boronic acid (COF-102, Figure 2). The increase of the surface area can be accredited to introduction of the 3 dimensional monomer. This 3-D design principle is exploited throughout this thesis.

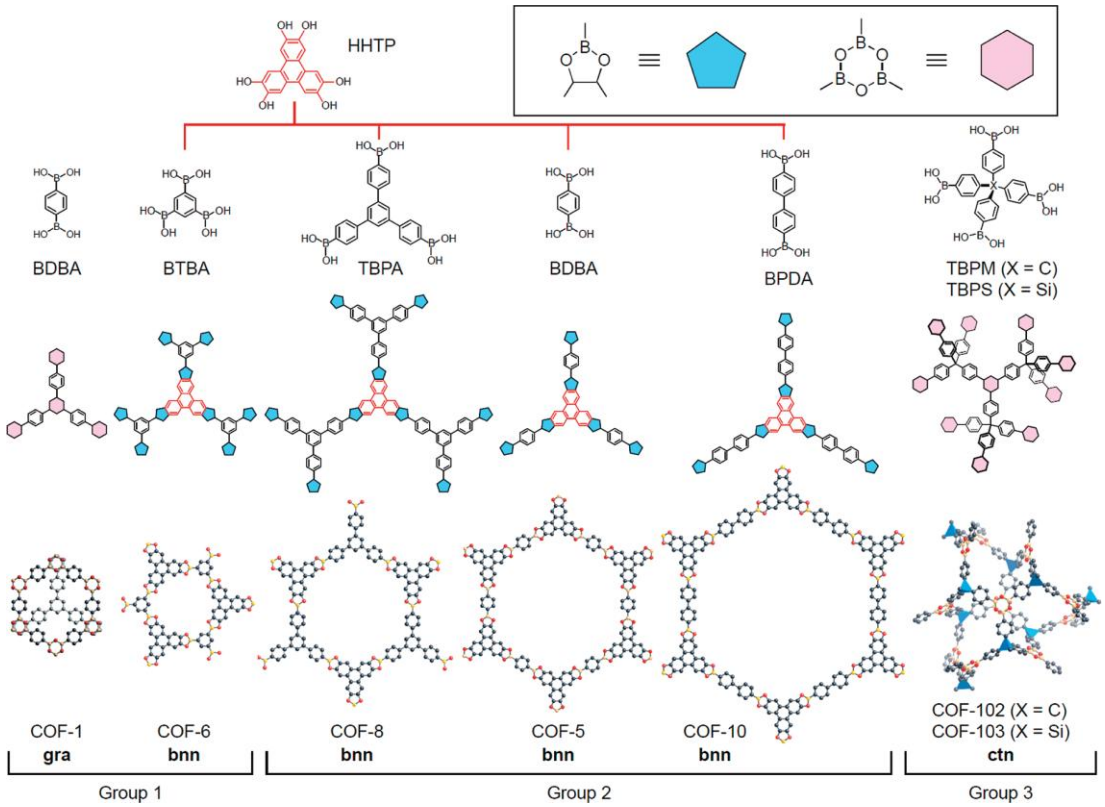

Figure 2: Condensation reactions of boronic acids and HHTP used to produce COFs (top), and resulting fragments of the COFs (middle). (bottom) Atomic connectivity and structure of crystalline products of 2D (COF-1, -5, -6, -8, and -10) and 3D (COF-102 and -103) COFs. B, orange; O, red; C, black; atom X in COF-102 and -103, blue tetrahedron; all hydrogen atoms are omitted for clarity. Inset: the C2O2B (blue) and the B3O3 (pink) rings formed by condensation reactions. The topology and the group classification number are indicated for each COF (Figure from reference 37)

1.2.2.3 Polymers of Intrinsic Microporosity (PIMs)

PIMs were among the first wholly microporous polymers reported.[38] They are amongst the most studied microporous polymers with a wide range of applications in gas storage,[39] separations[40] and catalysis.[41] The microporosity of PIMs is a result of a rigid bent monomer that contains a tetrahedral carbon atom, known as the site of contortion. The first PIMs were based on phthalocyanines and porphorins (B3 and B1, Figure 3) and contained metal ions or $2H^+$ ions in their cavities. The first PIMs exhibited BET surface areas of 450 to 1000 m^2/g.[39]

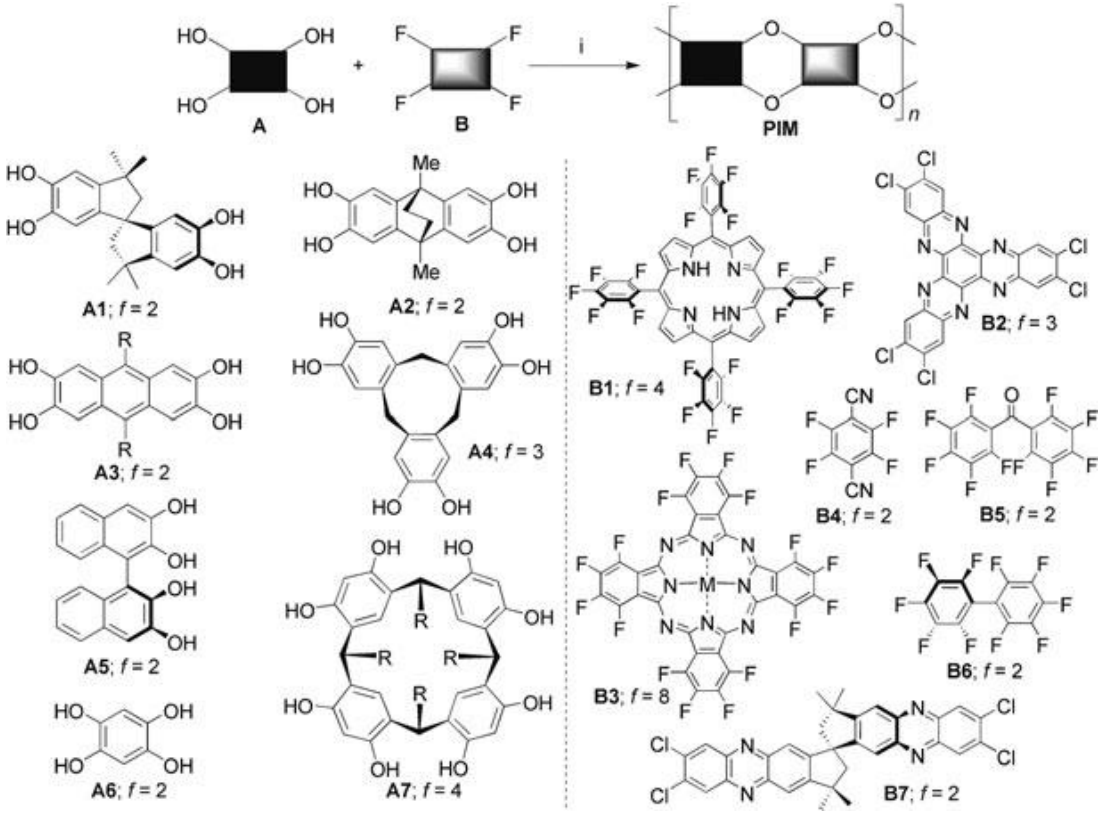

Figure 3: some of the monomers used in the synthesis of PIMs (adapted from [38d])

1.2.2.4 Organic Microporous Polymers

Organic microporous polymers are made of hydrogen, boron, carbon, nitrogen and oxygen. The nature of the polymers means that these have many advantages especially compared to MOFs.[41] In terms of gas storage, the uptake can increase if the material does not contain metal centres and is therefore less dense. Also, MOFs can sometimes be highly moisture and air sensitive[42] whereas the organic materials synthesised in our laboratories and elsewhere tend not to be sensitive to air or moisture,[1] with the exception of boronate ester COFs which tend to be unstable under atmospheric conditions.[43] Due to the nature of the way in which MOFs are synthesised, the reaction can be reversible when exposed to moisture. Organic microporous materials can also be more easily synthesised as a vast number of organic reactions, that are applicable, have been tested and established for the formation of porous networks.

1.2.2.5 Hypercrosslinked Polymers (HCPs)

Hypercrosslinked polymers (HCPs) are polymers which are synthesised by cross-linking reactions, such as Friedel-Crafts chemistry. HCPs were some of the first purely microporous synthetic materials. Hypercrosslinked polystyrene networks have been recognised since the 1970s. They were originally synthesised by the cross-linking reaction of linear polystyrene in a suitable solvent system.[45] HCPs were developed by cross-linking macroporous polymers further to make them microporous (e.g, in PolyHIPEs).[46]

The aim of these cross-linking reactions is to decrease the pore size by making the pores more rigid and stopping them from collapsing due to the cross-linking, thus forming smaller pores in the scaffold of the larger pores. This method was first developed by Davankov[47] and these type of HCPs are now sometimes referred to as Davankov resins.[45(b), 48] HCPs have also shown to adsorb large quantities of hydrogen[49] and thus their hydrogen storage capacity is widely investigated.

Traditionally, HCPs were prepared by swelling the polymer in a suitable solvent and then 'hyper-crosslinked' by use of Friedel-Crafts chemistry with the use of a Lewis acid such as iron (III) chloride (Figure 4).

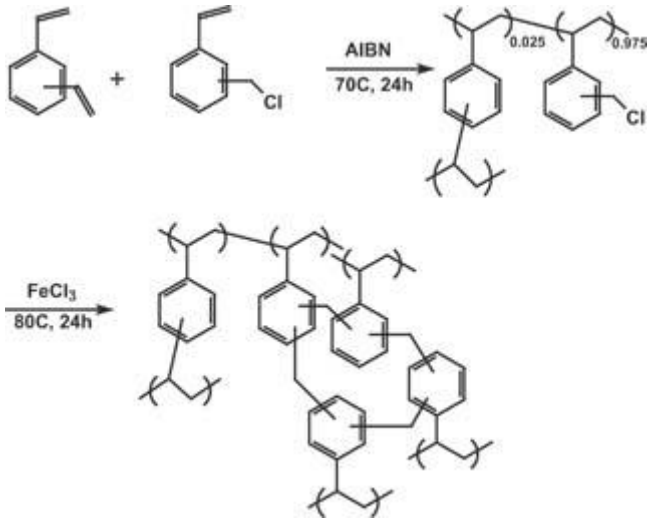

Figure 4: Reaction scheme for the synthesis of a hypercrosslinked polymer prepared from gel poly(chloromethylstyrene-*co*-divinylbenzene). The final polymer is a crosslinked polystyrene in which most aromatic rings have attachments to a polymer backbone plus two crosslinks[46]

By this method, monodispersed particles can be prepared from polystyrenes with particle diameters in the micrometer range. As these particles absorb significant amounts of solvent, they can be used as separation media in HPLC methods.[49]

A different way to synthesise HCPs is by direct cross-linking. By applying Friedel-Crafts chemistry to bifunctional monomers, the polymer is cross-linked in situ. There is no need to synthesise a precursor prior to cross-linking. Cooper *et al.*[48] developed a route to synthesising HCPs this way. The networks were synthesized by the self-condensation of bischloromethyl monomers such as *para*-dichloroxylene (*p*-DCX), 4,4'-bis(chloromethyl)-1,1'-biphenyl (BCMBP) and 9,10-bis(chloromethyl) anthracene (BCMA) (Figure 5). In both cases, a 1:3 molar ratio (*p*-DCX : BCMBP or BCMA) resulted in materials with the highest surface areas.

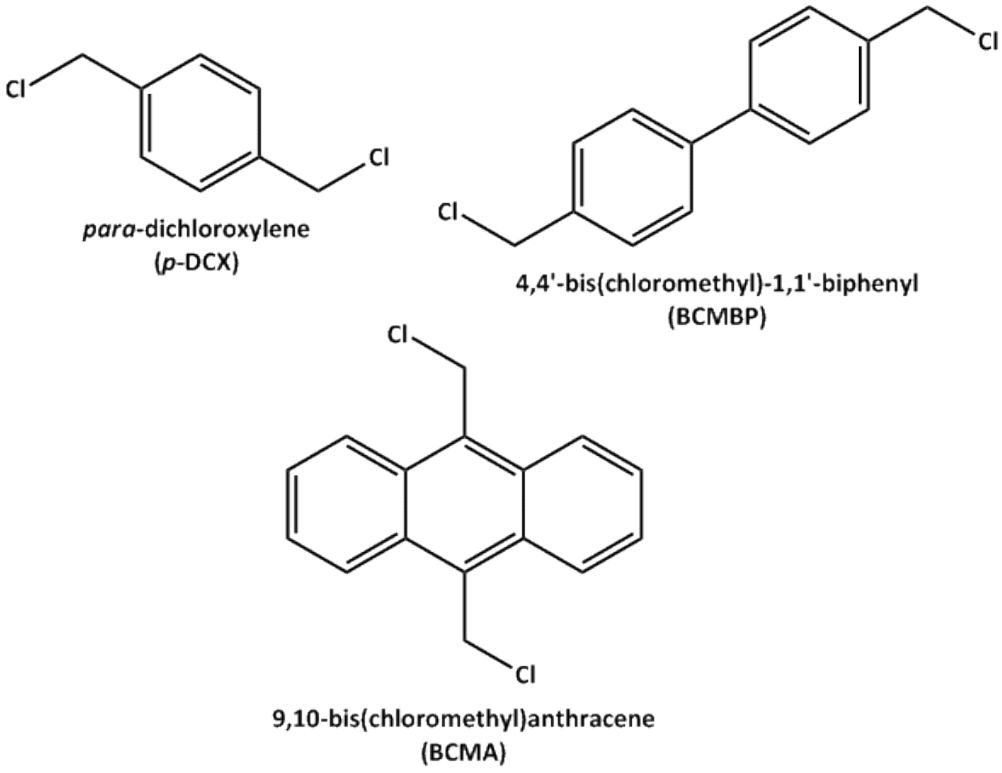

Figure 5: monomers used to form HCPs by Friedel-Crafts chemistry

HCPs synthesised by this method have shown to have Brunauer-Emmet-Teller surface area (SA_{BET}) of up to 1900 m^2/g[48] and are capable of storing hydrogen of up to 1.13 wt% (77 K, 1 bar), methane[49] up to 5.2 mmol/g (20 bar, 298 K) and

carbon dioxide[50] up to 1.7 mmol/g (1 bar, 298 K). Atomistic simulations confirm the experimental values and gave an idea on how the network is formed.[51]

HCPs can also be synthesised by other routes. A series of hyper-crosslinked polysilanes was synthesised by organolithiation reaction between tetraethylorthosilicate and dibromoaromatics to form so called element organic frameworks (EOFs).[52] These EOFs (Figure 6) have shown to be very thermally stable and to have hydrophobic properties.

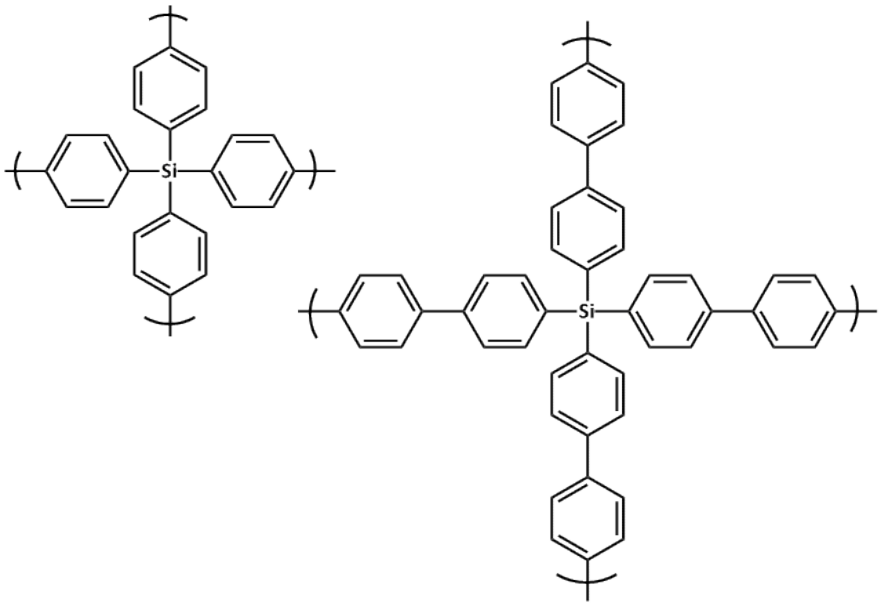

Figure 6: representation of element organic frameworks redrawn after [52], EOF-1 left and EOF-2 right

The EOFs exhibit surface areas of 800 m^2/g and 1000 m^2/g (EOF-1 and EOF-2 respectively) and hydrogen uptakes of 0.9 wt% (EOF-1) and 1.2 wt% (EOF-2) at atmospheric pressures and 77 K.[52]

Germain *et al.* developed HCPs from polyanilines and polypyroles.[53] In this case, there was no need to use lithiating agents or large quantities of Lewis acids. During the network formation, the production of HCl gas was therefore decreased significantly, making the reactions less harsh. The BET surface areas for these HCPs

were around 630 m^2/g if synthesised using diiodomethane and around 480 m^2/g if synthesised using formaldehyde. The HCPs also showed a hydrogen uptake of 1 wt% and 0.8 wt% respectively.

Recently HCPs have also been synthesised by imide bond formation using relatively mild conditions,[54] compared to Friedel-Crafts chemistry. In this case, tetraamino-spirobifluorene was reacted with pyromellitic acid anhydride to form a network that is comparable to a PIM network (Figure PI 1, Figure 7), although PIMs are linear.

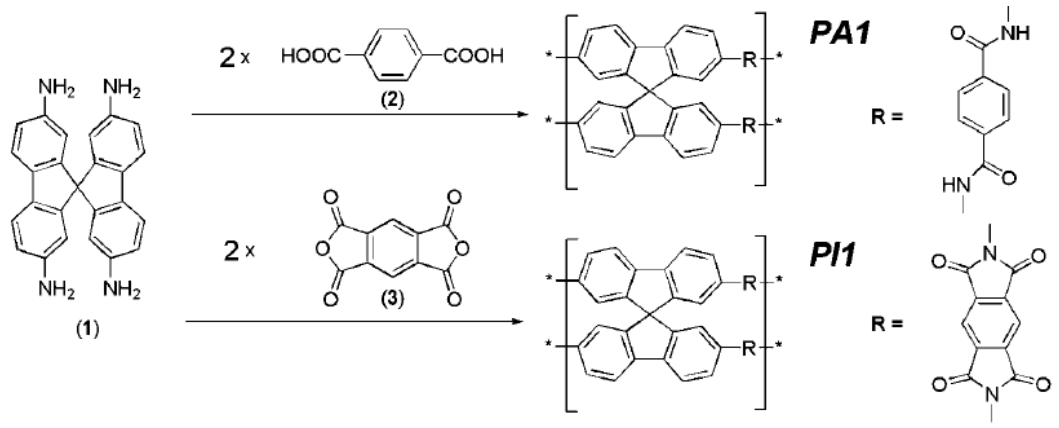

Figure 7: reaction scheme for synthesis of PI 1 (adapted from [54a])

The networks surface area arises from the space inefficient packing due to its 3 dimensional nature.[55] Surface areas of up to 1000 m^2/g have been reported.[54a] When the analogous polyamide network was formed from tetraaminobiphenyl the surface area decreased to 50 m^2/g. This suggests that the high surface area in the polyimide networks is caused by the inefficient packing. The polyimide network (PI-1) also showed a hydrogen uptake of 1.1 wt% (77 K, 1 bar).

1.2.2.6 Conjugated Microporous Polymers (CMPs)[56] and Porous Aromatic Frameworks (PAFs)

Conjugated microporous polymers (CMPs) are highly microporous polymers, which are synthesised by well-established organic cross-coupling reactions. They find application in gas storage, gas separation and catalysis.[56] Porous aromatic frameworks (PAFs) are very high surface area materials with high thermal stability[57] with potential applications in gas storage, gas capture and gas separation.[1] Uniquely, CMPs can have extended π-conjugation in the network backbone, distinguishing these materials from MOFs, COFs, IMs, HCPs and other synthetic microporous materials.

CMPs were first established in the Cooper group and were the basis for the work carried out in this thesis. The first CMPs were organic conjugated poly(aryleneethynylene) networks with surface areas of up to 830 m^2/g.[58] They were synthesised by applying Sonogashira-Hagihara coupling reactions between a di-, tri- or tetra-halide benzene and a di- or triethynyl benzene, catalysed by palladium (0) and copper iodide (Figure 8).

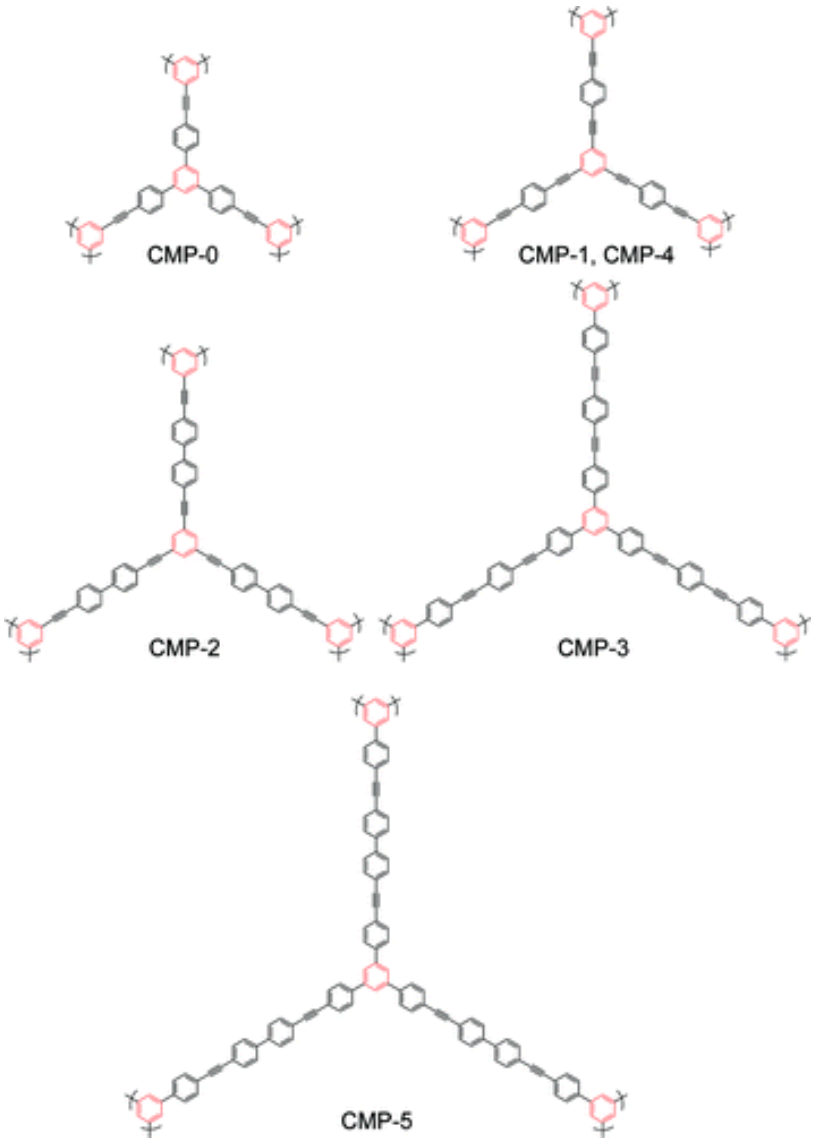

Figure 8: series of CMPs synthesised by Sonogashira cross-coupling[61]

These CMPs showed reasonable hydrogen storage capacities and could adsorb up to 130 cm^3/g of hydrogen (1.2 wt% for CMP-1, 77K, 1 bar).[61] The pore size distribution of CMP networks was very narrow, making them wholly microporous materials.

While analysing the original CMP networks, it was discovered that the networks do not just cross-couple but that a degree of homo-coupling of the ethynyl monomer can be observed.[61] By purposefully homo-coupling, the triethynyl

benzene monomer (previously used to synthesise CMP-1, Figure 8), a polymer could be synthesised (HCMP-1) which exhibited a similar surface area to that of CMP-1 of 840 m^2/g.[62] The hydrogen storage capacity was measured as 1 wt% of hydrogen at 1 bar, 77K. By analysing both the homo-coupled and the cross-coupled networks of HCMP-1 and CMP-1, respectively, by solid state NMR it was confirmed that they are different networks.

Jiang *et al.* also investigated the influence of the strut length on the surface area and on the gas sorption properties[63] (Figure 9). It was discovered that by increasing the strut length the surface area and the cumulative pore volumes were decreased. This was put down to the flexibility of the struts and therefore the ability of the struts to twist and collapse pores within the network.

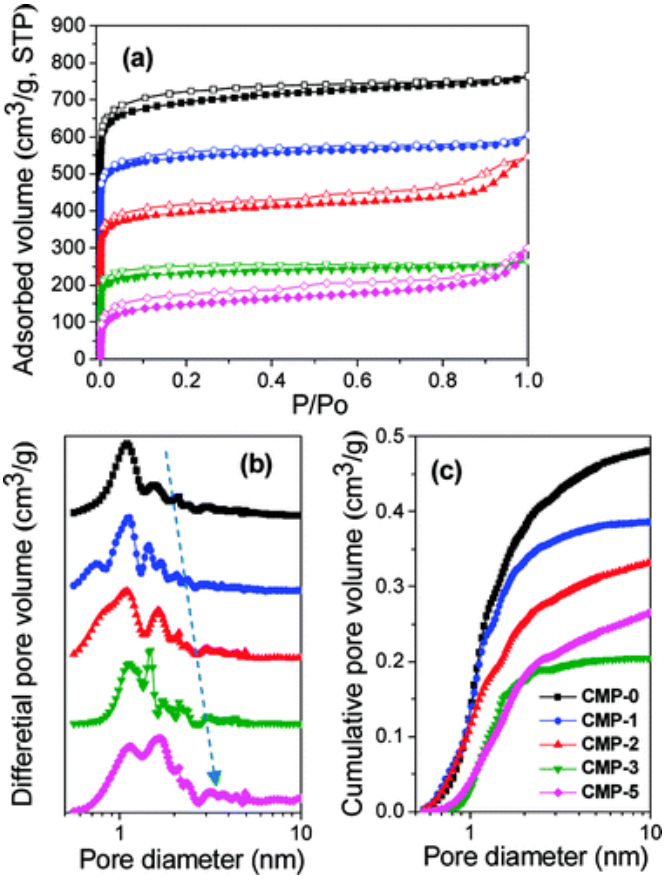

Figure 9: gas sorption (a), pore size distribution (b) and cumulative pore volume (c) for CMP networks with increasing strut length (arrow in (b) signifies the increase in strut length between the networks) (Figure from reference 63)

By increasing the strut length, the hydrogen uptake was also decreased from 1.4 wt% (CMP-0) to 0.6 wt% (CMP-5) at 1bar, 77K.

CMP-type networks can also be synthesised by Yamamoto cross-coupling reaction. Ben *et al.*[64] published in 2009 a Yamamoto coupled porous aromatic framework (PAF) that had the highest surface area reported to date for any material at that time. The apparent BET surface area was 5600 m^2/g for homo-coupled tetrakis(4-bromophenyl) benzene. The reaction was catalysed by $[Ni(cod)_2]$. This extreme high surface area outshone all previously published organic microporous polymers.

1.3 Gas Storage

The gas storage of hydrogen, methane and carbon dioxide has been heavily investigated in recent years.[65] Applications include hydrogen fuel cells,[66] carbon dioxide scrubbers[67] and safe methane storage.[65b] All of these applications are aimed at the reduction of greenhouse gases or the improved safety of gas storage.

1.3.1 Definition of Adsorption of Gases onto Accessible Surfaces

Adsorption is the physical adhesion of atoms or molecules of a gas to a surface.[68] During the process, a film of adsorbates, that is a film of the gas atoms or molecules, is created on the surface of the adsorbent. The difference between adsorbance and absorbance is that in absorption, a fluid permeates or is dissolved

by a liquid or a solid.[69] The term 'sorption' is applicable to both adsorption and absorption whereas desorption is the reverse of adsorption.[70]

As in surface tension, adsorption occurs due to the surface energy of the material. As atoms in a material are not wholly surrounded by other adsorbents, they can attract adsorbates such as gas atoms or molecules. The nature of the attraction and consequently of the bonding depends on the material itself. The adsorption process can generally be classified as physisorption or chemisorption: physisorption has characteristics of weak Van-der-Waals forces, while chemisorption has characteristics of covalent bonding.[71]

Adsorption is widely used in industrial applications for capture, storage, purification and catalytic processes. Because adsorption can be very selective, it can be used for the purification of gas mixtures[72] and in water purification.[73]

Adsorption is described through isotherms, which are a correlation of the amount adsorbed to the pressure in the system at a constant temperature. The adsorbed quantity is always normalized to the mass of adsorbent to allow for comparison with other materials. The first mathematical fit to an isotherm was published by Freundlich and Küster in 1894.[75] It was a purely empirical formula for gaseous adsorbates:

$$x_{ab}/m = kp^{1/n}$$

where x_{ab} is the quantity adsorbed, m is the mass of the adsorbent, p is the pressure of adsorbate and k and n are empirical constants for each adsorbent-adsorbate pair at a given temperature.[76] The function has an asymptotic maximum as pressure increases without bound. As the temperature increases, the variables k and n

change to reflect the empirical observation that the quantity adsorbed rises more slowly and higher pressures are required to saturate the surface.[77]

In 1916, Irving Langmuir published a new theory based on Freundlich's isotherms. It was a new model isotherm for gases adsorbed onto solids and is still know as the Langmuir isotherm.[78] It is a semi-empirical isotherm, which explains the difference in adsorption with different pressures. Langmuir proposed a kinetic mechanism for adsorption based on the following assumptions:[79]

1. A Fixed number of vacant or adsorption sites are available on the surface of solid.
2. All the vacant sites are of equal size and shape on the surface of adsorbent.
3. Each site can hold maximum of one gaseous molecule and a constant amount of heat energy is released during this process.
4. Dynamic equilibrium exists between adsorbed gaseous molecules and the free gaseous molecules.

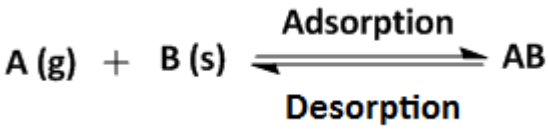

where A (g) is non-adsorbed gaseous molecule, B(s) is unoccupied surface and AB is adsorbed gaseous molecule.

5. Adsorption is monolayer or unilayer.

These assumptions are rarely all true at once. The surface of a material is seldom perfect,[81] the adsorbed molecules are not necessarily inert and the mechanism is

not the same for the first molecule to be adsorbed and the last molecule to be adsorbed.[82] The Brunauer-Emmet-Teller (BET) theory addresses some of these problems,[83] the main one being the assumption that the gas molecules only adsorb as a monolayer.[83] Even though the Langmuir theory has some limitations, it is still applied widely in adsorption measurements. For the purpose of this thesis, it was decided that the BET model is most applicable. In general, the Langmuir isotherm is applied for chemisorptions and the BET isotherm for physisorption.[84] Traditionally BET theory has been used for microporous materials in the Cooper research group and most other groups in the area of microporous solids.

1.3.2 Adsorption of Gases in CMPs and DoE Guidelines

One potential application, which is not fully studied yet, is the use of CMPs in fuel cells as a storage material for hydrogen. Figure 10 shows a schematic view of a hydrogen fuel cell. The microporous materials would be used as storage material to supply the hydrogen flow for the fuel cell.

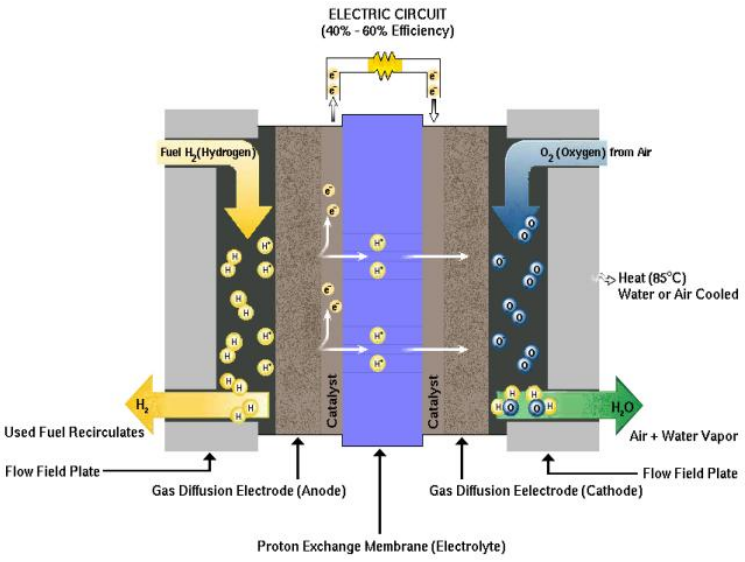

Figure 10: Schematic view of a hydrogen fuel cell[85]

For the use of storage materials in fuel cells, guidelines have been established by the US Department of Energy (US DoE).[86] These guidelines have been adjusted several times over the last couple of years. Some of the most relevant targets are shown in Table 1 below as published by the US DoE.

Table 1: DoE Targets of Onboard Hydrogen storage systems for Light-duty vehicles, technical targets[6] adapted from the DoE homepage.[87]

Storage Parameter	Units	2010	2015	Ultimate
Durability/Operability				
• Operating ambient temperature[d]	ºC	-30/50 (sun)	-40/60 (sun)	-40/60 (sun)
• Operational cycle life (1/4 tank to full)[e]	Cycles	1000	1500	1500
• Min delivery pressure from storage system; FC= fuel cell, ICE= internal combustion engine	bar (abs)	5FC/35 ICE	5FC/35 ICE	3FC/35 ICE
• Max delivery pressure from storage system[f]	bar (abs)	12	12	12
• Onboard Efficiency	%	90%	90%	90%
Charging/discharging Rates				
• System fill time (for 5-kg H_2)	min (kg H_2/min)	4.2 min (1.2 kg/min)	3.3 min (1.5 kg/min)	2.5 min (2.0 kg/min)
Fuel Purity (H_2 from storage)[i]	% H_2	SAE J2719 and ISO/PDTS 14687-2 (99.97% dry basis)		

Footnotes for Table 1: (d) Stated ambient temperature plus full solar load. No allowable performance degradation from –20 °C to 40 °C. Allowable degradation outside these limits is to be determined. (e) Equivalent to 200,000; 300,000; and 300,000 miles respectively (current gasoline tank specs) (f) the storage system should be capable of delivering 10,000 psi (700 bar) compressed hydrogen, liquid hydrogen, or chilled hydrogen (77K) at 5,000 psi (350 bar). In the long term, it is anticipated that delivery pressures will be reduced to between 50 and 150 bar for materials-based storage systems. (i) The storage system is not expected to provide any purification for the incoming hydrogen, and will receive hydrogen at the purity levels required for the fuel cell. Note that some storage technologies may produce contaminants for which effects are unknown; these will be addressed by system engineering design on a case by case basis as more information becomes available, adapted from [87]

The targets quoted by the DoE are based on the lower heating value of hydrogen, compared to gasoline, and are stated for a complete system, comprised of tank, material, valves, regulators, piping, mounting brackets, insulation, added cooling capacity and other balance-of-plant components. The capacities are defined as useable capacities, which can be delivered to the fuel cell or internal combustion engine. The targets have to be met at the end of a service life cycle that is 1500 cycles or 5000 operation hours (equivalent of 150,000 miles). The targets are for use in hydrogen internal combustion engines as well as for hydrogen fuel cells.[88]

All of the 2015 targets set by the US DoE are very challenging as they are based on the performance of a hydrocarbon-fuelled car. From many researchers' point of view, the most important targets are that the fuel tank system should contain 9 wt% gravimetric hydrogen density and that the system should be capable of being recharged in less than 5 minutes.[89,66]

In order for polymeric materials to achieve such a high hydrogen uptake, it is thought[90] that they need to have very high surface areas of more than 1000 m^2/g. Surface areas of above 1000 m^2/g usually indicate a material which is suitable for hydrogen storage.[90] The surface area needs to be high because molecular hydrogen even if very small tends to need a vast amount of space for adsorption. In theory, one can say that the higher the surface area, the higher the hydrogen uptake.[91]

The idea of using a 3-dimensional monomer (Figure 11) in the network formation arose from the need to increase the surface area of polymers. We proposed that the introduction of tetrahedral monomers into the networks would increase the local order in the network, and hence stabilise the pores within the network and hence increase the surface area. The idea was to force the network to

obtain a higher degree of conformity, with respect to other CMPs,[8] without using a templating agent, which is normally used to create order within a non-ordered network. Increased surface area should also cause the gas uptake to increase.

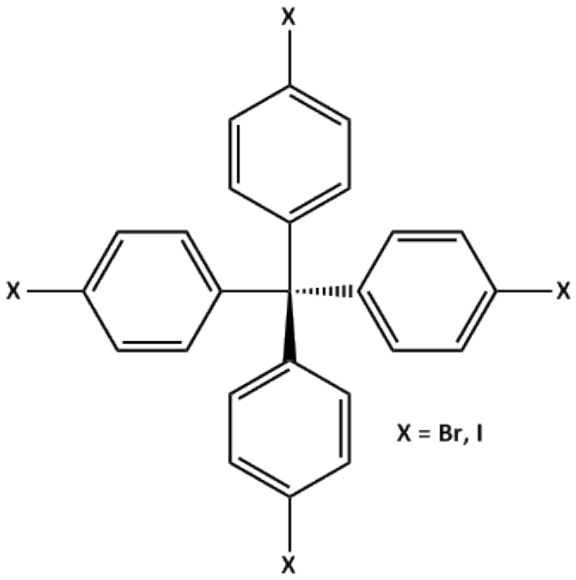

Figure 11: 3 dimensional monomer used for the formation of networks in this study

The use of the tetrahedral monomer (Figure 11) in the formation of the network might also allow the network to obtain a smaller pore size distribution, i.e. the network has only a narrow distribution of pores, which will exclusively be in the micro pore region of < 2 nm, due to the tetrahedral character of the monomer. Our assumption was that the pore size would be essentially defined by the monomer in advance, and can therefore be 'designed' depending on the strut length of the monomer or linker.

For the purpose of hydrogen storage in microporous materials with pores sizes of less than 2 nm are desired.[90] The pore size of a polymer is calculated from the nitrogen adsorption isotherm. By IUPAC definition, there are six types of sorption isotherms (Figure 12).

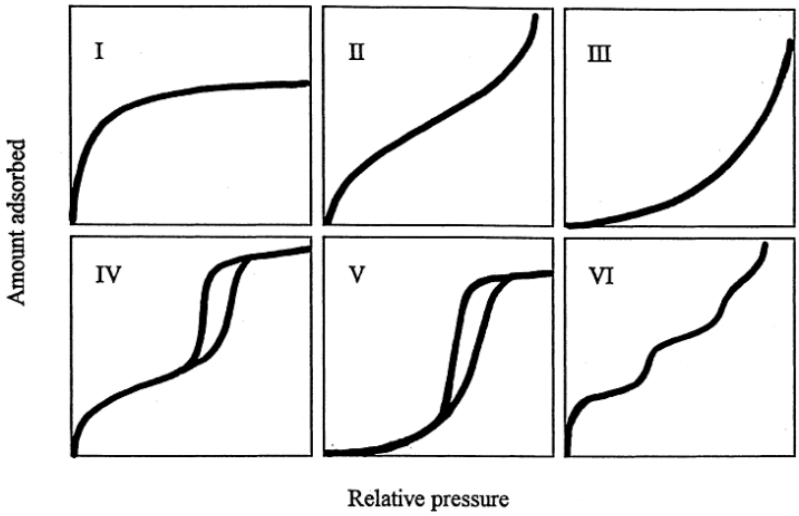

Figure 12: The IUPAC Classification of Adsorption Isotherms for Gas/Solid Equilibria[90-93]

The shape of the isotherm depends on the porosity in the polymer. Small pores are filled first at lower pressures and give rise to the so-called 'micropore step' within the isotherm. Larger pores are filled at higher pressures. Hence Type I isotherms are typical for microporous materials and Type IV isotherms for macroporous materials. For the purpose of hydrogen storage and most other gas storage applications, microporous materials with a Type I isotherm are most desirable. Type II isotherms do not exhibit a saturation limit as can be observed in Type I isotherms. The isotherm indicates a wide distribution of pore sizes present. Type I isotherms therefore can be found in mesoporous materials such as silicas. Type III isotherms are not common, but a number of systems, such as nitrogen on polyethylene, can give rise to isotherms with a gradual increase in gas adsorbed. The Type V isotherm is uncommon; it is related to the Type III isotherm in that the adsorbent-adsorbate interaction is weak, but is obtained with certain porous adsorbents. The Type VI isotherm represents a stepwise multilayer adsorption on a uniform non-porous surface. The sharpness of the steps depends on the system and

the temperature. The step-height represents the monolayer capacity for each adsorbed layer and, in the simplest case, remains nearly constant for two or three adsorbed layers. Amongst the best examples of Type VI isotherms are those obtained with argon or krypton on graphitised carbon blacks at liquid nitrogen temperatures.[93]

1.4 Overview of the work described in this thesis

The aim of this work has been the synthesis and characterisation of Sonogashira-coupled CMP networks and Yamamoto-coupled PAF networks. These will be discussed in the subsequent Chapters 2 and 3. A study on the influence of templating agents in the synthesis of CMPs by Sonogashira coupling reactions was also undertaken (Chapter 4). The general outcome of gas sorption measurements of all networks will be discussed in Chapter 5.

1.5 References

[1] Cooper, A. I., *Adv. Mat.*, **2009**, 21, 1291

[2] Chun, H., *et al., Chem. - A Eur. J.*, **2005**, 11, 3521

[3] Steele, B. C. H., Heinze, A., *Nature*, **2001**, 414, 345

[4] Düren, T., *et al.*, *Langmuir*, **2004**, 20, 2683

[5] Keith, D., Mahmoudkhani, M., WO Patent, WO/2009/155,539, **2009**

[6] Chinchilla, R., *et al.*, *Chem. Rev.*, **2007**, 107, 874

[7] Jhaveri, S. B., *et al., Chem. Eur. J.*, **2008**, 14, 6845

[8] Morris, R. E., *et al., Angew. Chem. Int. Ed.*, **2008**, 47, 4966

[9] Sederel, W. L., *et al., J. App. Polym. Sci.*, **1973**, 17, 2835

[10] Sing, K. S. W., *P. and App. Chem.*, **1985**, 57, 603

[11] Galarneau, A., *et al.,* F., *Langmuir*, **2001**, 17, 8328

[12] Hernández, M. A., *et al., J. Por. Mat.*, **2000**, 7, 443

[13] Kitagawa, H., *et al., Carbon,* **1981**, 19, 470

[14] Jacobs, P. A., *et al., Zeolites*, **1981**, 1, 161

[15] Karanfil, T., *Environ. Sci. Technol.*, **1999**, 33, 3217

[16] Srivastava, N. C., *et al., App. Therm. Eng.*, **1998**, 18, 707

[17] (a) Matranga, K. R., *et al., Chem. Eng. Sci.*, **1992**, 47, 1569 (b) Jonas, L. A., *et al., Carbon*, **1974**, 12, 95, (c) Mota, J. P. B, *Carbon*, **1997**, 35, 1259, (d) Siriwardane, R. V., *et al.*, *Energy & Fuels* **2001**, 15, 279 (e) Foster, K. L., *et al., Chem. Mater.*, **1992**, 4, 1068, (f) Chue, K. T., *et al.,* Ind. *Eng. Chem. Res.,* **1995**, 34, 591 (g) Chiang, Y.-C., *et al.*, *Carbon*, **2001**, 39, 523

[18] Khimmich, N. N., *Gl. Phy. Chem.,* **2004,** 30, 430

[19] (a) Lenza, R. F. S., Vasconcelos, W. L., *Mat. Res.*, **2001,** 4, 189, (b) Harris, R., Wick, A. N., *Ind. Eng. Chem. Anal. Ed.*, **1946**, 18, 276

[20] Schüth, Handbook of Porous Solids, **2002,** Wiley-VCH

[21] (a) Meier, W. M., *J. Sol. State Chem.*, **1979**, 27, 349 (b) Barrier, R. M., *Pure Appl. Chem.* **1979**, 51, 1091, (c) Barrer, R. M., *et al., J. Chem. Soc., Ser. A.* **1970**, 765, 775, (d) Barrer, R. M., *J. Chem. Soc.*, **1948**, 2158, (e) Zhdanov, S. P., *ACS Adv. Chem. Ser.,* **1971**, 101, 20, (f) Breck, D. W., *et al., J. Am. Chem. Soc.,* **1956**, 78, 2338, (g) Dessau, R. M., *et al., Zeolites,* **1984**, 4, 315, (h) Barre, R. M., *Zeolites,* **1981**, 1, 130 - 140

[22] Li, H., *et al., Nature*, **1999**, 402, 276

[23] Long, J. R., Yaghi, O. M., *Chem. Soc. Rev.*, **2009**, 38, 1213

[25] (a) http://www.basf.com/group/pressrelease/P-10-428 (accessed 21/05/2011) (b) http://www.catalysts.basf.com/Main/adsorbents/basf_adsorbent_technologies/metal_organic_frameworks (accessed 23/06/2011)

[27] Wong-Foy, A. G., *et al., J. Am. Chem. Soc.*, **2006**, 128, 3494

[28] O'Keeffe, M., *Chem Soc Rev*, **2009**, 38, 1215

[29] (a) Lin, X., *et al., J. Am. Chem. Soc.*, **2009**, 131, 2159, (b) Eddaoudi, M., *et al., Science*, **2002**, 295, 469

[30] Han, S. S., *et al., Chem. Soc. Rev.*, **2009**, 38, 1460

[31] Rosi, N. L. *et al., Science,* **2003**, 300, 1127

[32] Murray, L. J., *et al., Chem. Soc. Rev.*, **2009**, 38, 1294

[33] Wang, L., *et al., En. & Environ. Sci.*, **2008**, 1, 268

[35] Côté, A. P., *et al., Science*, **2005**, 310, 1166

[36] Severin, K., *Dalton Trans.*, **2009**, 5254

[37] Furukawa, H., *et al., J. Am. Chem. Soc.*, **2009**, 131, 8875

[38] (a) Budd, P. M., *et al., Phys. Chem. Chem. Phys.*, **2007**, 9, 1802 (b) McKeown, N. B., *et al., Macromolecular Rapid Commun.*, **2007**, 28, 995 (c) Germain, J., *et al., Small*, **2009**, 5, 1098 (d) McKeown, N. B., *et al.*, *Chem. Eur. J.* **2005**, 11, 2610

[39] Campbell, N. L., *et al.*, *Chem. Mater.*, **2009**, 21, 204

[40] (a) Tsyurupa, M. P., *et al., Reac. Funct. Polym.*, **2002**, 53, 193, (b) Davankov, V. A., *et al., USSR Pat*. 299 165 (**1969**); *US Pat*. 3 729 457 (**1973**); *Chem. Abstr*., 75 (**1971**) 6841B, (c) Davankov, V. A., *et al., React. Polym.,* **1990**, 13, 27–42

[41] Sherrington, D. C., *Chem. Comm.*, **1998**, 2275

[42] Tsyurupa, M. P., *et al., Reac. Funct. Polym.*, **2006**, 66, 768

[44] Fontanals, J., *et al., J. Polym. Sci. Part A: Polym. Chem.*, **2005**, 43, 1718,

[45] Zhou, J. *et al., Small*, **2009**, 5, 244

[46] Germain, J., *et al.*, *Chem. Mater.*, **2006**, 18, 4430

[47] Cormack, P. A. G., *et al., Adv. Mater.*, **2008**, 20, 1298

[48] Wood, C. D., *et al., Chem. Mat*., **2007**, 19, 2034

[49] Wood, C. D., *et al., Adv. Mater*., **2008**, 20, 1916

[50] Martín C. F., *et al., J. Mater. Chem*., **2011**, 21, 5475

[51] Trewin, A., *et al., J. Phys. Chem. C.,* **2008***,* 112*,* 20549

[52] Rose, M., *et al., Chem Comm*, **2008**, 2462

[53] (a) Germain, J., *et al., J. Mater. Chem.,* **2007**, 17, 4989 (b) Germain, J., *et al., Chem Comm*, **2009**, 1526 (c) Germain, J., *et al., Chem*. *Mater*., **2008**, 20, 7069

[54] (a) Weber, J., *et al., Macro.*, **2008**, 41, 2880 (b) Ritter, N., *et al., Macro.*, **2009**, 42, 8017 (c) Farha, O. K., *et al., Chem. Mater*., **2009**, 21, 3033

[55] (a) McKeown, N. B., *et al., Chem Comm*, **2002**, 2780 (b) McKeown, N. B., *et al.,Chem Comm*, **2002**, 2782

[56] (a) Budd, P. M., *et al., Phys. Chem. Chem. Phys.*, **2007**, 9, 1802 (b) McKeown, *et al., Macromolecules Rapid Comm*, **2007**, 28, 995

[57] Budd, P. M., *et al., J Mater Chem*, **2005**, 15, 1977

[58] Cooper, A. I., *Adv*. *Mater*., **2009**, 21, 1291

[59] (a) Mackintosh, H. J., *et al., J. Mater. Chem.* **2008**, *18*, 573, (b) McKeown, N. B., Budd, P. M., *Chem. Soc. Rev.* **2006**, *35*, 675, (c) Morris, R. E., Wheatley, P. S., *Angew. Chem., Int. Ed.* **2008**, *47*, 4966, (d) Schmidt, J., *et al., Adv. Mater.,* **2009**, *21*, 702

[60] Ten, B., *et al., Angew*. *Chem*. *Int*. *Ed*., **2009**, 48, 9457

[61] Jiang, J., *et al., Angew*. *Chem*. *Int*. *Ed*., **2007**, 46, 8574

[62] Jiang, J., *et al., J. Am. Chem. Soc.*, **2008**, 130, 7710

[63] Jiang, J.-X., Cooper, A. I., *Topics Curr. Chem.*, **2010**, *293*, 1

[64] Ben, T., *et al., Angew*. *Chem*. *Int*. *Ed*., **2009**, 48, 9457

[65] (a) C.D. Wood, , *et al., Chem. Mat*., **2007**, *19*, 2034, (b) R. Dawson, , *et al., Chem. Sci*., **2011**, *2*, 1173

[66] Ross, D. K., *Vacuum***, 2006,** 80 (10), 1084

[67] C. F. Martín, *et al., J. Mater. Chem.,* **2011,** *21*, 5475

[68] Brandt, R. K., *et al., Surface Science*, **1993**, 286 (1-2), 15

[69] Cussler, E. L. (1997). *Diffusion: Mass Transfer in Fluid Systems* (2nd ed.). New York: Cambridge University Press. pp. 308–330.

[70] Eischens, R. P., Pliskin, W. A., *Ad. Catal.,* **1958**, 10, 1

[71] Henderson, A. P., *et al., Langmuir,* **2009**, 25 (2), 931

[72] (a) FW Giacobbe - US Patent 4,717,406, **1988**, (b) MA Jonqueres - US Patent 4,786,294, **1988** (c) Li, J.-R., *et al., Chem. Soc. Rev.*, **2009**, 38, 1477

[73] Spahn, H., *et al., Chem. Eng. Sci.*, **1975**, 30 (5-6), 529

[74] (a) Davies, J. T., *et al., Proc. R. Soc. Lond. A,* **1958,** *245*, 417, (b) Giles, C. H., *J. Soc. Dy. Col.*, **1973,** 410 (c) Zhou, C. F., *et al., J. Phys. Chem. C*, **2007**, 111, 4347 (d) Kralj, D., K et al., *WSEAS TRANS. ENVIRO. DEVEL.*, **2009**, 4

[75] http://www.xamplified.com/freundlich-adsorption-isotherm/ (accessed 21/06/2011)

[76] Kralj, D., K et al., *WSEAS TRANS. ENVIRO. DEVEL.*, **2009**, 4

[77] http://www.xamplified.com/langmuir-adsorption-isotherm/ (accessed 21/06/2011)

[78] http://www.xamplified.com/langmuir-adsorption-isotherm/ (accessed 21/06/2011)

[79] http://www.chem.ufl.edu/~itl/4411L_f00/ads/ads_1.html (accessed 22/06/2011)

[81] http://www.micromeritics.com/Repository/Files/ Gas_Adsorption_Theory_poster.pdf (accessed 22/06/2011)

[82] S. Brunauer, P. H. Emmett and E. Teller, *J. Am. Chem. Soc.*, **1938**, 60, 309

[83] http://www.iesmat.com/img/Productos-QC-General/DOCUMENTACION/Porous%20Materials%20Primer_gas%20sorption%20calculation%20methods.pdf (accessed 22/06/2011)

[84] Kreuer, K. D., *J. Membr. Sci.,* **2001,** 185, 29

[85] http://www.itwm.fraunhofer.de/en/departments/flow-and-material-simulation/microstructure-simulation-and-virtual-material-design/simulation-supported-design-of-fuel-cells.html (accessed 23/06/2011)

[86] http://www1.eere.energy.gov/hydrogenandfuelcells/storage/ pdfs/targets_onboard_hydro_storage.pdf (accessed 23/05/2011)

[87] Fuel Cell Technologies Programm - U. S. Department of Energy http://www1.eere.energy.gov/hydrogenandfuelcells/storage/current_technology.html (accessed 04/04/2011)

[88] Yang, Z., *et al., J. Am. Chem. Soc.*, 2007, 129, 1673

[89] Cheng, H.-M., *et al., Carbon*, **2001**, 39, 1447

[90] Yushin, G., *et al., Adv. Funct.* Mater., **2006**, 16, 2288

[91] IUPAC Recommendations, *Pure App. Chem.,* **1985**, 57, 603

[92] IUPAC Recommendations, *Pure App. Chem.,* **1994**, 66, 1739

[93] Brunauer, S., *et al., J. Am. Chem. Soc.,* **1940**, 62, 1723

Chapter 2

Synthesis of 3-Dimensional Conjugated Microporous Polymers (CMPs) by Sonogashira-Hagihara cross-coupling

2.1 Introduction

For the formation of the polymeric materials presented here, well known organic coupling reactions have been applied and optimised for polymer formation.[1] Some of the polymer syntheses were carried out by applying Sonogashira-Hagihara cross-coupling reactions.[2] A general reaction pathway is shown below (Figure 13).

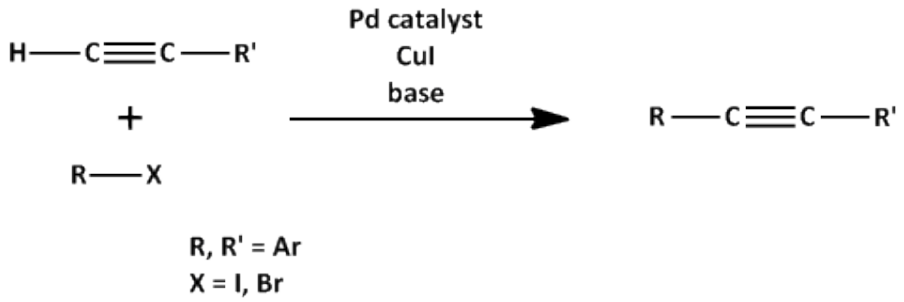

Figure 13: Sonogashira-Hagihara Coupling reaction scheme; simplified pathway

The Sonogashira coupling is a modification of the Castro-Stephens coupling[3] with added palladium and *in situ* preparation of the copper acetylide. The reaction mechanism is not clearly understood, but the textbook mechanism revolves around a palladium cycle and a copper cycle[4] (Figure 14).

Looking at the palladium cycle, the $Pd(0)L_2$ (**A**) reacts first with an aryl halide in an oxidative addition to give a Pd(II) complex (**B**). The next step is the rate limiting step, the transmetallation with the copper acetylide, which is produced in the copper cycle, to give complex **C**, releasing the copper halide CuX (**G**). Complex **D** is formed in the trans-cis isomerisation, as previously both organic ligands are trans orientated. The product is released by reductive elimination alongside with the regeneration of the Pd(0) catalyst. Regarding the copper cycle, the main limitation is

the inability to account for the deprotonation of the terminal alkyne. The amines normally used, such as diethylamine or *N,N*-diisopropylethylamine, are generally speaking not basic enough. It is suggested that the deprotonation is still possible after π-alkyne complex **E** is formed. Compound **F**, an organo-copper compound, is formed after reaction with the base. It continues to react with the palladium intermediate **C** and regenerates the copper halide **G** at the same time.

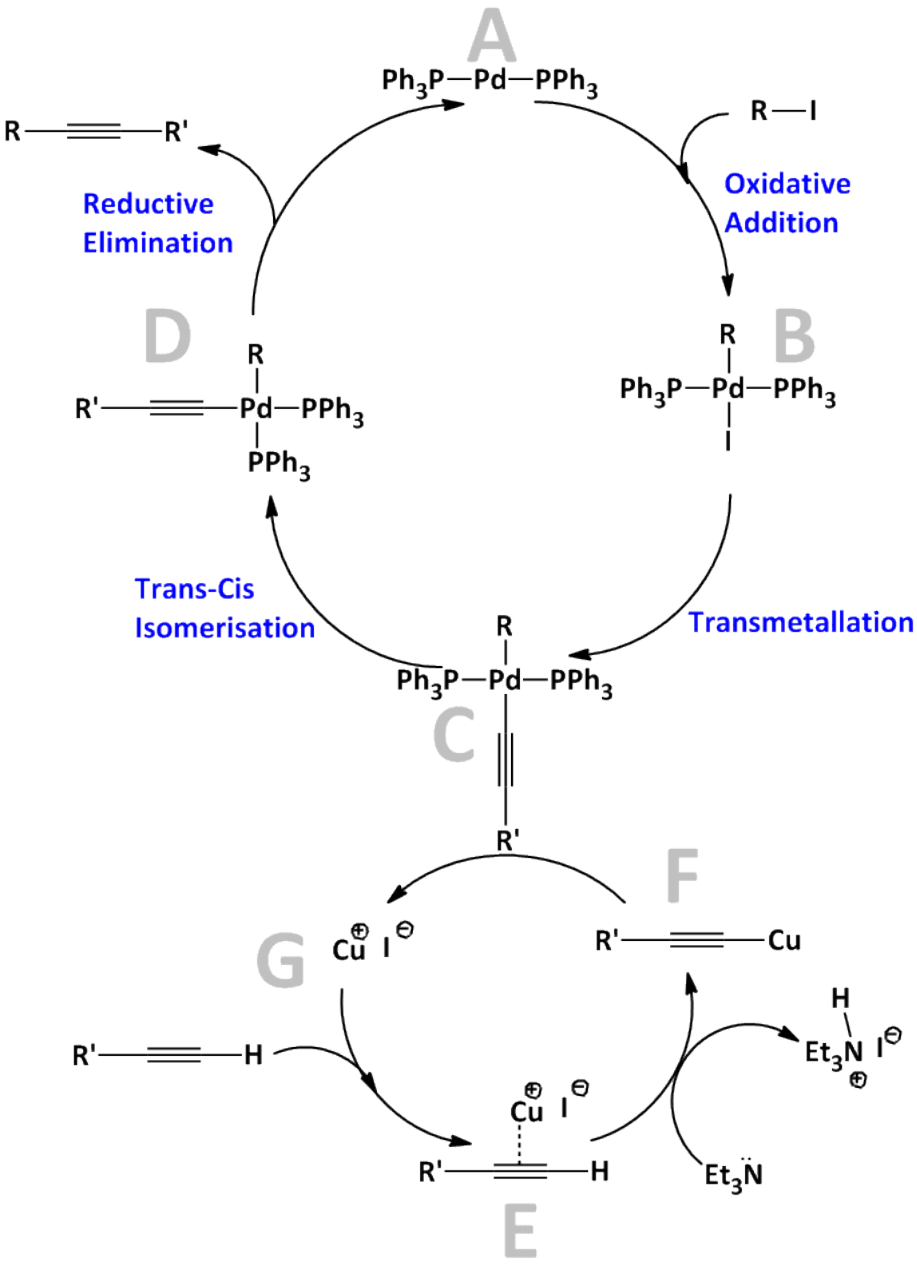

Figure 14: catalytic cycle for Sonogashira-Hagihara cross coupling reaction (redrawn after reference [4])

2.2 Results and Discussion

Polymeric materials were synthesised by applying Sonogashira-Hagihara cross-coupling reactions between 1,4-diethynylbenzene (DEB) or 1,3,5-triethynylbenzene (TEB) and tetrakis(4-iodophenyl) methane (TPM-I) (Figures 15 and 16, respectively).[5] Tetrakis(triphenylphosphine) palladium(0) (Pd(0)) or bis(triphenylphosphine) palladium(II) dichloride (Pd(II)) and copper(I) iodide (CuI) were used as the catalysts.

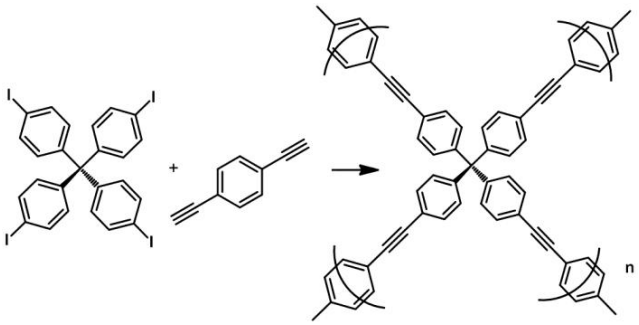

Figure 15: reaction scheme of the reaction between TPM-I and DEB, to give the idealised network

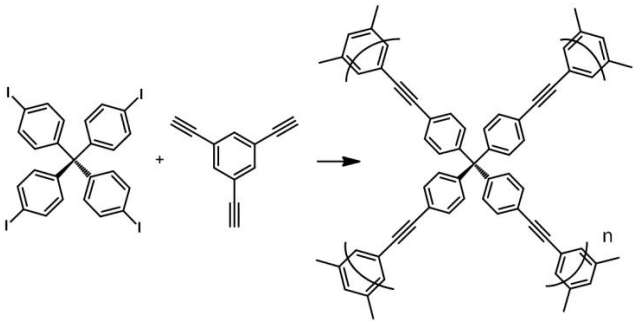

Figure 16: reaction scheme of the reaction between TPM-I and TEB, to give the idealised network

In all cases, after reacting for 24 hours under nitrogen, insoluble solids were isolated in good yields. The effect of catalyst and base on the structure and surface area was investigated. The apparent BET surface area and the elemental microanalysis were recorded as means of comparison of the different networks. All reactions are repeatable within 10 m^2/g surface area and within 1 % in terms of the

microanalysis. The following five Tables (Table 1-5) show the results of the catalyst study conducted.

Tables 2-6 show the results for the surface area measurements (SA_{BET}), the results of the microanalyses carried out and the calculated iodine contents per gram of material for each of the polymeric networks. The surface area measurements were carried out on a Micromeretics 2420 ASAP sorption apparatus and all BET surface areas (SA_{BET}) were calculated in the relative pressure range of 0.01 to 0.1 (p/p_0). This low-pressure range is used for the calculation of surface areas as microporous materials are considered here. In most guidelines for sorption sample preparation, e.g for the Quantachrome systems,[6] it is advised to use this low-pressure range and to apply the density functional theory (DFT) for microporous solids. All surface areas were calculated with a maximum error bar of ± 25 m^2/g, ensuring positive C-values and Y-intercepts of approximately zero.

As part of the analysis process for the porous materials, microanalysis was carried out. The common discrepancy in the microanalysis for materials of this nature raised questions as to what was the missing mass and whether it can be used to explain the degree of completion of the reactions, e.g., by means of identifying unreacted end groups based on the halogen contents.

The missing mass can be calculated based on the microanalysis results. As there should ideally be only carbon and hydrogen in the network, these two elements should add up to 100 %, based on the microanalysis. If carbon and hydrogen contents do not add up to 100 % the percentage left to make up 100 % is considered as the 'missing' mass. Any nitrogen content observed can be explained by trapped base within the pores: triethylamine and diisopropylamine were used as

the bases during the reactions (see the Experimental Section, Chapter 6, for detailed description of the synthesis of the networks). The assumed iodine content, stated in the following five tables, is based on example elemental analyses carried out at Butterworth Laboratories UK for four networks. Based on these results, the amount of palladium used in the reaction and the microanalysis carried out in the Chemistry department, the missing mass can be calculated by the following formula:

$$\text{Missing mass (act.)} = \text{Missing mass} - \text{Assumed } I_2 - \text{Assumed Pd}$$

The initial calculations show that there is a possibility that not all of the palladium catalyst is being washed out. For simplicity in these calculations, it is assumed that the palladium contents used in the reactions are equal to the palladium content in the remaining networks. These assumptions can be made as EDX measurements of one of the networks (Table 2, reaction 11) showed that 1 wt% of remaining palladium was present in the network. Based on these numbers, and the assumption of remaining palladium catalyst, the actual iodine content and therefore the percentage of unreacted halogenated end-groups per gram of material was calculated. As only the actual numbers for the carbon, hydrogen, and nitrogen contents are measured, assumptions were made for the iodine and palladium contents. The calculations are therefore approximate, but give an indication of the amount of unreacted end groups and hence the degree of completion of the reactions. These calculations are necessary, as the chemical analysis of these materials is difficult due to their insoluble nature. The networks

are mainly analysed by surface area measurements, since this is the main characteristic this work was focused on. The means of analysis by CHN gives only an indication as to how well the network has formed. Solid-state NMR could have been applied to all of the networks to confirm network formation and this could have quantified alkyne end-groups.[7] This method of analysis is however time and cost consuming, and not readily available. Therefore, these calculations of 'missing' mass and iodine end-groups were applied to give an indication as to why some surface areas are higher than others, and to optimise reaction conditions.

Table 2, below, shows the first part of the catalyst study. In the first part of this study, Pd (II) was the catalyst of choice. Palladium (II) was chosen as the catalyst because it is a less expensive alternative to the palladium (0) catalyst traditionally used.[8] Bis(triphenylphosphine) palladium (II) dichloride, for example, costs £25.30 per gram whereas tetrakis(triphenylphosphine) palladium (0) costs £40.80 per gram as supplied by Sigma Aldrich at the same purity grade. In addition, palladium (II) can be reduced to palladium (0) *in situ* within the catalytic cycle, thus the choice of catalyst should not influence the network formation. A comparison with palladium (0) as the catalyst is drawn in later reactions. The polymeric material was synthesised by Sonogashira-Hagihara cross coupling reaction between TPM-I (2 mmol) and DEB (6 mmol) (Figure 15), ensuring that the previously optimised 1 : 1.5 functional group ratio,[9, 10] between halide and alkyne, was maintained.

The reactions were carried out in duplicate, changing the base used to triethylamine instead of diisopropylamine in reactions denoted with 'a'. Diisopropylamine, although having a similar pK_a to triethylamine,[11] is a slightly more potent base than triethylamine and has been used in coupling synthesis before.[12]

Table 2: Palladium study part 1; synthesis of networks from 6 mmol DEB and 2 mmol TPM-I using palladium (II) as the catalyst, (a) theoretical values for CHN analysis if optimum network was formed, (b) mass of palladium (II) used in mg, (c) mass of copper iodide used in mg, (d) BET surface area in m^2/g as calculated from the nitrogen adsorption isotherm, (e) carbon contents of network, (f) hydrogen contents of network, (g) nitrogen contents of network, (h) missing mass calculated from CHN analysis, (i) assumed iodine contents as measured on one example network by Butterworth Laboratories UK, (k) palladium content used in the reaction, (l) actual missing mass calculated with taking iodine and palladium contents in to consideration, (m) iodine contents of network, 'degas' is the analysis of the same network after gas sorption measurements have been carried out

Experiment Ref	Pd(II) (mg)[b]	CuI (mg)[c]	SA_{BET} (m^2/g)[d]	Carbon (%)[e]	Hydrogen (%)[f]	Nitrogen (%)[g]	Missing mass (%)[h]	Assumed I_2 (%)[i]	Assumed Pd (%)[k]	Missing mass (act.) (%)[l]	Adjusted I_2 (%)[m]
THEORY[a]				95.72	4.28	0	0	0	0	0	0
1	100	30	620	74.67	4.97	4.99	15.37	4.8	8.13	2.44	-5.69
DEGAS	100	30	620	78.3	4.49	2.93	14.28	4.8	8.13	1.35	-6.78
1a	100	30	750	80.41	3.97	0.5	15.12	4.8	8.13	2.19	-5.94
DEGAS	100	30	750	78.95	3.82	0.25	16.98	4.8	8.13	4.05	-4.08
2	80	24	840	75.42	5.09	5.55	13.94	4.8	6.54	2.60	-3.93
DEGAS	80	24	840	82.22	4.31	1.18	12.29	4.8	6.54	0.95	-5.58
2a	80	24	830	80.17	3.89	0.5	15.44	4.8	6.54	4.10	-2.43
DEGAS	80	24	830	78.45	3.82	0	17.73	4.8	4.93	8.00	3.08
3	60	18	660	75.67	5.04	5.59	13.7	4.8	4.93	3.97	-0.95
DEGAS	60	18	660	81.06	4.45	2.27	12.22	4.8	4.93	2.49	-2.43
3a	60	18	800	73.4	3.7	0.5	22.4	4.8	4.93	12.67	7.75
DEGAS	60	18	800	79.99	4.09	0.42	15.5	4.8	4.93	5.77	0.85
4	40	12	500	74.95	4.88	4.77	15.4	4.8	3.30	7.30	4.00
DEGAS	40	12	500	76.86	4.2	2.7	16.24	4.8	3.30	8.14	4.84
4a	40	12	850	72.54	3.54	0.5	23.42	4.8	3.30	15.32	12.02
DEGAS	40	12	850	80.87	3.86	0	15.27	4.8	3.30	7.17	3.87
5	40	12	540	74.47	4.86	4.75	15.92	4.8	3.30	7.82	4.52
DEGAS	40	12	540	77.77	4.2	2.44	15.59	4.8	3.30	7.49	4.19
5a	40	12	780	75.34	3.72	0.5	20.44	4.8	3.30	12.34	9.04
DEGAS	40	12	780	82.11	3.92	0	13.97	4.8	3.30	5.87	2.57
6	20	6	300	74.13	4.69	4.34	16.84	4.8	1.66	10.38	8.72
DEGAS	20	6	300	77.09	4.17	2.73	16.01	4.8	1.66	9.55	7.89
6a	20	6	720	73	3.58	0.5	22.92	4.8	1.66	16.46	14.80
DEGAS	20	6	720	80.16	3.85	0	15.99	4.8	1.66	9.53	7.87
7	10	3	420	77.92	4.8	4.33	12.95	4.8	0.83	7.32	6.49
DEGAS	10	3	420	80.05	4.12	1.97	13.86	4.8	0.83	8.23	7.40
7a	10	3	490	70.61	3.48	0.5	25.41	4.8	0.83	19.78	18.95
DEGAS	10	3	490	73.93	3.54	0	22.53	4.8	0.83	16.90	16.07
8	5	1.5	340	75.09	4.79	3.39	16.73	4.8	0.42	11.51	11.10
DEGAS	5	1.5	340	75.52	3.82	1.53	19.13	4.8	0.42	13.91	13.50
8a	5	1.5	290	67.59	3.39	0.5	28.52	4.8	0.42	23.30	22.89
DEGAS	5	1.5	290	67.13	3.23	0	29.64	4.8	0.42	24.42	24.01

The assumed iodine contents are based on one analysis carried out by Butterworth Laboratories UK. This was assumed as a constant to simplify the calculations of missing mass. The assumption of remaining palladium contents are based on the amount of palladium added to the reaction. The results need therefore to be treated with caution but give an explanation as to why some networks have lower surface areas than others.

Considering only the reactions carried out with diisopropylamine as the base, a definite trend is noticeable when comparing the Surface Areas (SA_{BET}) between reactions. The surface area initially increases from 630 m^2/g to 840 m^2/g while decreasing the amount of catalyst by 20 % from 100 mg to 80 mg. The surface area then decreases further when decreasing the amount of catalyst and reaches its lowest point at 305 m^2/g, when the amount of catalyst is reduced by 80 % to 20 mg, thus showing that the amount of catalyst influences the surface areas of the materials significantly. A slight fluctuation of surface area can be observed when decreasing the amount further (Graph 1). This implies that the amount of catalyst used influences the degree of polycondensation of the material and therefore the surface area. If the amount of catalyst is too high, it cannot be removed completely from the network formed, and hence blocks pores within the network and decreases the surface area. However, when using a low amount of catalyst, e.g. in experiment 8, where 5 mg of Pd(II) were used, a surface area of 288 m^2/g can still be observed, compared to a surface area of 837 m^2/g when using 80 mg of Pd(II). This suggests that even a low amount of catalyst, gives rise to porous networks.

The experiments denoted with ‘a’ (reactions where triethylamine was used as the base) were carried out to see if the catalyst or the base used during the

reactions had a greater influence on the network formation. In organic chemistry, triethylamine is often used as the base for Sonogashira coupling reactions.[12] Diisopropylamine was chosen as the base as its pK_a is slightly higher compared to triethylamine and therefore should be the better base for the reaction.[13] The pK_a of triethylamine is 10.75 and of diisopropylamine is 11.05.

The general trend (Graph 1) observed was that when using triethylamine (red line) as the base during the reaction, the surface areas were higher than when using diisopropylamine (black). The surface area was highest for this series, when using triethylamine as the base, of materials when using 40 mg of catalyst and not 80 mg like in the case of diisopropylamine. This is a further 50 % decrease in amount of catalyst compared to the reactions where diisopropylamine was used and shows that the base, as well as the catalyst, influences the Sonogashira coupling mechanism significantly. The trend lines added to Graph 1 for the two sets of reactions (black for diisopropylamine reactions and red for triethylamine reactions) show that with decreasing catalyst used in the reaction the surface area decreased as well. This trend was expected and shows that the surface area of the network is dependent on the catalyst concentration used in the reactions.

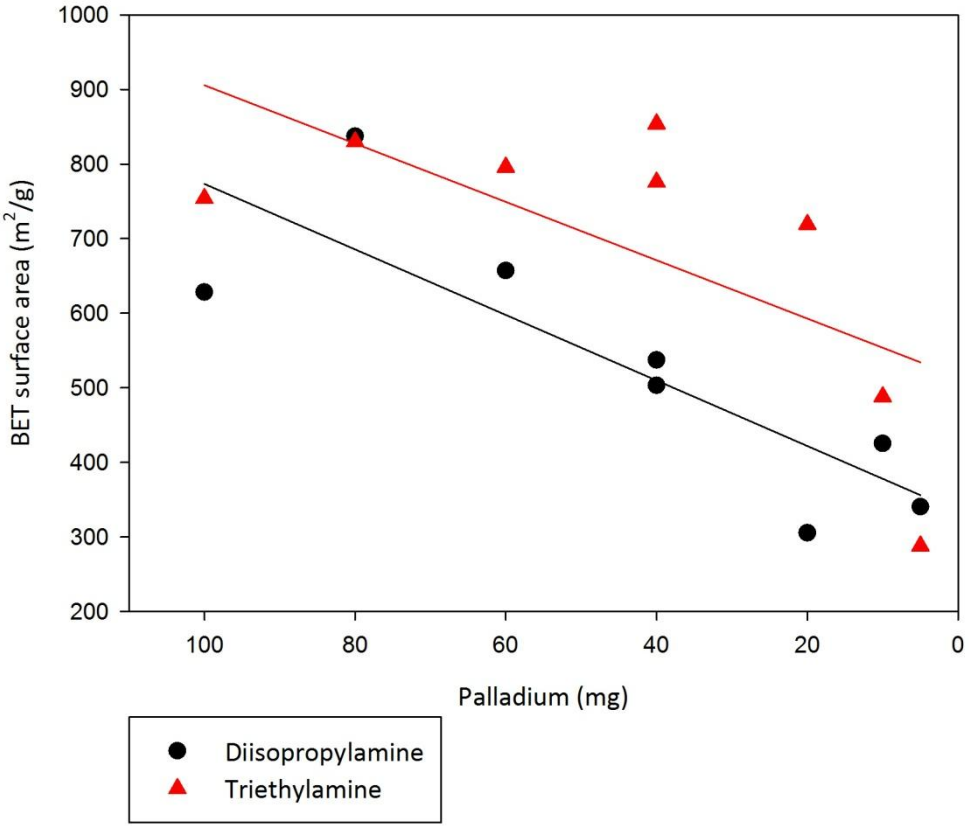

Graph 1: comparison of surface areas of networks from Table 1 in relation to amount of palladium used in the reaction, black line for reaction carried out in diisopropylamine, red line for reactions carried out in triethylamine, solid lines show trends of surface areas (linear relationship between the surface areas)

Calculating the missing mass from the microanalysis shows that all materials have some unreacted end groups and / or trapped residual catalyst present. All materials have a missing mass of over 10 % before adjusting for iodine and palladium contents. As the theoretical values in the microanalysis refer to the ideal network, which, in our experience, is not always formed (known exception is the PAF-1 network discussed in Chapter 3), a deviation of up to 5% in the microanalysis is acceptable, but a mass discrepancy of over 10% implies that the reaction has not gone to completion. The calculation of missing mass and iodine contents can be adjusted when using representative sample measurements for halogens in the network. The adjustments are based on the assumption that the catalyst is not

washed out during the work up process and that the amount of iodine measured on one of the samples at Butterworth is representative for all samples from the series. Only one of each series of samples was analysed at Butterworth as the analysis of halogen contents is highly expensive and time-consuming. If we allow theoretical adjustment of missing mass and iodine contents, it is noticeable that the highest surface area material, experiment 2, when using diisopropylamine as the base in this series, also has one of the lowest missing masses and one of the lowest iodine contents.

Where triethylamine was used as the base the highest surface area was measured when using 40 mg, 60% less than the original conditions, of catalyst and triethylamine as the base (Experiment Reference 4a). This surface area is significantly higher than that of the same reaction when using diisopropylamine as the base. All isotherms are of type I by IUPAC classification and the materials are hence microporous. A difference of 350 m^2/g indicates that triethylamine is the better base for these reactions. However, when comparing the CHN results for reaction 4 and 4a, before degassing the samples, it is noticeable that the missing mass was much higher for the triethylamine reaction (4a) than for the diisopropylamine reaction (4). The microanalysis results indicated that the reaction carried out with triethylamine had twice as many unreacted iodine end groups, therefore indicating that triethylamine was a weaker base for this set of reactions and hinders, rather than drives, the polycondensation of the network. This contradiction cannot be explained easily.

All materials had some base trapped within the network, as shown by the presence of nitrogen in the elemental analysis. This can be seen when comparing

the CHN results before and after degassing of the samples. The samples were degassed at 120 °C for 24 hrs prior to surface area measurements and the CHN contents were measured before and after these measurements. It was observed that, in general, the nitrogen contents decreased and the carbon contents increased after degassing, thus indicating that some trapped base was removed upon degassing of the sample.

The polymeric materials synthesised with only 5 mg of catalyst, experiments 8 and 8a, even though still porous, have the highest missing masses and iodine contents. This suggests that, although still porous, the polymers are the least condensed in this series, presumably due to an insufficient amount of catalyst present. Based on these initial results, it can be seen that the conditions used in experiment 2, i.e. 80 mg of Pd(II) as catalyst and diisopropylamine as base, are the ideal conditions resulting in materials with a high surface area, a low amount of missing mass, and a low amount of unreacted iodine end groups.

Table 3 below shows the second part of the catalyst study. In the second part of this study, Pd (II) was the catalyst of choice. The polymeric material was synthesised by Sonogashira-Hagihara cross coupling reaction between TPM-I (2 mmol) and TEB (4 mmol), ensuring that the previously optimised 1 : 1.5 functional group ratio,[7] between halide and alkyne, was maintained.

The reactions were carried out in duplicate, again changing the base used to triethylamine instead of diisopropylamine in reactions denoted with ‘a’.

Table 3: Palladium study part 2; synthesis of networks from 4 mmol TEB and 2 mmol TPM-I using palladium (II) as the catalyst, (a) theoretical values for CHN analysis if optimum network was formed, (b) mass of palladium (II) used in mg, (c) mass of copper iodide used in mg, (d) BET surface area in m^2/g as calculated from the nitrogen adsorption isotherm, (e) carbon contents of network, (f) hydrogen contents of network, (g) nitrogen contents of network, (h) missing mass calculated from CHN analysis, (i) assumed iodine contents as measured on one example network by Butterworth Laboratories UK, (k) palladium content used in the reaction, (l) actual missing mass calculated with taking iodine and palladium contents in to consideration, (m) iodine contents of network, 'degas' is the analysis of the same network after gas sorption measurements have been carried out

Experiment Ref	Pd(II) (mg)[b]	CuI (mg)[c]	SA_{BET} (m^2/g)[d]	Carbon (%)[e]	Hydrogen (%)[f]	Nitrogen (%)[g]	Missing mass (%)[h]	Assumed I_2 (%)[i]	Assumed Pd (%)[k]	Missing mass (act.) (%)[l]	Adjusted I_2 (%)[m]
THEORY[a]				95.72	4.28	0	0	0	0	0	0
9	100	30	320	72.14	4.83	5.04	17.99	14.6	8.70	-5.31	-14.00
DEGAS	100	30	320	80.03	4.77	5.25	9.95	14.6	8.70	-13.35	-22.04
9a	100	30	1620	65.63	3.12	0.5	30.75	14.6	8.70	7.45	-1.24
DEGAS	100	30	1620	75.35	3.44	0.31	20.9	14.6	8.70	-2.40	-11.09
10	80	24	1030	77.38	3.63	0	18.99	14.6	6.99	-2.60	-9.60
DEGAS	80	24	1030	76.36	3.42	0.56	19.66	14.6	6.99	-1.93	-8.93
10a	80	24	770	64.13	3.04	0.5	32.33	14.6	6.99	10.74	3.74
DEGAS	80	24	770	75.25	3.41	0.25	21.09	14.6	6.99	-0.50	-7.50
11	60	18	1080	80.25	3.66	0.18	15.91	14.6	5.27	-3.96	-9.23
DEGAS	60	18	1080	78.16	3.49	0.56	17.79	14.6	5.27	-2.08	-7.35
11a	60	18	890	68.13	3.19	0.5	28.18	14.6	5.27	8.31	3.04
DEGAS	60	18	890	74.59	3.39	0.26	21.76	14.6	5.27	1.89	-3.38
12	50	15	990	77.6	3.58	0	18.82	14.6	4.41	-0.19	-4.59
DEGAS	50	15	990	75.87	3.35	0.47	20.31	14.6	4.41	1.30	-3.10
12a	50	15	940	65.02	3.04	0.5	31.44	14.6	4.41	12.43	8.03
DEGAS	50	15	940	72.62	3.3	0.26	23.82	14.6	4.41	4.81	0.41
13	40	12	960	77.67	3.58	0	18.75	14.6	3.53	0.62	-2.92
DEGAS	40	12	960	76.95	3.44	0.55	19.06	14.6	3.53	0.93	-2.61
13a	40	12	850	64.27	2.98	0.5	32.25	14.6	3.53	14.12	10.58
DEGAS	40	12	850	74.85	3.39	0.21	21.55	14.6	3.53	3.42	-0.12
14	20	6	870	77.49	3.58	0	18.93	14.6	1.78	2.55	0.78
DEGAS	20	6	870	75.61	3.32	0.36	20.71	14.6	1.78	4.33	2.56
14a	20	6	770	66.05	3.04	0.5	30.41	14.6	1.78	14.03	12.26
DEGAS	20	6	770	74.31	3.29	0.24	22.16	14.6	1.78	5.78	4.01
15	10	3	720	75.21	3.42	0	21.37	14.6	0.89	5.88	4.99
DEGAS	10	3	720	73.11	3.18	0.28	23.43	14.6	0.89	7.94	7.05
15a	10	3	930	70.83	3.21	0.5	25.46	14.6	0.89	9.97	9.08
DEGAS	10	3	930	78.6	3.45	0.28	17.67	14.6	0.89	2.18	1.29
16	5	1.5	570	71.6	3.29	0	25.11	14.6	0.45	10.06	9.62
DEGAS	5	1.5	570	71.32	3	0.2	25.48	14.6	0.45	10.43	9.99
16a	5	1.5	620	58.17	2.71	0.5	38.62	14.6	0.45	23.57	23.13
DEGAS	5	1.5	620	67.17	2.95	0	29.88	14.6	0.45	14.83	14.39

In this part of the study, a similar general trend was observed as before. The BET surface area decreased with decreasing amount of catalyst, indicating that the degree of polycondensation decreased with less catalyst (Graph 2). Interestingly, in this set of data, the difference in surface area between reaction 9 and 9a was exceptionally large. Reaction 9 has a very low surface area of 300 m^2/g and its duplicate reaction, where triethylamine was used as the base, had a surface area of 1600 m^2/g. This suggests that triethylamine is the better base for this reaction and that the network was formed to a higher degree of completion.

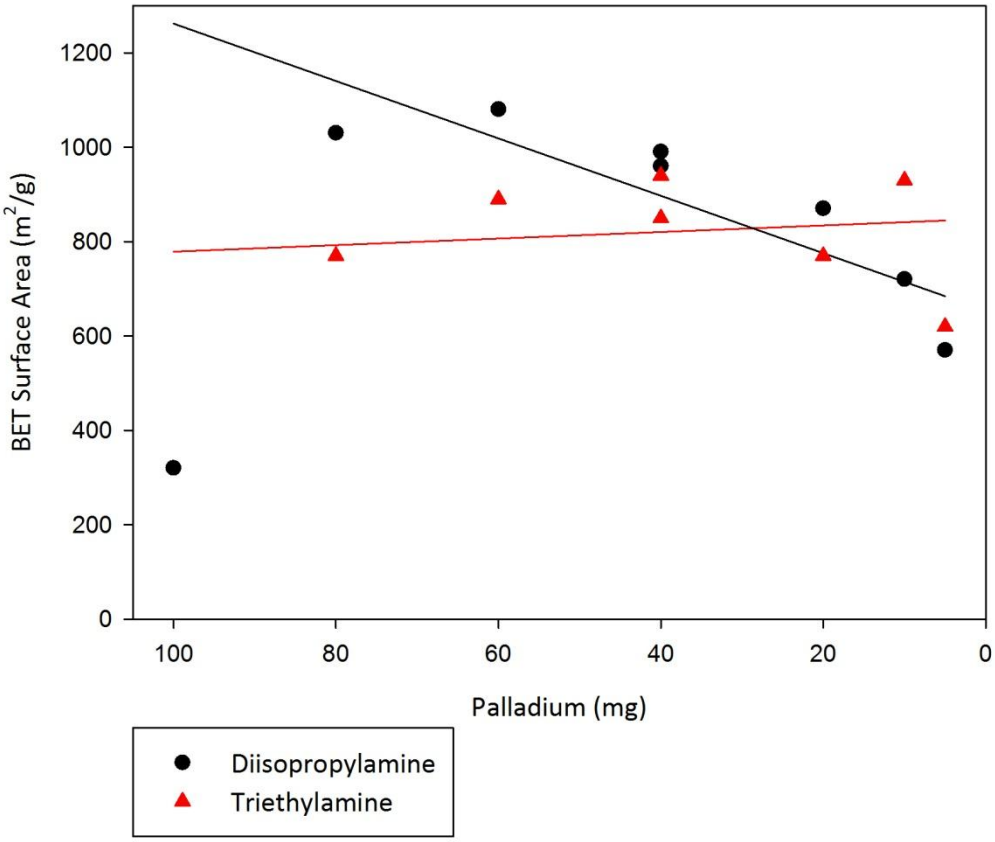

Graph 2: comparison of surface areas of networks from Table 3 in relation to amount of palladium used in the reaction, black line for reaction carried out in diisopropylamine, red line for reactions carried out in triethylamine, solid lines show trends of surface areas (linear relationship between the surface areas)

The degree of completion is in some cases directly linked to the surface area. As discussed by Irwin *et al.,* the extent of condensation of the polymerisation is parallel to the surface area.[14] However, looking at the results from the microanalysis for these two reactions, the opposite could be deduced. The lower surface area material has a closer match to the theoretical values for the carbon and hydrogen contents with an initial missing mass of 18 % compared to 31 % for the higher surface area material. After adjusting for unreacted iodine end groups and palladium contents, both materials had a negative amount of actual missing mass, i.e. the assumption for iodine and palladium in the materials is an overestimation. It was also noticeable in both cases that after degassing, the CHN analysis becomes closer to the theoretical values, by approximately 10 % for carbon, while the amount of hydrogen and nitrogen does not change significantly. This indicates that other elements, perhaps oxygen, were present in the network before degassing. This could be due to the materials absorbing moisture from the air.

The rest of the series followed a more easily explained trend. The surface areas in the materials show that diisopropylamine is the better base for this set of reactions, resulting in higher surface areas compared to their triethylamine repeats, with differences in surface areas of about 100 – 200 m^2/g. The microanalysis confirmed that the reactions carried out using diisopropylamine as the base have a higher degree of condensation, compared to reactions carried out with triethylamine as the base, and therefore a lower amount of missing mass.

Table 4 below shows the third part of the catalyst study. In the third part of this study, Pd (0) was chosen as the catalyst. The polymeric material was

synthesised by Sonogashira-Hagihara cross coupling reaction between TPM-I (2 mmol) and DEB (6 mmol), ensuring that the previously optimised 1 : 1.5 functional group ratio,[7] between halide and alkyne, was maintained.

The reactions were also carried out in duplicate, changing the base used to triethylamine instead of diisopropylamine in reactions denoted with 'a'. Based on the initial results in this catalyst study (Table 2) it was decided to decrease the number of reactions carried out and only use the amount of catalyst that gave the best results for the first set of reactions. Hence, amounts of Pd (0) of 80 mg, 60 mg and 40 mg were used.

Table 4: Palladium study part 3; synthesis of networks from 6 mmol DEB and 2 mmol TPM-I using palladium (0) as the catalyst, (a) theoretical values for CHN analysis if optimum network was formed, (b) mass of palladium (II) used in mg, (c) mass of copper iodide used in mg, (d) BET surface area in m^2/g as calculated from the nitrogen adsorption isotherm, (e) carbon contents of network, (f) hydrogen contents of network, (g) nitrogen contents of network, (h) missing mass calculated from CHN analysis, (i) assumed iodine contents as measured on one example network by Butterworth Laboratories UK, (k) palladium content used in the reaction, (l) actual missing mass calculated with taking iodine and palladium contents in to consideration, (m) iodine contents of network, 'degas' is the analysis of the same network after gas sorption measurements have been carried out

Experiment Ref	Pd(0) (mg)[b]	CuI (mg)[c]	SA_{BET} (m^2/g)[d]	Carbon (%)[e]	Hydrogen (%)[f]	Nitrogen (%)[g]	Missing mass (%)[h]	Assumed I_2 (%)[i]	Assumed Pd (%)[k]	Missing mass (act.) (%)[l]	Adjusted I_2 (%)[m]
THEORY[a]				95.72	4.28	0	0	0	0	0	0
17	80	24	1230	87.01	4.38	0	8.61	4.8	6.54	-2.73	-9.26
DEGAS	80	24	1230	85.46	4.36	0.37	9.81	4.8	6.54	-1.53	-8.06
17a	80	24	1200	72.51	3.58	0.5	23.41	4.8	6.54	12.07	5.54
DEGAS	80	24	1200	86.28	4.11	0	9.61	4.8	6.54	-1.73	-8.26
18	60	18	1220	87.01	4.38	0	8.61	4.8	4.93	-1.12	-6.04
DEGAS	60	18	1220	86.49	4.15	0.27	9.09	4.8	4.93	-0.64	-5.56
18a	60	18	1000	75.11	3.76	0.5	20.63	4.8	4.93	10.90	5.98
DEGAS	60	18	1000	84.65	4.07	0	11.28	4.8	4.93	1.55	-3.37
19	40	12	1110	85.95	4.39	0.22	9.44	4.8	3.30	1.34	-1.96
DEGAS	40	12	1110	85.47	4.19	0.24	10.1	4.8	3.30	2.00	-1.30
19a	40	12	940	73.5	3.62	0.5	22.38	4.8	3.30	14.28	10.98
DEGAS	40	12	940	81.26	3.92	0	14.82	4.8	3.30	6.72	3.42

It is noticeable from Table 4 that the surface areas were higher compared to these when using Pd (II) as catalyst. A difference between the surface areas of up to 400 m^2/g, compared to results from Table 1, is very significant. Pd (0) seems to be the better catalyst for these reactions, resulting in higher surface areas and lower iodine contents, and hence higher degrees of condensation. This could be because the catalyst does not need to be reduced first in the reaction mixture before the reaction can begin. However, the advantage would be very small as the turnover is very quick[15] within the catalytic cycle. The original Sonogashira[8] coupling reaction was carried out with palladium (II) and Sonogashira showed that yields of 70 % to 99 % can be achieved. Sonogashira also comments that palladium (0) species can also be used but that the presence of copper iodide is required for the reaction to occur at room temperature.[2] This suggests that the copper iodide is an important component of the reaction cycle.[4] Comparing the reactions carried out using diisopropylamine as the base, and their duplicates where triethylamine was used as the base, it was observed that the surface areas were higher than for the diisopropylamine reactions. The missing mass was overestimated for the majority of the reactions, most of which where diisopropylamine was used as the base. Only reactions where triethylamine was used as the base demonstrated missing masses of more than 20 %. This indicates that the combination of Pd (0) and diisopropylamine is the optimum combination of reagents for the coupling of TPM-I with DEB.

The same trend, as in the previous Tables, was observed in Table 4. The decreasing amount of catalyst resulted in a decrease in SA_{BET} of the materials (Graph 3). Decreasing the amount of catalyst by 50 % of its original amount (i.e.,

from 80 mg to 40 mg) resulted in a decrease in SA_{BET} of 118 m^2/g, in the case of the diisopropylamine reactions, and 260 m^2/g in the case of the triethylamine reactions.

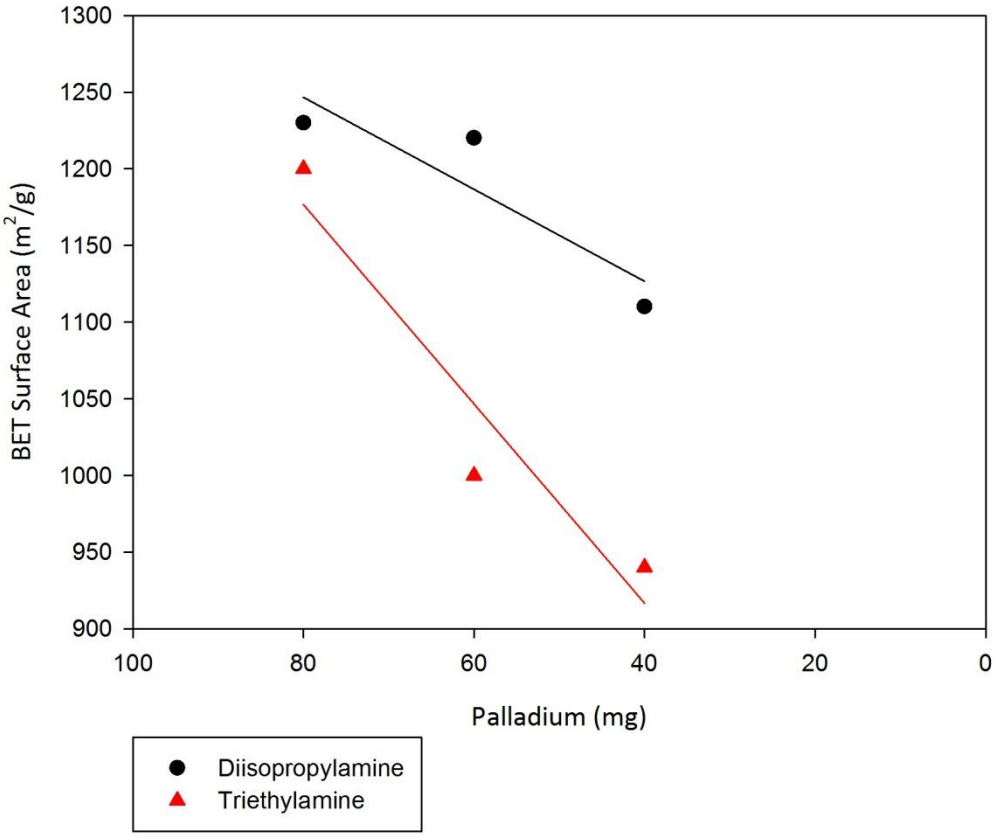

Graph 3: comparison of surface areas of networks from Table 4 in relation to amount of palladium used in the reaction, black line for reaction carried out in diisopropylamine, red line for reactions carried out in triethylamine, solid lines show trends of surface areas (linear relationship between the surface areas)

Comparing the surface areas for the diisopropylamine and for the triethylamine reactions, one can see a difference of up to 200 m^2/g was observed between the duplicate reactions. This suggests that for this set of reactions, a combination of 80 mg of catalyst and diisopropylamine as the base is the best combination. This was also confirmed by the missing mass and the percentage of iodine in the material. The overestimation of missing mass and iodine contents show that, in this case, for reaction 17 the palladium catalyst was almost washed out completely. It was

assumed that only 2.7 % of the original 6.5 % of palladium remain in the network, based on the missing mass calculation. Reaction 17 is the sample that was analysed at Butterworth Laboratories for iodine. Therefore, the missing mass is solely due to the palladium trapped in the network.

Table 5 below shows the fourth part of the catalyst study. In the fourth part of this study, Pd (0) was chosen as the catalyst and the networks were synthesised by Sonogashira-Hagihara cross coupling reaction between TPM-I (2 mmol) and TEB (4 mmol). Again, the previously optimised 1 : 1.5 functional group ratio,[7] between halide and alkyne, was maintained.

The reactions were also repeated with triethylamine as the base instead of diisopropylamine. The numbers of reactions were minimised again based on the initial results of this catalyst study (Table 1). Hence, amounts of Pd (0) of 80 mg, 60 mg and 40 mg were used.

Table 5: Palladium study part 4; synthesis of networks from 4 mmol TEB and TPM-I using palladium (0) as the catalyst, (a) theoretical values for CHN analysis if optimum network was formed, (b) mass of palladium (II) used in mg, (c) mass of copper iodide used in mg, (d) BET surface area in m^2/g as calculated from the nitrogen adsorption isotherm, (e) carbon contents of network, (f) hydrogen contents of network, (g) nitrogen contents of network, (h) missing mass calculated from CHN analysis, (i) assumed iodine contents as measured on one example network by Butterworth Laboratories UK, (k) palladium content used in the reaction, (l) actual missing mass calculated with taking iodine and palladium contents in to consideration, (m) iodine contents of network, 'degas' is the analysis of the same network after gas sorption measurements have been carried out

Experiment Ref	Pd(0) (mg)[b]	CuI (mg)[c]	SA_{BET} (m^2/g)[d]	Carbon (%)[e]	Hydrogen (%)[f]	Nitrogen (%)[g]	Missing mass (%)[h]	Assumed I_2 (%)[i]	Assumed Pd (%)[k]	Missing mass (act.) (%)[l]	Adjusted I_2 (%)[m]
THEORY[a]				96.06	3.94	0	0	0	0	0	0
20	80	24	1300	78.38	3.77	0.16	17.69	14.6	6.99	-3.90	-10.90
DEGAS	80	24	1300	79.97	3.65	0.3	16.07	14.6	6.99	-5.52	-12.52
20a	80	24	1200	63.06	2.91	0.5	33.53	14.6	6.99	11.94	4.94
DEGAS	80	24	1200	76.29	3.38	0.27	20.06	14.6	6.99	-1.53	-8.53
21	60	18	450	60.32	3.04	0	36.64	14.6	5.27	16.77	11.50
DEGAS	60	18	450	59.36	3.07	0.32	37.25	14.6	5.27	17.38	12.11
21a	60	18	1500	60.07	2.68	0.5	36.75	14.6	5.27	16.88	11.61
DEGAS	60	18	1500	81.02	3.57	0	15.41	14.6	5.27	-4.46	-9.73
22	40	12	300	75.92	4.89	5.59	13.6	14.6	3.53	-4.53	-8.07
DEGAS	40	12	300	67.56	3.79	2.25	26.4	14.6	3.53	8.27	4.73
22a	40	12	1090	72.41	3.23	0.5	23.86	14.6	3.53	5.73	2.19
DEGAS	40	12	1090	79.55	3.56	0	16.89	14.6	3.53	-1.24	-4.78

It is again noticeable that the surface areas were significantly higher compared to the same set of reactions where Pd (II) was used as the catalyst. The decrease in surface area was more significant regarding the separate parts of this series, i.e. diisopropylamine and triethylamine used as base (trend shown in Graph 4). Regarding the diisopropylamine reactions (reactions 20, 21 and 22) the decrease in surface area was significant when decreasing the amount of catalyst from 80 mg to 60 mg. The decrease in surface area of 850 m^2/g can be explained by a lack of condensation of the reaction. This can also be seen when comparing the CHN analysis for these reactions. Reaction 20 shows the overestimation of the missing

mass, as seen before, meaning that the catalyst and / or the iodine content have been overestimated, and for reaction 21 it can be observed that the lowest match in CHN was measured and therefore the highest missing mass was calculated. This shows that the formation of this network was more difficult than for the network containing 1,4-diethynylbenzene.

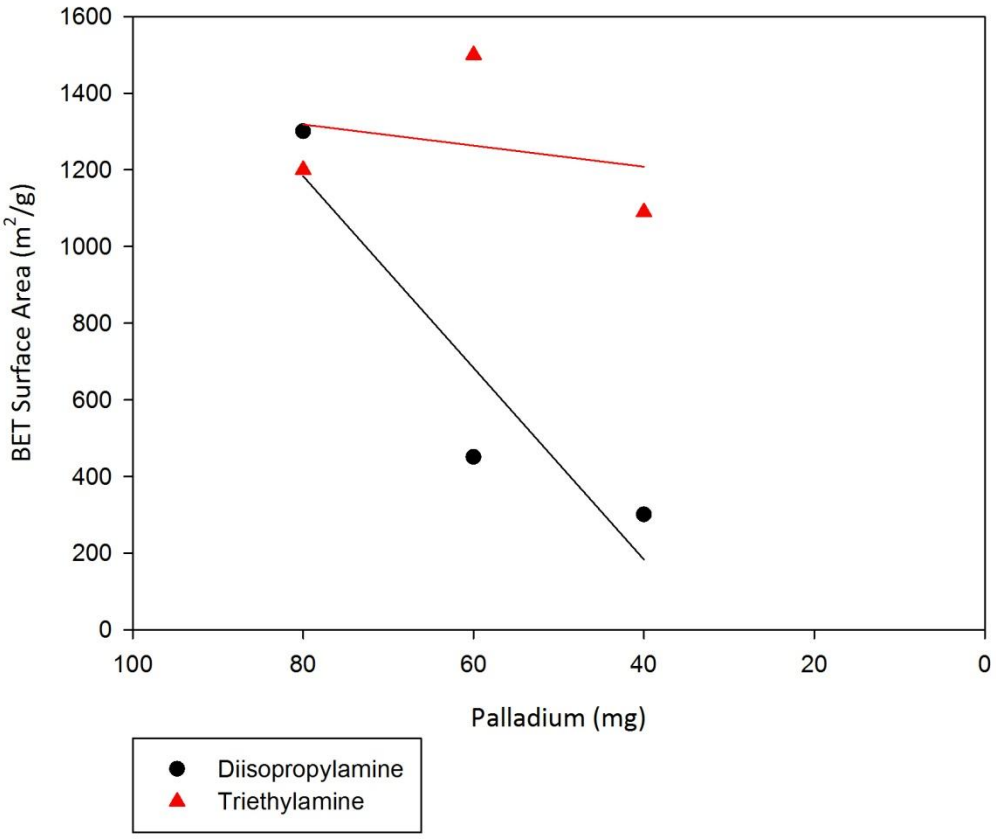

Graph 4: comparison of surface areas of networks from Table 5 in relation to amount of palladium used in the reaction, black line for reaction carried out in diisopropylamine, red line for reactions carried out in triethylamine, solid lines show trends of surface areas (linear relationship between the surface areas)

Regarding the reactions carried out where triethylamine was used as the base (reactions 20a, 21a and 22a) the trend of surface area fluctuation is clearer. While decreasing the amount of catalyst from 80 mg to 60 mg, an increase in surface area from 1200 m^2/g to 1500 m^2/g was observed. Although the results for

the CHN analyses were significantly different before degassing the samples (reactions 20a and 21a), adjusting for palladium and iodine contents, the samples have a similar, if overestimated, percentage for unreacted iodine in the material. The overestimation shows, again, that if we assume that the measurement at Butterworth for one of the samples is representative for the entire series, then the palladium does wash out fully in the extraction process.

The surface area decreased when decreasing the catalyst to 40 mg from 60 mg. The decrease of 400 m^2/g shows that the network is not formed optimally. Comparing the results in this series, it is apparent that the optimum conditions are 60 mg of palladium and triethylamine as the base.

As well as varying the catalyst concentration for the new materials, the known reaction for the formation of CMP-1 (Figure 17) was tested for the influence of catalyst on the surface area and the elemental analysis (Table 6). This part of the catalyst study, in which the experiments were carried out as 'proof of principle' with 100 mg of Pd (0), is to compare directly with earlier studies.[8]

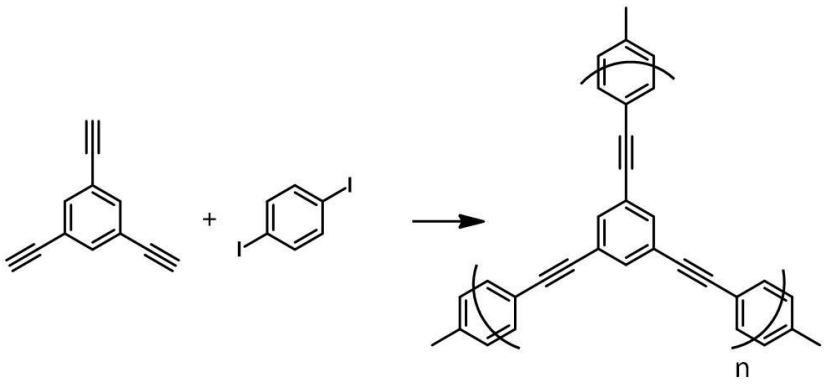

Figure 17: Schematic view of the reaction between TEB and DIB to form ideal CMP network

Table 6 below shows these results. Palladium (0) and palladium (II) were used as the catalysts. The reactions were again carried out in duplicate, changing the base to triethylamine for the repeat reactions denoted with 'a'. Reactions were carried out with 100 mg and with 50 mg of catalyst, with the aim to show that the reduction of catalyst will influence the surface area. The SA_{BET} for the original CMP-1 network was 834 m^2/g.[7]

Table 6: Palladium study part 5; control experiments; synthesis of networks from 2 mmol TEB and 2 mmol Diiodobenzene (DIB) using palladium (0) or palladium (II) as the catalyst, (a) theoretical values for CHN analysis if optimum network was formed, (b) mass of palladium used in mg, (c) mass of copper iodide used in mg, (d) BET surface area in m^2/g as calculated from the nitrogen adsorption isotherm, (e) carbon contents of network, (f) hydrogen contents of network, (g) nitrogen contents of network, (h) missing mass calculated from CHN analysis, (i) assumed iodine contents as measured on one example network by Butterworth Laboratories UK, (k) palladium content used in the reaction, (l) actual missing mass calculated with taking iodine and palladium contents in to consideration, (m) iodine contents of network, 'degas' is the analysis of the same network after gas sorption measurements have been carried out

Experiment Ref	Pd(II) (mg)[b]	Pd(0) (mg)[b]	CuI (mg)[c]	SA_{BET} (m^2/g)[d]	Carbon (%)[e]	Hydrogen (%)[f]	Nitrogen (%)[g]	Missing mass (%)[h]	Assumed I_2 (%)[i]	Assumed Pd (%)[k]	Missing mass (act.) (%)[l]	Adjusted I_2 (%)[m]
THEORY[a]					96.53	3.47	0	0	0	0	0	0
23		100	30	570	85.87	3.55	0	10.58	2.73	10.10	0.48	-9.62
DEGAS		100	30	570	85.62	3.47	0.21	10.7	2.73	10.10	0.60	-9.50
23a		100	30	760	74.85	3.13	0.5	21.52	2.73	10.10	11.42	1.32
DEGAS		100	30	760	82.77	3.55	0	13.68	2.73	10.10	3.58	-6.52
24	100		30	620	83.68	3.49	0.19	12.64	2.73	10.10	2.54	-7.56
DEGAS	100		30	620	82.23	3.37	0.35	14.05	2.73	10.10	3.95	-6.15
24a	100		30	670	74.3	3.21	0.5	21.99	2.73	10.10	11.89	1.79
DEGAS	100		30	670	78.23	3.41	0.17	18.19	2.73	10.10	8.09	-2.01
25		50	15	580	90.06	3.58	0	6.36	2.73	5.13	1.23	-3.90
DEGAS		50	15	580	88.64	3.5	0	7.86	2.73	5.13	2.73	-2.40
25a		50	15	800	86.59	3.49	0.5	9.42	2.73	5.13	4.29	-0.84
DEGAS		50	15	800	89.37	3.82	0	6.81	2.73	5.13	1.68	-3.45
26	50		15	650	88.61	3.6	0.14	7.65	2.73	5.13	2.52	-2.61
DEGAS	50		15	650	87.01	3.35	0.25	9.39	2.73	5.13	4.26	-0.87
26a	50		15	800	77.41	3.21	0.5	18.88	2.73	5.13	13.75	8.62
DEGAS	50		15	800	84.21	3.44	0	12.35	2.73	5.13	7.22	2.09

It is noticeable that none of the repeat reactions for the CMP-1 network, had exactly the same surface area as the original network,[7] but that three of the eight reactions had a surface area with 60 m^2/g off the published CMP-1; namely reactions 23a, 25a and 26a. Looking at the results, one can notice immediately that the materials with surface areas of approximately 800 m^2/g are the reactions where triethylamine was used as the base, as in the original CMP-1 reactions. The reactions where diisopropylamine was used as the base gave porous CMP-1 networks but with surface areas of only 600 m^2/g, and not 830 m^2/g like the original network.[7] This indicates that triethylamine is the best choice of base for the synthesis of CMP-1. Interestingly, neither the catalyst nor the amount of catalyst influences the surface area significantly for these networks, unlike before in the previous catalyst studies. Comparing reactions 25a and 26a, one can see that the surface areas are the same although Pd(0) and Pd(II) were used as catalysts, respectively. Also, for these reactions the amount of catalyst was reduced by 50 %, to 50 mg from 100 mg, from the original conditions[8] and the network was still formed and was as porous as the original network, as also been shown by Jiang *et al.* in 2008.[16] This shows that the oxidation state of the catalyst does not influence the network formation significantly in this case, and that the amount of catalyst used previously was unnecessarily high and can be reduced without compromising the resulting sorption properties. In fact, taking the CHN analysis into account, the decrease in catalyst gives a closer match to the theoretical values. The percentage of carbon is only 7 % too low in case of reactions 25a and 25. This is an indication that the decrease in catalyst means that a higher degree of polycondensation is

achieved and the remaining catalyst is removed more easily in the extraction process.

Recently, it has also been discovered by Dawson *et al.* that the solvent for these types of reactions can influence the surface area of CMP networks formed.[7] In these studies, DMF was used as the solvent for Sonogashira coupling reactions resulting in an increase in surface area.[10] However, when using DMF for the syntheses of the tetrahedral monomer containing networks, no improvement on the surface area was found. Further experiments have been carried out on the influence of the solvent on these types of networks. See Chapter 6 for further details and discussions.

2.3 Conclusion

In conclusion, we have increased the surface area (SA_{BET}) of conjugated microporous polymer networks by introducing a three-dimensional monomer. A maximum increase in surface area of 700 m^2/g was achieved compared to the original CMP networks,[7] which have surface areas of 800 m^2/g and which were obtained from the trigonal planar monomers. The general trend for the increase in surface area is an increase of around 300 $m^2/g \pm 100$ m^2/g, when changing the reaction conditions. The characterisation of these networks showed that the amount of catalyst used, as well as the type of base used in the reactions influenced not only the surface area but also the degree of polycondensation in the networks. This could be seen by the percentage of unreacted iodine end-groups per gram of material.

The analyses of the networks showed that optimal conditions for the synthesis of CMPs with three-dimensional monomers with high surface areas could be achieved by decreasing the amount of catalyst used to 80 mg from the original 100 mg. The base used for these reactions also influenced the degree of polycondensation and thus the surface area. When comparing the effect of triethylamine on the surface area and the effect of diisopropylamine on the surface area, in general triethylamine is the better base. The slightly lower pK_a of triethylamine compared with diisopropylamine seems to be favourable for the Sonogashira coupling reactions.

In conclusion, it can be said that the oxidation state of the catalyst, i.e. whether palladium (0) or palladium (II) is used, does not affect the surface area

significantly but that the choice of base for the syntheses of these type of networks is important if the highest possible surface area is desired.

2.4 References

[1] (a) Leal, M. P., *et al., Chem. Eur. J.* **2011**, 17, 1828, (b) Singh, V., *et al.*, Prog*r. Mat. Sci.*, **2011,** 56, 1178, (c) Kinder, L., *et al., Polymer,* **1991,** 32, 2096, (d) Grigoras, M., *et al., Europ. Poly. J.,* **2005,** 41, 1079, (e) Jiang, J., *et al., Chem. Sci.,* **2011**, (f) Dawson, R., *et al., Chem. Sci*., **2011**, *2*, 1173

[2] Sonogashira, K., *Tet. Lett.,* **1975,** 50, 4467

[3] Stephens, C., *J. Org. Chem* **1963**, 28, 3313

[4] Chinchilla, R. C. N., *Chem. Rev.,* **2007**, 107, 874

[5] Stöckel, E., *et al., Chem. Comm.*, **2009,** 2, 214

[6] http://www.iesmat.com/img/Productos-QC-General/DOCUMENTACION/Porous%20Materials%20Primer_gas%20sorption%20calculation%20methods.pdf (accessed 11/07/11)

[7] Lappan, U., *et al., Polymer,* **2002,** 43, 4325

[8] Sonogashira, K., *et al., Tetrahedron Letters,* **1975,** 16, 4467

[9] Jiang, J., *et al., Angew. Chem. Int. Ed.,* **2007**, 46, 8574

[10] Dawson, R., *et al., Macromolecules*, **2010**, 43, 8524

[11] http://www.zirchrom.com/organic.htm (accessed 03/05/2011)

[12] (a) Karpov, A. S., Müller, T. J. J., *Org. Lett.*, **2003**, 5, 3451 (b) Eckhardt, M., *J. Am. Chem. Soc.*, **2003**, 125, 13642 (c) Wüst, F. R., Kniess, T., *J. Lab. Comp. Radiopharm.*, **2003**, 46, 699

[13] Franks, M. A., *et al.,Bioorg. Medic. Chem.,* **2005,** 13, 2221

[14] Irwin, A. D., *et al., Mat. Let.,* **1987**, 6, 25

[15] Kozuch, S., *et al., Organometallics*, **2005**, 24, 2319

[16] Jiang, J., *et al., J. Am. Chem. Soc*., **2008**, *130*, 7710

[17] (a) Csékei, M., *et al., ARKIVOC,* **2004,** vii, 285, (b) Yang, J., *et al., Inorg. Chim. Act.,* **2005**, 358, 389, (c) Imoto M., *et al., Res. Chem. Intermed.,* **2009,** 35, 957

Chapter 3

Synthesis of Conjugated Microporous Polymers by Yamamoto Cross Coupling

3.1 Introduction

We hypothesised that a change in the coupling chemistry might improve the surface area for conjugated microporous polymers. This hypothesis was based on a publication by Thomas *et al.* in which the use of Yamamoto coupling to synthesise high surface area amorphous polymers was described.[1] In the Yamamoto coupling reaction (Figure 18), aromatic units are coupled directly. Based on the tetrahedral monomer used for Sonogashira couplings (Chapter 2), it was anticipated that an increase in rigidity, achieved by applying Yamamoto coupling, might result in a network less likely to collapse. In this case, pores would not be blocked and hence could be pre-defined, perhaps more so than in the Sonogashira-Hagihara coupling case.

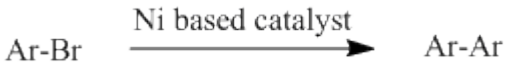

Figure 18: reaction scheme for Yamamoto coupling

A proposed catalytic cycle of the Yamamoto coupling reaction (Figure 19) involves in general the transmetallation of an aryllithium intermediate with a nickel (II) species.[2] Following that, a second transmetallation of the Ar-Ni(II)-X species forms an Ar-Ni(II)-Ar species. That species undergoes reductive elimination to form the Ar-Ar coupled product and active Ni (0). The Ni (0) species can then undergo oxidative addition to another Ar-Br molecule.

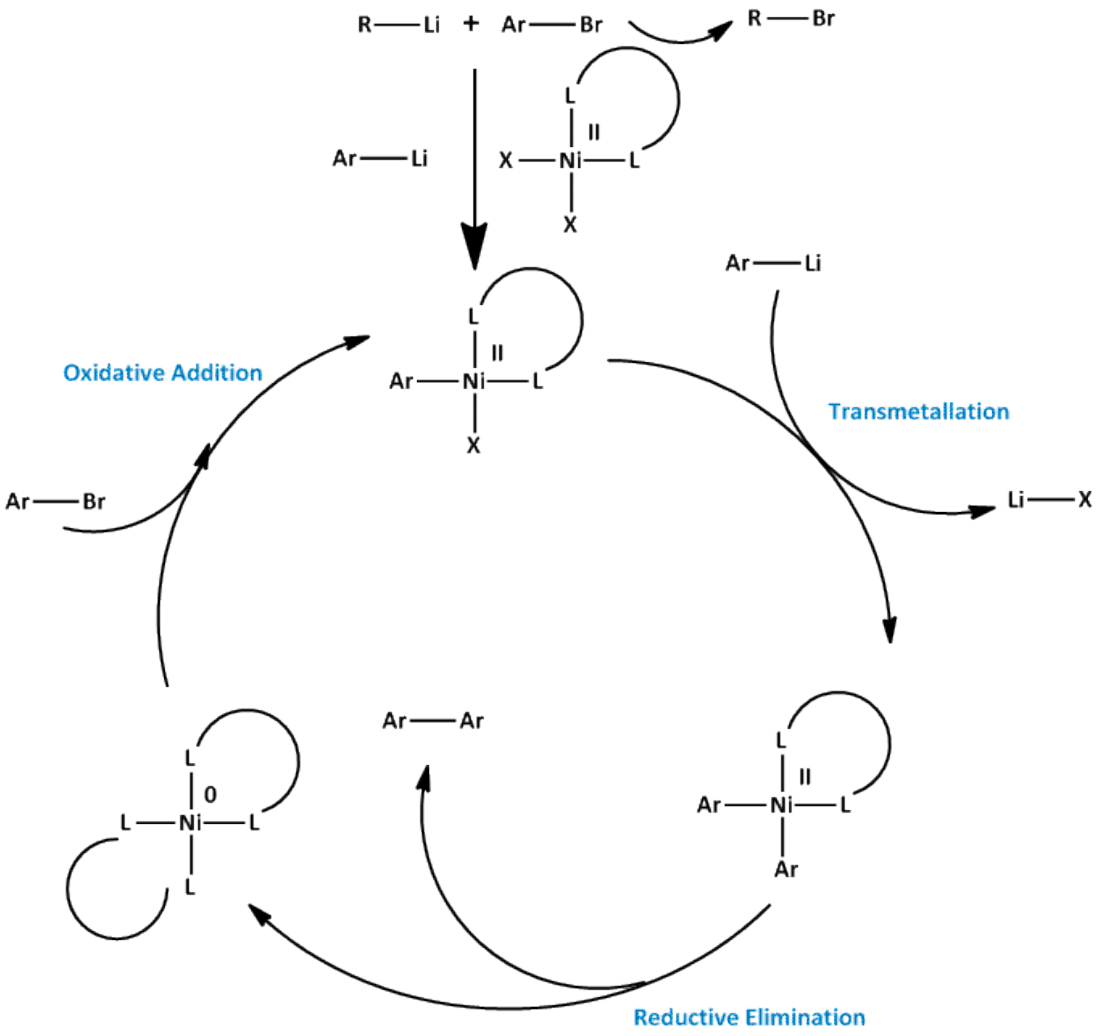

Figure 19: Proposed catalytic cycle of Yamamoto Coupling, redrawn after [3], where X = halogen atom, in the case of the networks synthesised as part of this thesis, no lithium is used in the reactions

The reactions discussed as part of this project do not have a transmetallation step, as no lithium is used in the reactions. Since we are trying to synthesise complex porous networks, it would be unfavourable to include additional metals and ligands, which can potentially block the pores of the network. It was therefore important to use the fewest possible different complexes, needed for the reaction. The catalytic cycle is therefore broken to an extent. The proposed mechanism is given in Figure 20. It was hypothesised that the additional ligands in the reaction

would 'mop up' the halogens. The aromatic rings are coordinated to the nickel, before undergoing reductive elimination to form the new C-C bond between two aromatic rings. The excess of ligand ensures that no elemental nickel is formed before the reaction is quenched. The reaction is quenched with concentrated hydrochloric acid, which causes the nickel complexes to decompose and therefore will terminate the reaction. This mechanism is in good agreement with previously published work[3-10] on Yamamoto coupling reactions.

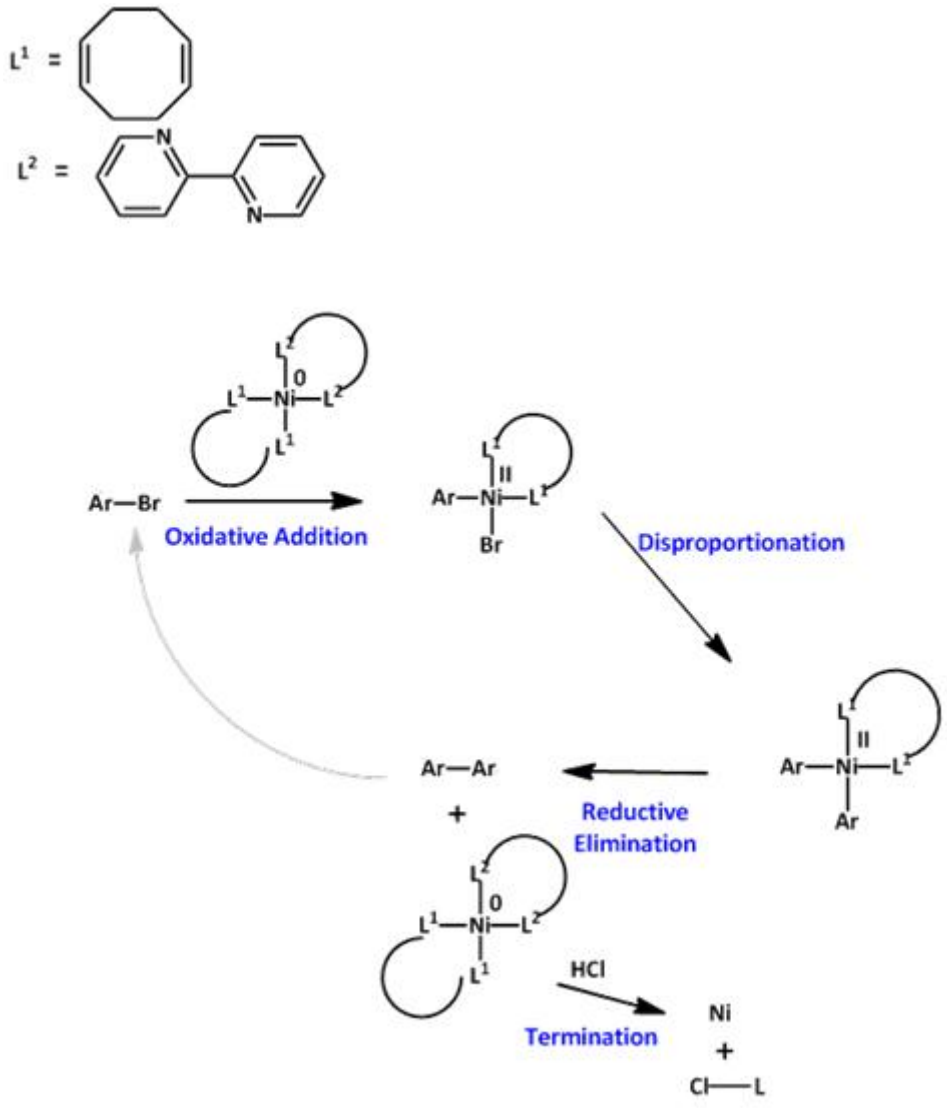

Figure 20: Proposed reaction mechanism for Yamamoto coupling discussed here

The advantage of Yamamoto coupling over Sonogashira-Hagihara coupling reactions for the formation of polymeric networks is the direct coupling of aromatic groups. The strut lengths is minimised, thus increasing the rigidity.[11] Also, axial rotation about biphenyl struts might be expected to be less facile than for arylene ethynylene struts. Even though the amount of catalyst was increased from previously used 0.1 mmol,[24] in case of the Sonogashira couplings, to 5 mmol for the Yamamoto couplings, the reactions seem to result in a higher degree of completion, for example, as in the PAF-1 system published by Ben *et al.*[10] PAF-1 was the first example of a porous network with a BET surface area of over 5500 m^2/g. It was claimed that the network shows some degree of crystallinity,[10] although this is disputed by others. PAF-1 has a hydrogen uptake of 7.0 wt% at 273 K and 48 bar, and a CO_2 uptake of 33.5 mmol/g at 298 K and 40 bar.

The different nature of the catalyst also needs to be taken into account. The nickel-based catalyst for the Yamamoto coupling reactions is less expensive than the palladium catalysts used in the Sonogashira couplings. The degree of polymerisation for PAF-1[10] as gauged by the very close match between calculated and measured carbon contents, is increased dramatically compared with previous Sonogashira-coupled networks. Thus, the decision was made to carry out a range of reactions to see if previously published results for PAF-1 were reproducible and also if novel networks with similar surface areas and gas sorption properties could be synthesised.

3.2 Results and Discussion

Figure 21 shows the reaction scheme for the synthesis of PAF-1.[10] This network has the highest surface area reported for an organic material and is comparable to the surface area of MOF-177, COF-103 and UMCM-2.[12-16] The gas uptake of PAF-1 is also very similar to those materials, showing that in high surface area materials, high pressures are necessary to saturate the material.

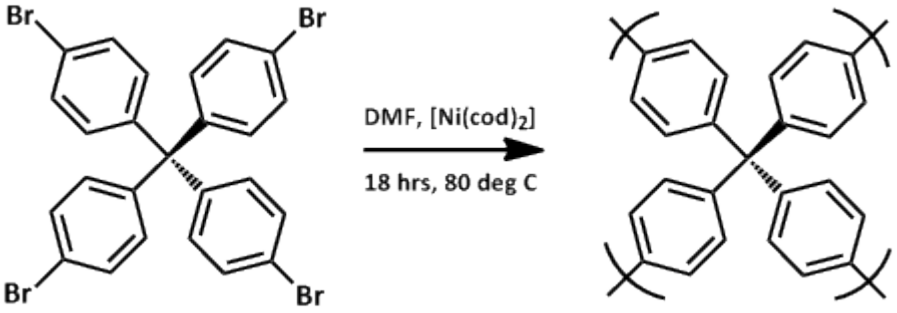

Figure 21: Idealised reaction scheme for the synthesis of PAF-1

Repeating the synthesis of PAF-1 as described in the literature[10] resulted in a PAF network with an apparent BET surface area of 4300 m^2/g, which is somewhat lower than the 5600 m^2/g which have been published by Ben *et al.* but still very high. This can be explained by comparing the CHN analyses of both the published and our synthesised material. The elemental analysis of the original PAF-1 material almost matched the calculated values for carbon and hydrogen content. However, the PAF-analogue network synthesised here was found to result in materials with carbon contents ranging from 84 to 90 %; that is, there was a discrepancy in carbon contents between 5 to 11 % in the materials synthesised here (Table 7). Although this discrepancy was not as large as for the Sonogashira-coupled polymers (Chapter 2), it demonstrates that, even though nominally the exact same procedure was

followed there is 'missing' mass that can be accredited to unreacted bromine end-groups. Although the reaction was repeated several times, the surface area of 5600 m^2/g was never achieved with this network in our hands.

Table 7: CHN analysis for PAF-1 networks (1-6), theoretical values based on $C_{25}H_{16}$ repeating unit, the published results were taken from reference [10]

	calculated	published	1	2	3	4	5	6
Carbon	94.94	94.73	84.98	83.94	90.21	89.19	84.50	84.15
Hydrogen	5.06	5.27	5.06	5.01	5.21	5.13	4.98	4.97

The purity of monomer and catalyst were checked by NMR spectroscopy and found to be 98 % pure, so only the reaction set-up could have been the influence for these reactions. All reactions were carried out on a Radleys 6 station carousel. Although the PAF-1 paper does not state the exact reaction set-up, it was assumed that the reaction was carried out under an inert atmosphere in a glove box, as the catalyst $[Ni(cod)_2]$ is extremely air-sensitive. The reactions carried out in our laboratories on the Radleys carousel are potentially not completely under inert conditions, as the system cannot be sealed entirely, even though all efforts were made to seal the system. Additionally dried nitrogen was also used to ensure no moisture in the system.

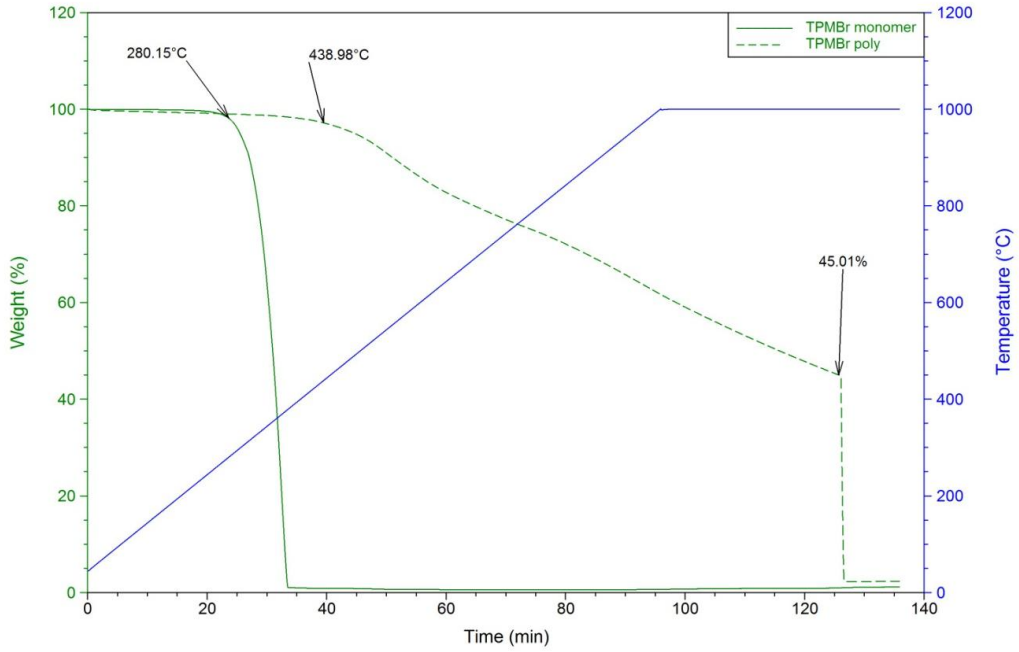

Figure 22: TGA comparison between PAF-1 network and tetrahedral monomer, run at 5 °C/min under inert atmosphere, holding for 30 minutes after reaching maximum temperature of 1000 °C and then switched to oxygen to test for any remaining catalyst, percentage represents the weight loss of the network

From comparison of the TGA for the network compared with the monomer (Figure 22) it was observed that a stable network had formed (dashed line) and that no detectable amount of monomer (solid line) was trapped in the network. The decrease in weight for the network (dashed line) with temperature was a lot slower than for the monomer (solid line) and showed that the network has indeed been formed. However, we cannot determine to what degree the network is formed. With decreasing solubility during the reaction the network could only have a few repeating units when it first precipitates. As these materials are not soluble in any solvent, no GPC or mass spectrometry can be obtained, which would determine the molecular weight of the material and therefore the number of repeat units. The decomposition of the monomer starts at 280 °C and that of the polymer begins at

approximately 440 °C. After holding the temperature at 1000 °C for 30 minutes under nitrogen, the weight of the polymer had decreased by 45 %. The weight decreased to 0 % when switching from inert conditions to oxygen, showing that no metal (i.e. no catalyst) remained in the network.

3.2.1 Novel Porous Networks

Building on the PAF-1 network and its extremely high surface and good gas uptake ability, analoguous networks were synthesised. The monomers used for the networks are shown in Figure 23. These tetrahedral monomers, featuring adamantane and silicon as the central unit, formed networks which are comparable to the PAF-1, network. The tetrahedral monomer with a carbon centre and iodine as the end group would be expected to form the same network as PAF-1, and was used to test whether iodine or bromine is the better leaving group in Yamamoto coupling reactions. The literature traditionally suggests that bromine would be the better leaving group.[17-20] The di-, tri- and tetra-bromobenzenes were mainly used as co-monomers in coupling reactions with the tetrahedral monomers. However, to test the reactions and to form novel networks, the tri- and tetra-bromobenzenes were also used to synthesise networks on their own.

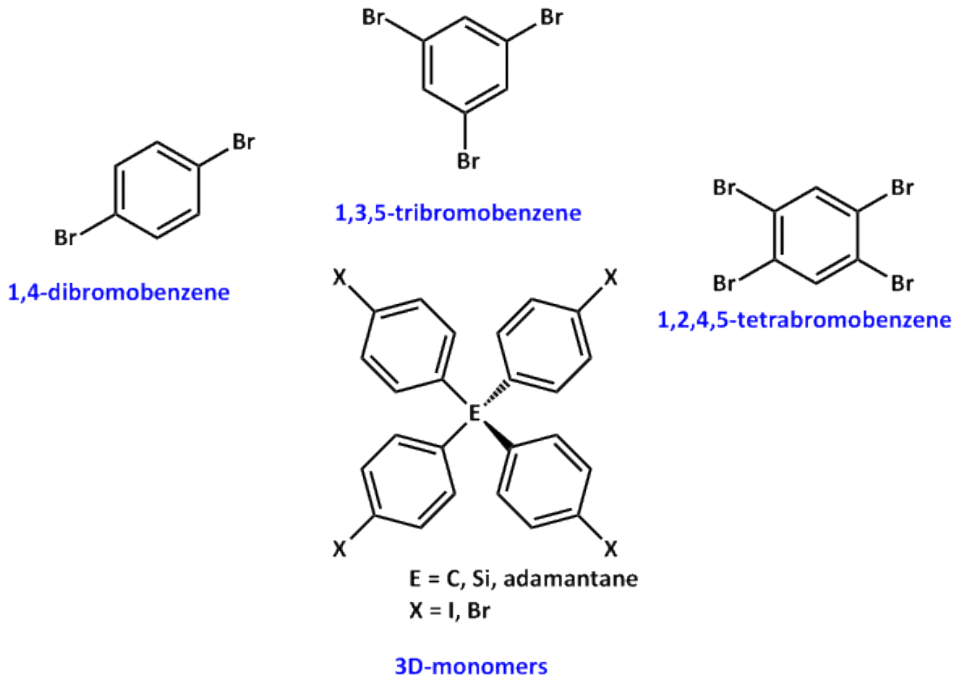

Figure 23: monomers used for Yamamoto coupling reactions

The adamantane-centred tetrahedral monomer was investigated, as it is an analogue to the PAF-1 network. The reaction scheme is shown in Figure 24. The adamantane monomer was synthesised from 1-bromoadamantane with benzene following direct bromination[21, 22] (see experimental section for full details). The Yamamoto coupling of the 1,3,5,7-tetrakis(4-bromophenyl) adamantane was carried out under identical conditions to the PAF-1 synthesis to ensure the comparability with the published network.

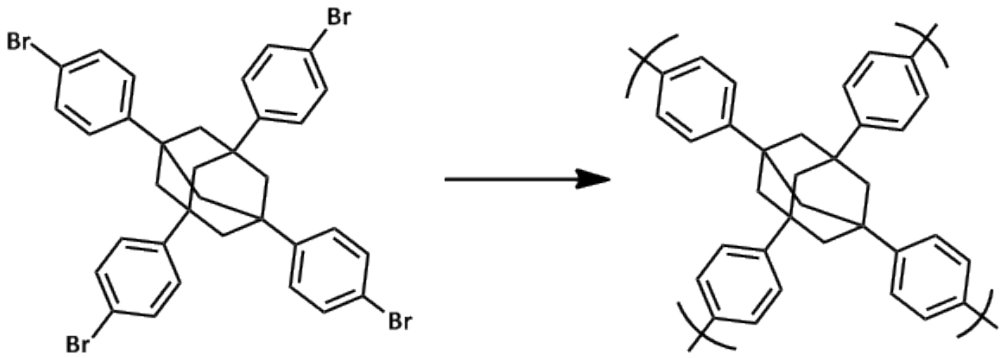

Figure 24: reaction scheme for the synthesis of poly-tolyladamantane

The surface area of the network was measured and an apparent BET surface area of 3700 m^2/g was calculated. This surface area is comparable to the surface area of the PAF-1 network synthesised in our laboratories. The carbon content was calculated to be 93.53 % and the hydrogen content to be 6.45 %. By elemental analysis, the CHN contents of the material gave good agreement with the calculated values. The carbon content was found to be 90.15 % and the hydrogen content 6.56 %. From the CHN measurements, one can deduce that only approximately 3.4 wt% can be assigned to bromine end groups, which translates on average to approximately one unreacted bromine for every repeating unit, which consists of five adamantanes.

Comparing the TGA of the adamantane monomer and polymer (Figure 25) showed that, potentially, a small amount of trapped, unreacted monomer was present. The monomer started to decompose at around 330 °C and the polymer at 460 °C. The monomer showed the expected steep weight-loss but the polymer showed an initial weight-loss of approximately 30 % that might be due to the decomposition of monomer trapped in the network that was not washed out in the purification process. As the monomer would not be incorporated in the network,

but also not be able to freely move around within the network, it might take higher temperatures for the monomer to decompose and to escape from the network. For reference, the melting point of 1,3,5,7-tetrakis(4-bromophenyl)adamantane was reported to be 120.3 °C by Reichert and Mathias.[23]

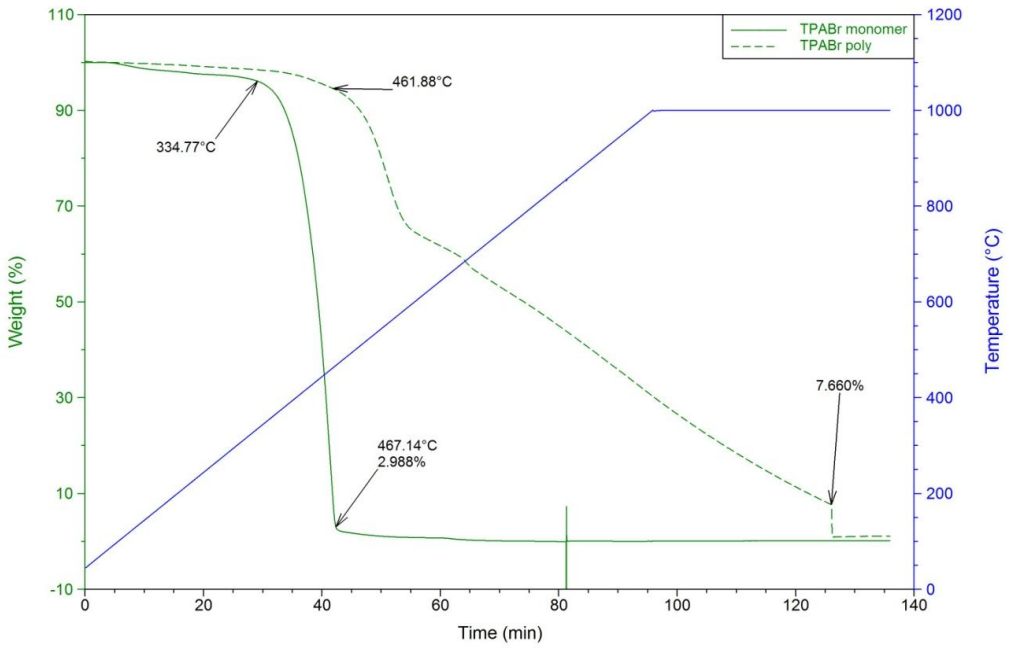

Figure 25: TGA comparison between TPA-Br network and its tetrahedral monomer, run at 5 °C/min under inert atmosphere, holding for 30 minutes after reaching maximum temperature of 1000 °C and then switched to oxygen to test for any remaining catalyst

After this initial decomposition step, the polymer decomposed at a slow rate, as expected, leaving 7.5 % of weight under inert conditions after holding the temperature at 1000 °C. When switching the gas to oxygen from nitrogen, the polymer decomposed completely, showing that no catalyst was left in the network, as any metal contents would not decompose, and would leave some mass behind. The extraction of the network was therefore complete, and the missing mass from the CHN analysis arises from unreacted bromine end-groups.

Figure 26 shows the next reaction carried out in this series. In this case, the tetrahedral monomer with a silicon core instead of a carbon core was chosen. The monomer was synthesised as reported by Stöckel *et al.*[24]

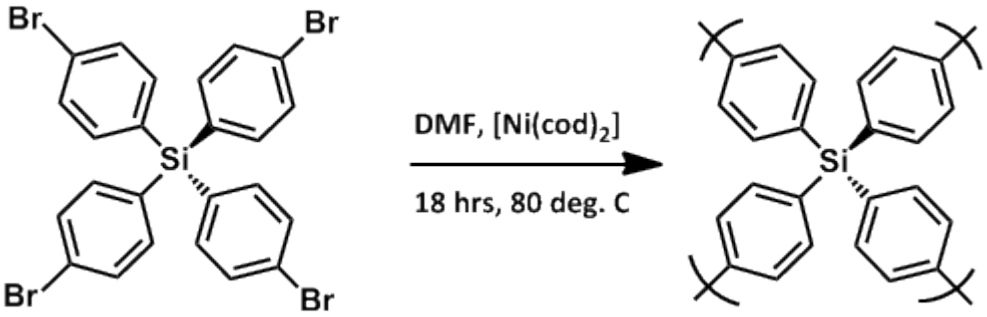

Figure 26: Idealised reaction scheme for the synthesis of poly-tolylsilane

This network was found to have an apparent BET surface area of 910 m^2/g which is considerably lower than the previously-synthesised networks. This trend was observed previously when synthesising CMPs with the same monomer plus diethynylbenzene via Sonogashira coupling.[24] In the case of the Sonogashira coupling, an additional peak in the solid state NMR[24] spectrum in the region of 90 ppm could be observed. This was ascribed to a side reaction with the base in the reaction mixture. In the case of the Yamamoto couplings, the reaction conditions are different and no ethyl source is present to cause such a side reaction.

The CHN analysis for the network shows that the results disagree with the theoretical values for the idealised network. The calculated amount of carbon and hydrogen should have been 86.7 % and 4.9 % respectively in the case of complete conversion, but the measured amount of carbon and hydrogen were 82.9 % and 5.2 % respectively, thus showing a discrepancy of approximately 3.5 %. The theoretical

values also take the silicon content of 8.4 % into account, which element could not be measured in the department. This translates on average to one bromine end group per six repeating units of material within the network. This suggests that, even though the surface area for this material is relatively low, the network has formed with a similarly high degree of condensation compared to the previous adamantane and PAF-1 materials. Perhaps the most likely explanation for the low surface area (910 m^2/g) is therefore the poor solubility of the monomer and of the resulting network as well, since the sorption properties (see Chapter 5 for discussion) and CHN results are comparable to the previous two networks.

Looking at the TGA for the silicon network (Figure 27, dashed line) compared with the TGA of its monomer (solid line), it can be seen that the polymer starts to decompose approximately 100 °C after the monomer starts to decompose (260 °C) showing that the network has formed and no trapped monomer is present.

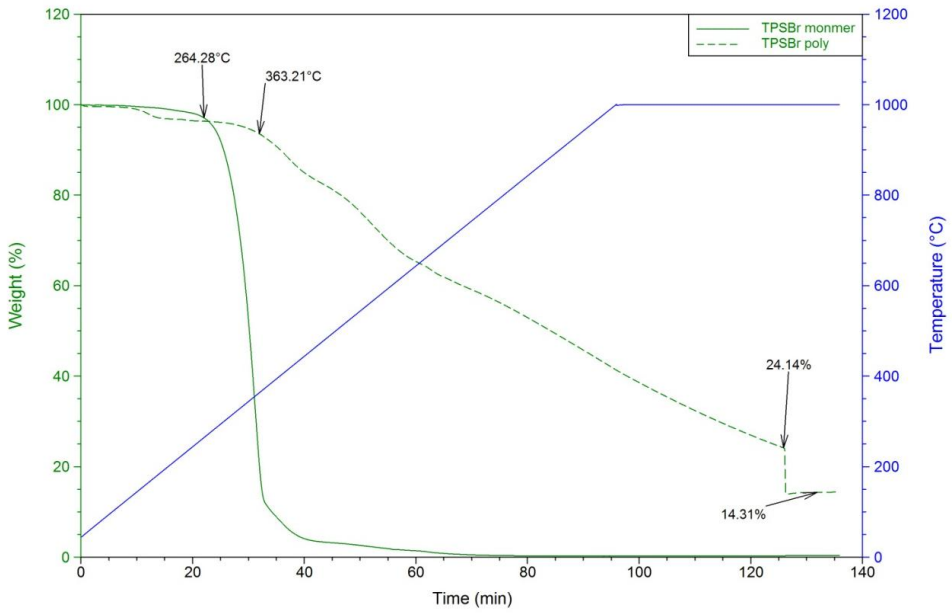

Figure 27: TGA comparison between TPM-Br network and its tetrahedral monomer, run at 5 °C/min under inert atmosphere, holding for 30 minutes after reaching maximum temperature of 1000 °C and then switched to oxygen to test for any remaining catalyst

The network decomposes on heating under nitrogen losing 76 % of its weight when reaching 1000 °C and holding it at this temperature for 30 minutes. On switching from inert conditions to oxygen the network shows a remaining mass of 14 % indicating that some remaining catalyst was trapped in the system. The 14 % remaining mass was due to nickel (II) oxide forming once switching to oxygen. A green tinge in the weighing pan could be observed hence proving the presence of nickel (II) oxide. From the CHN analysis it was seen that a mass discrepancy of 3.5 % was measured. The TGA showed that approximately 14 % of the mass of the network could be due to trapped nickel in the polymer network. Even when taking into account that the nickel is oxidised to nickel (II) oxide in the thermogravimetric analysis, it showed that the proposed repeating unit is an overestimate and that it is more likely that the mass discrepancy in the CHN analysis is due to trapped nickel and not due to unreacted bromine end groups.

Figure 28 shows the reaction scheme of the formation of the PAF-1 network from tetrakis(4-iodophenyl) methane. This reaction was carried out as comparison to the PAF-1 network synthesised from the analogous tetrahedral bromo monomer. The iodo monomer was used to see whether iodine or bromine is the better leaving group for the Yamamoto coupling reaction.[17-20]

Figure 28: reaction scheme of the synthesis of PAF-1 from the tetrahedral iodo monomer

The material synthesised showed an apparent BET surface area of 3600 m^2/g which was close to the same network synthesised from tetrakis(4-bromophenyl) methane. Comparing the CHN analysis for this network with the network synthesised from tetrakis(4-bromophenyl) methane, it was noticeable that similar results for the carbon and hydrogen content are measured. Namely 90.2 % and 5.2 % for the carbon and hydrogen content, respectively, for the network synthesised from tetrakis(4-bromophenyl) methane and 91.2 % and 5.5 % for the carbon and hydrogen content, respectively, for the network synthesised from tetrakis(4-iodophenyl) methane. The iodo network therefore has a slightly closer match with the theoretical CHN data than the bromo network. Whereas the PAF-1 network synthesised from tetrakis(4-bromophenyl) methane has a missing mass of 6.6 % which is likely to be due to unreacted bromine end groups, the PAF-1 network synthesised from the iodo monomer has a mass of just 3.3 % of unreacted iodine end groups.

The results from the CHN analysis show that the network formed from the iodine monomer is more condensed than the network formed from the bromine monomer. This is a surprising result, as the bromine end group is in theory the better leaving group for this kind of chemistry.[25] From these results, one can assume, however, that iodine is the better leaving group, for these reactions, and that the maximum surface area for this type of network is achieved, leaving only 3 % of material unreacted. No explanation can be made as to why the surface area of the original PAF-1 network is so much higher (5600 m^2/g compared to 4300 m^2/g for the PAF-1 synthesised in our laboratories). We speculate that the amount of

oxygen in the reaction vessels and / or the quality of the catalyst might be the cause for the decrease in surface area, as either would prevent the reaction from going to completion. Since no glove box was at hand to carry out the reaction under completely inert conditions, it was not possible to test this theory.

Considering the TGA of the network, compared to its monomer (Figure 29), it can be observed that the network, dashed line, is formed and started decomposing at 400 °C, approximately 115 °C after the monomer decomposed (solid line).

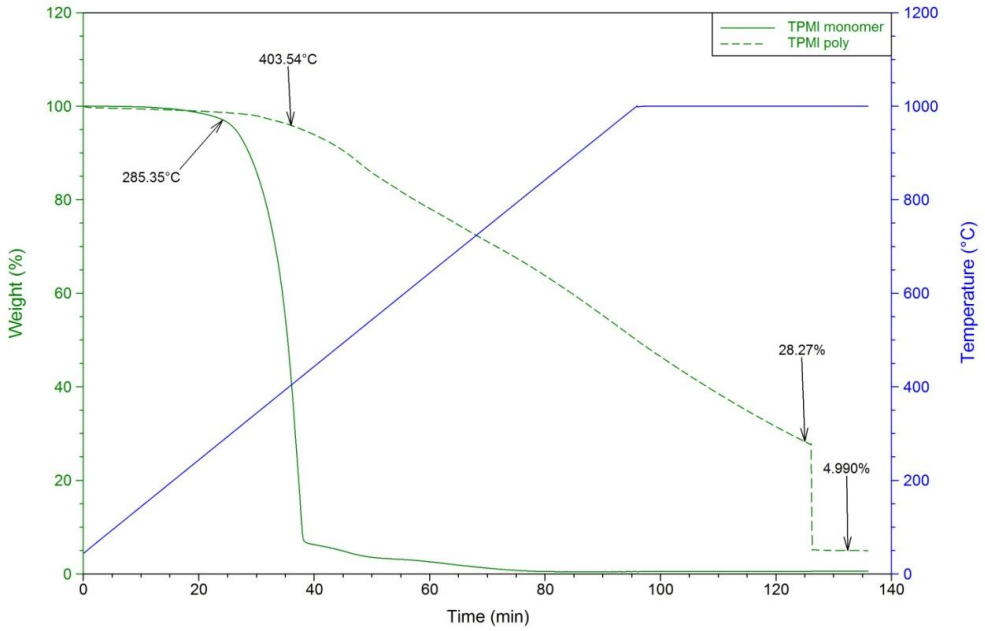

Figure 29: TGA comparison between TPM-I network and its tetrahedral monomer, run at 5 °C/min under inert atmosphere, holding for 30 minutes after reaching maximum temperature of 1000 °C and then switched to oxygen to test for any remaining catalyst

The network decomposed almost completely after switching from inert conditions to oxygen, losing 95 % of its weight. The remaining 5 % of the mass are due to trapped catalyst in the network, which was oxidised during the

measurement to give nickel (II) oxide, which can be observed by a green tinge in the weighing pan after the measurement was taken.

Figure 30 below shows the idealised synthesis of a polyphenylene network by Yamamoto coupling from 1,3,5-tribromobenzene. This network was formed as a comparison for the cross-coupled networks discussed later on. In order to be able to compare the homo-coupled network with the cross-coupled networks discussed below, BET, CHN and TGA measurements were all carried out.

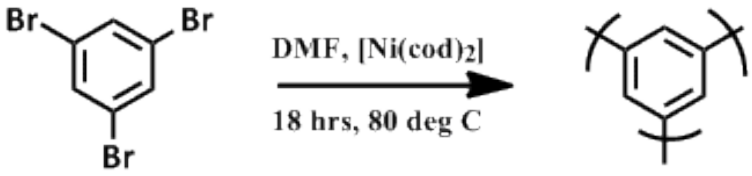

Figure 30: reaction scheme for the synthesis of polyphenylene from 1,3,5-tribromobenzene

The BET surface area for this polyphenylene network was found to be 1060 m^2/g. The surface area was significantly lower than for the homo-coupled networks synthesised from the tetrahedral monomers. This shows that the surface area is dependent on the monomer as the 2-dimensional monomer forms an insoluble network, with less impressive surface area.

Looking at the TGA of the network (Figure 31) it was observed that no monomer is present. The monomer has a melting point of 117 – 121 °C (lit.) and a boiling point of 271 °C (lit.). From the TGA, it was observed that the decomposition of the network starts at around 340 °C. No significant weight decrease was observed before then. The network was therefore free of monomer and stable up to a temperature of 330°C under nitrogen. After heating to 1000 °C a 60 % mass decrease was observed, losing a further 20 % when holding the temperature at

1000 °C under nitrogen for another 30 minutes. Only when switching the gas from nitrogen to air did the network decompose completely leaving 1.5 % of the mass. This residual mass can be accounted for by remaining metal content within the network, assuming that the soxhlet extraction (see Chapter 6 for full experimental details) did not remove any remaining catalyst completely.

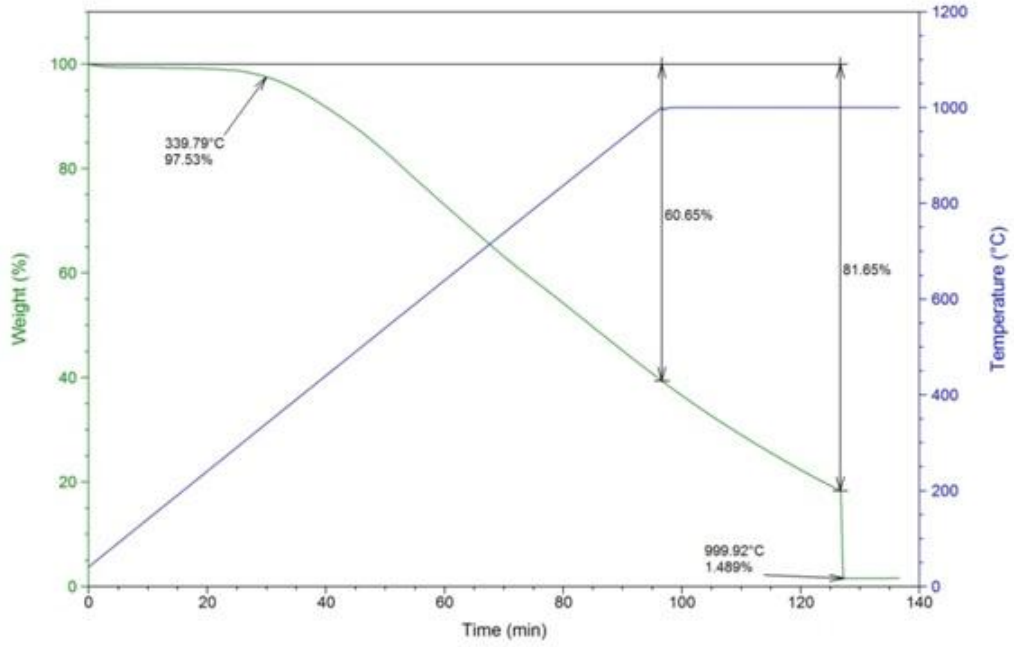

Figure 31: TGA of polyphenylene network synthesised from 1,3,5-tribromobenzene

It is also clear from the TGA is that the network decomposed without any fluctuation but at a steady rate while increasing the temperature. From the CHN analysis, we can determine the number of unreacted end groups and therefore assume that more than a few units are linked together. The CHN analysis for this material showed that 83.2 % of carbon and 4.8 % of hydrogen are present. A small nitrogen content of 2.1 % was also measured. In theory, 96 % of carbon and 4 % of hydrogen content should have been measured. If we take the 1.5 % left over mass from the TGA in to account and assume that this is equivalent to the metal content

in the network, it can be calculated that the network has four unreacted bromine end groups per one repeating unit. On average, one repeating unit consists of 41 benzene rings. The average repeating unit for the network synthesised from 1,3,5-tribromobenzene is purely representative. Solid state NMR spectroscopy would be the only possible method to prove this theory.

Considering the CHN analysis, one can say that the network, although it has formed, has not formed completely. Some trapped metal is still present, which during the reaction may have hindered the coupling, and some trapped nitrogen from the gas sorption measurement is still present. The CHN can be further explained when taking into account that hydrodehalogenation can occur in these types of reactions.[26-28] This is true for all networks discussed here but can only be seen in some cases when undergoing detailed theoretical analysis, as discussed previously, alongside with the carbon and hydrogen content measured, it can be proven to an extent.

Figure 32 below shows the reaction scheme of the synthesis of another polyphenylene network synthesised from 1,2,4,5-tetrabromobenzene. The network has an apparent BET surface area of 15 m^2/g and hence was non-porous to nitrogen.

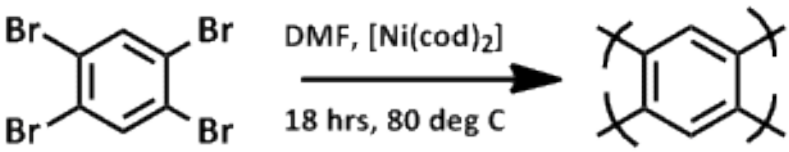

Figure 32: reaction scheme for the synthesis of polyphenylene from 1,2,4,6-tetrabromobenzene

The network was not expected to be highly porous, as the coupling would be hindered due to a 'crowded' monomer.[29] However, it needed to be tested as the monomer was also used in subsequent cross-coupling reactions. The CHN and TGA of this network were also recorded.

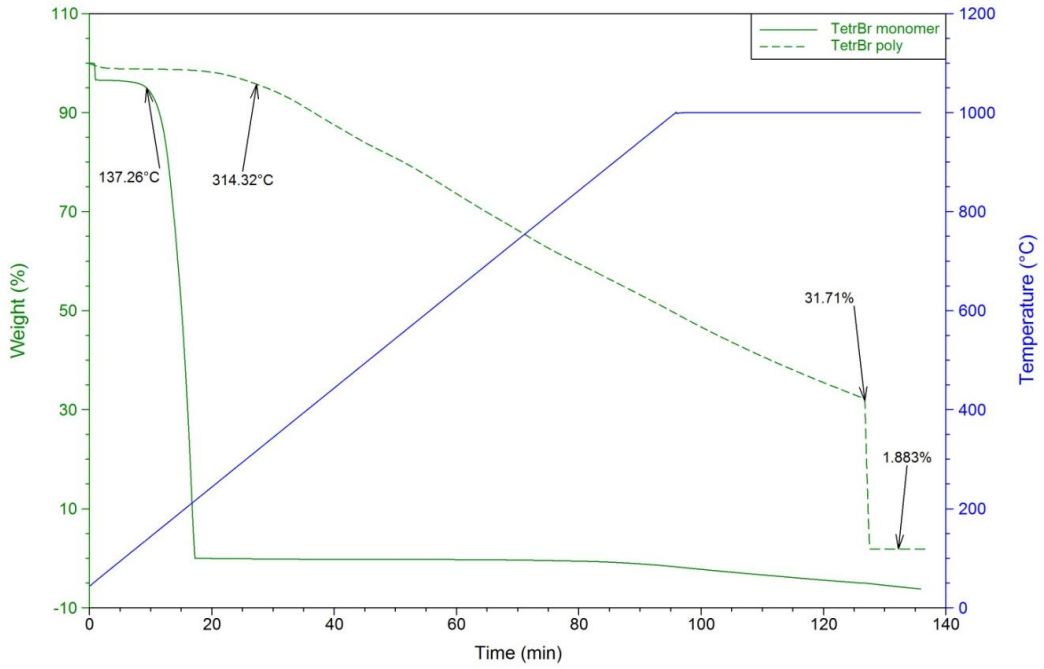

Figure 33: TGA of polyphenylene network synthesised from 1,2,4,5-tetrabromobenzene

The TGA of this network (Figure 33) shows that a stable weight loss from about 310 °C on can be observed for the network (dashed line). This shows that a stable network has formed. The TGA of the monomer was also run (solid line) and comparing the two it can be seen that the network (dashed line) has no remaining monomer within it. The network, as noticed before in the other networks, does not decompose completely under nitrogen. When 1000 °C was reached, under nitrogen, only 70 % of the mass was lost. Only when switching the gas used from nitrogen to air did the network decompose completely, leaving less than 2 % of the initial mass.

The 2 % of mass left is most likely due to left over catalyst, which was trapped in the pores, and could be seen by a light green tinge in the weighing pan, after the TGA was run, which was due to the nickel (II) oxide, which formed during the analysis.

The CHN analysis for this network showed that the network has not formed completely. The theoretical values, for a completely condensed network, would be 97.28 % for the carbon content and 2.72 % for the hydrogen content. The content found by CHN in the material were 81.53 % for carbon and 4.96 % for hydrogen. Additionally a nitrogen content of 2.35 % was detected which could arise from trapped nitrogen after the gas sorption measurements or trapped bipridyl which is used in the reaction. Taking the TGA results of left over metal into account the composition of one repeat unit for the material can be calculated as $C_{156}H_{93}Br_3N_4Ni$. The theoretical and experimental still do not match entirely, but are a closer match than for a perfectly formed network.

The amount of hydrogen can be rationalised if it is assumed that hydrodehalogenation[26-28] takes place. This would mean that on average only 2 of the 4 bromines are involved in the reaction which can be rationalised with the relative steric hindrance the monomer experiences, i.e. once a second monomer has reacted at one of the sites, the bromine adjacent to that is not easily accessible by the catalyst and hence cannot react again. However, as hydrodehalogenation is a catalysed reaction[26-28] it has to happen when the network is forming and therefore be in direct competition to the coupling reaction. These are all speculations and cannot be proven at this point. Potentially ssNMR spectroscopy could help solve this.

Figure 34 below shows the reaction scheme for the first cross-coupling Yamamoto reaction in the series. The network was synthesised by the reaction between tetrakis(4-bromophenyl) methane and 1,4-dibromobenzene. A stoichiometric ratio of 1:2 for the two monomers respectively was used to encourage cross-coupling and not only homo-coupling.

Figure 34: reaction scheme for the reaction between tetrakis(4-bromophenyl) methane and 1,4-dibromobenzene

The synthesised material had an apparent BET surface area of 1500 m^2/g. This surface area was significantly lower than for the homo-coupled PAF-1 network, which is an indication that either a cross coupled network had formed or that two individual networks formed and the linear network formed inside the network formed by the tetrahedral monomer, decreasing the surface area.

Looking at the TGA (Figure 35) of the network one can observe that there was no residual monomer in the network. The 1,4-dibromobenzene started to decompose at 70 °C (dashed line) whereas the network started to decompose from 430 °C onwards.

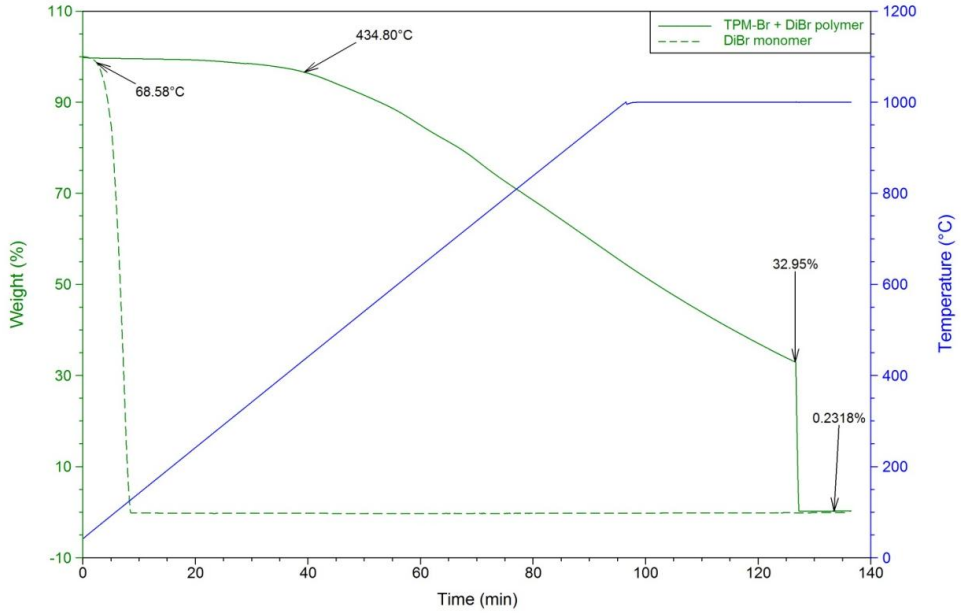

Figure 35: TGA of the polyphenylene network synthesised by cross-coupling reaction of tetrakis(4-bromophenyl) methane and 1,4-dibromobenzene, ramp to 1000 °C at 10 °C/min under N_2, 50 ml/min, switching to oxygen after holding temperature at 1000 °C for 30 minutes

The TGA showed a constant decomposition from about 410 °C for the network, confirming that a stable network was formed. On reaching a temperature of 1000 °C, 67 % of the initial mass was lost. The material decomposed completely when switching from inert conditions to oxygen, leaving 0.2 % of the mass in the pan, which is a negligible amount. This implies that the catalyst was washed out completely on work up and that any missing mass by elemental analysis can be accredited to unreacted bromine end groups.

The CHN analysis gave a carbon content of 90.55 % and a hydrogen content of 5.2 %. A nitrogen content of 0.38 % was also detected. As the amount for metal content from TGA and nitrogen are so low they were not taken in to consideration for the analysis of this material. The actual carbon and hydrogen contents of the material showed that the missing mass for this network is 4.3 %. Assuming that the

missing mass is due to unreacted bromine end groups, one can calculate that on average, two bromine end groups per repeating unit of the network are present. A plausible repeating unit consists of seven tetrahedral monomers and nineteen 2D monomers.

Figure 36 below shows the reaction scheme for the synthesis of a polyphenylene network from the cross coupling reaction between tetrakis(4-bromophenyl) benzene with 1,3,5-tribromobenzene.

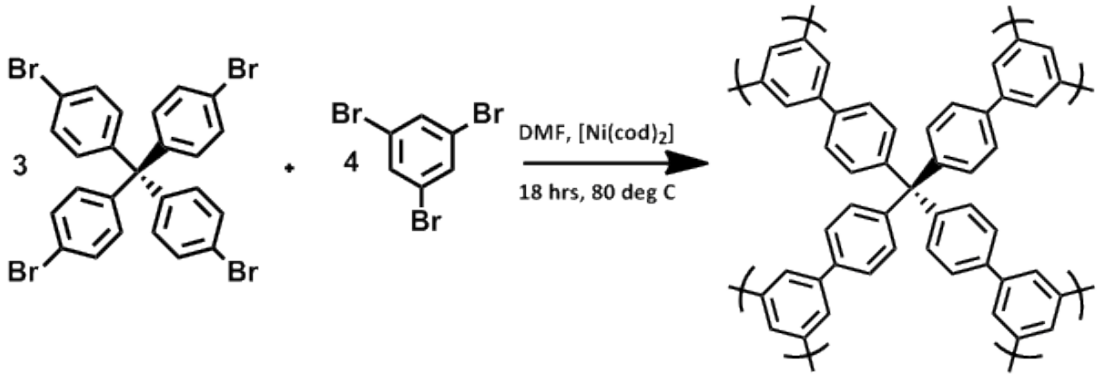

Figure 36: reaction scheme for the reaction between tetrakis(4-bromophenyl) methane and 1,3,5-tribromobenzene

This network exhibited a BET surface area of 1790 m^2/g. This surface area is slightly higher than that for the cross-coupled network between tetrakis(4-bromophenyl) methane and 1,4-dibromobenzene above. Although the surface area is higher than for the previous cross-coupled network it is apparent from looking at the TGA data (Figure 37) that the network has not formed efficiently. One can identify several steps in the TGA.

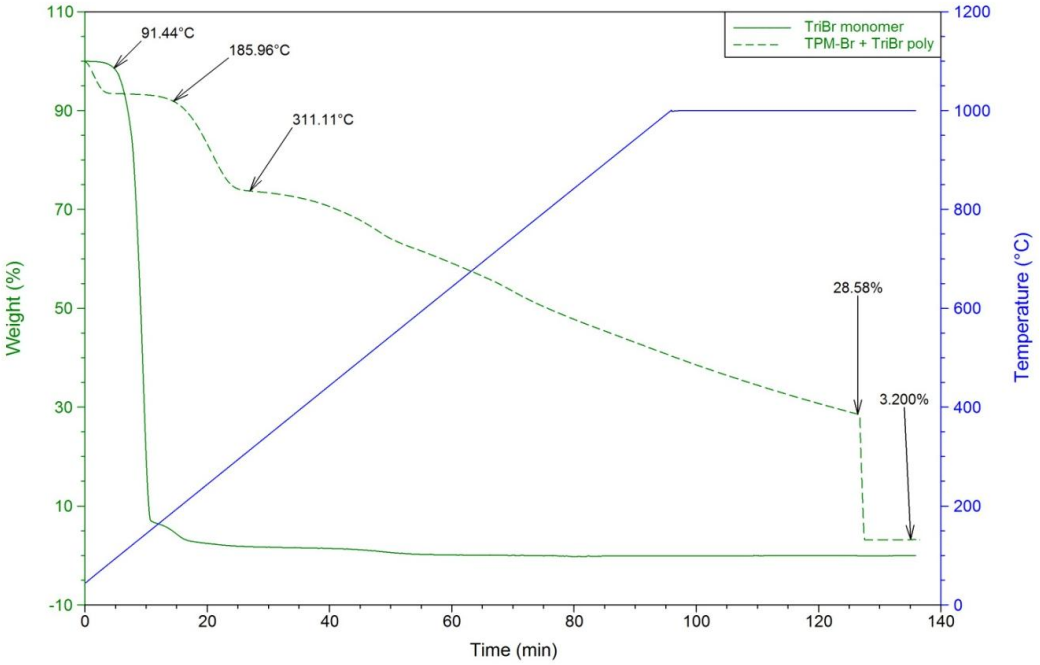

Figure 37: TGA of the polyphenylene network synthesised by cross-coupling reaction of tetrakis(4-bromophenyl) methane and 1,3,5-tribromobenzene, ramp to 1000 °C at 10 °C/min under N_2, 50 ml/min, switching to compressed air after holding temperature at 1000 °C for 30 minutes

The initial weight loss of 6 % until up to 75 °C can be assigned to solvent trapped in the system. Potential impurities in the network were extracted with methanol and the first step in the TGA can therefore be assigned to trapped methanol in the material due to insufficient drying. The next weight loss step was observed from about 180 °C, resulting in a weight loss of a further 19 %. This weight loss is most likely due to unreacted 1,3,5-tribromobenzene which is trapped in the network and hence has a higher decomposition temperature than if the monomer is analysed on its own (solid line).[30] The network started to decompose steadily from about 310 °C onwards. After switching from inert conditions to air, the network 'burns' almost completely, creating a residual mass of 3 %, which can be explained if taken into account that trapped nickel is present in the network.

When overlaying the TGA data for the network with the previous homo-coupled network formed from 1,3,5-tribromobenzene and tetrahedral monomer (Figure 38), one can see that the synthesised network was a mixed network. The decomposition of the cross-coupled network occurs slightly early than either of the homo-coupled networks. The PAF-1 type network synthesised from the tetrahedral monomer forms the most stable network with a decomposition temperature of 400 °C. The homo-coupled network formed by the homo-coupling of tribromobenzene with itself had a decomposition temperature of 340 °C. The cross-coupled network synthesised here started to decompose from 280 °C onwards.

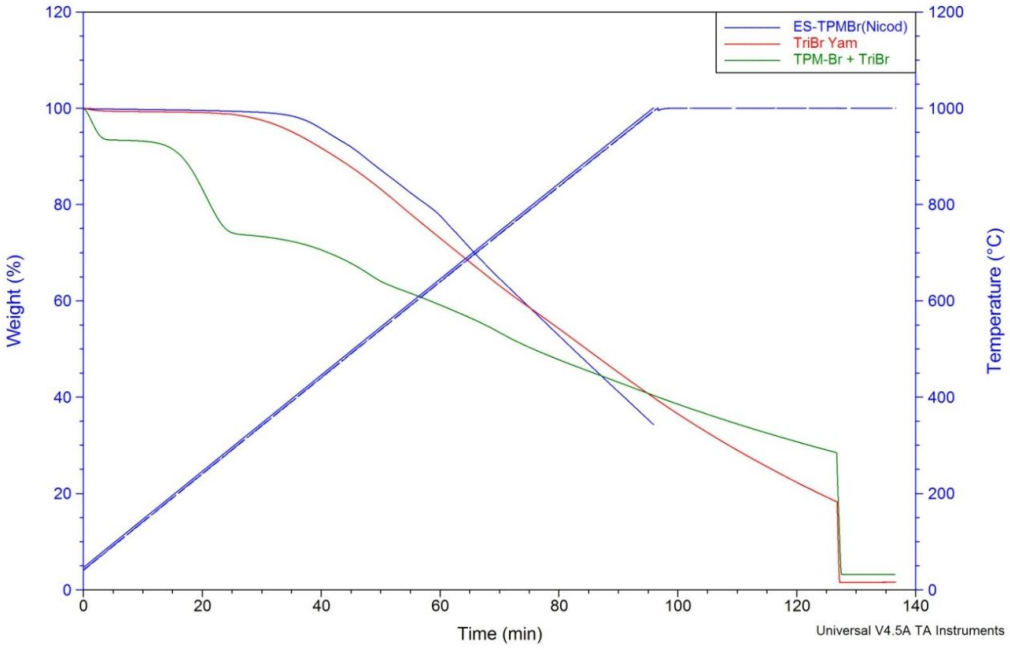

Figure 38: overlay of TGA data for homo-coupled and cross-coupled networks, homo-coupled TPM-Br blue, homo-coupled tribromobenzene red, cross-coupled network green

Figure 39 below shows the reaction scheme for the formation of the polyphenylene network from the cross-coupling reaction between TPM-Br and tetrabromobenzene. The network was found to have an apparent BET surface area

of 1780 m^2/g. The surface area is comparable to the previous cross-coupled network. As the 2D monomer is more sterically hindered than the tri- or di-substituted 2D monomer, it is not expected to form a completely condensed network with the tetrahedral monomer.

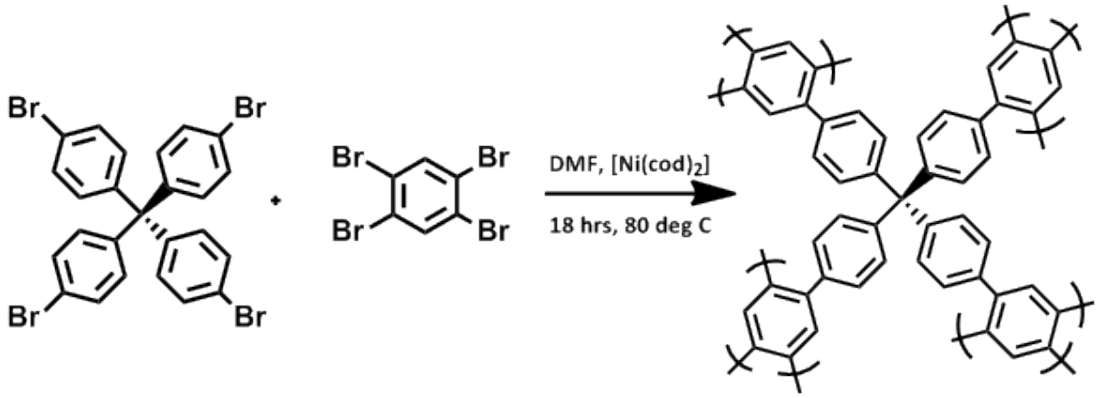

Figure 39: reaction scheme for the reaction between tetrakis(4-bromophenyl)methane and 1,2,4,5-tetrabromobenzene

Considering the TGA (Figure 40) for this material, it was observed that no additional decomposition steps for remaining monomers were present. We can therefore assume that the network has formed as predicted and has a decomposition temperature of approximately 285 °C. On reaching a temperature of 1000 °C, approximately 37 % of weight had been lost by the network, showing the high thermal stability of the network. On holding the temperature at 1000 °C for a further 30 minutes, a further 15 % of weight was lost. Only when switching from inert conditions to air did the network decompose completely, leaving 0.6 % of weight behind. The 0.6 wt% can be assigned to trapped metal in the material, which would not burn away on heating in air.

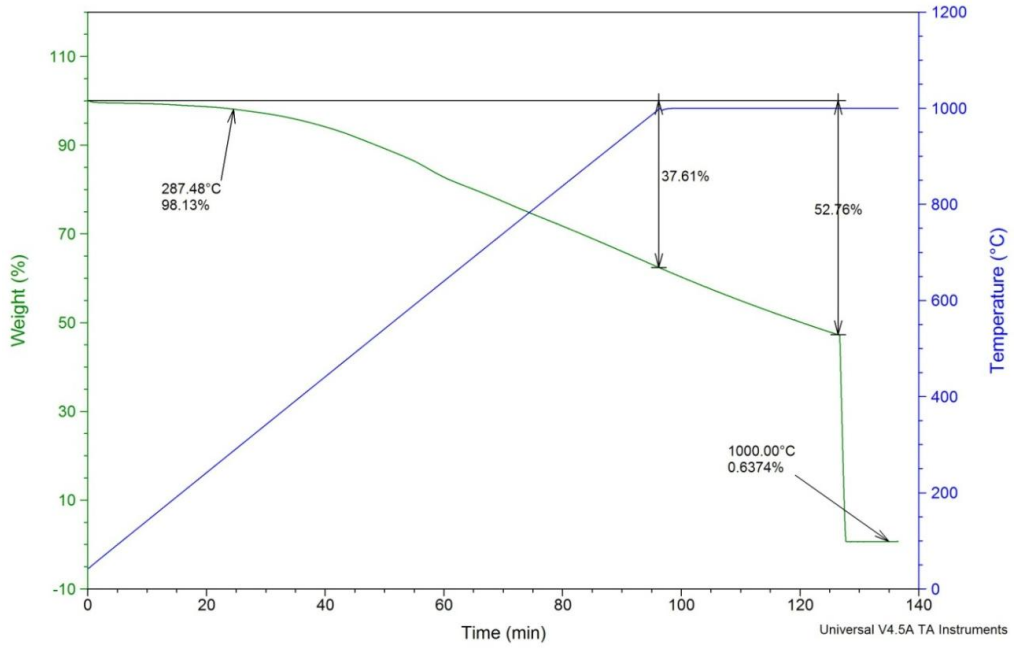

Figure 40: TGA of the polyphenylene network synthesised by cross-coupling reaction of tetrakis(4-bromophenyl) methane and 1,2,4,5-tetrabromobenzene, ramp to 1000 °C at 10 °C/min under N_2, 50 ml/min, switching to compressed air after holding temperature at 1000 °C for 30 minutes

When overlaying the TGA (Figure 41) data for the cross-coupled and the two homo-coupled networks, one can observe that the thermal stability of the cross-coupled (red line) network is initially comparable with the thermal stability of the 3D homo-coupled network (blue line). However, the cross-coupled network (red) had a slower decomposition than the homo-coupled 3D network (blue). The decomposition of the homo-coupled 2D material (green) occurred at a similar rate to the cross-coupled network (red), however, started to decompose at a slightly lower temperature.

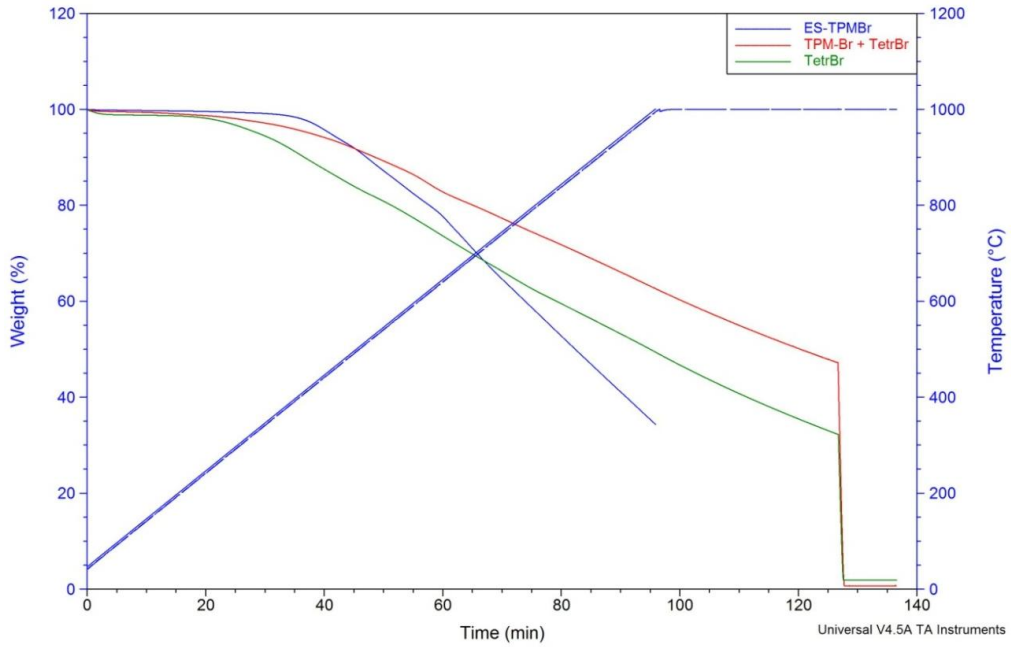

Figure 41: overlay of TGA data for homo-coupled TPMBr network (blue), homo-coupled tetra-functional benzene network (green) and cross-coupled network

Considering the CHN analysis for this network the theoretical contents of carbon and hydrogen were 96.05 % and 3.95 % respectively. Analysis showed that 87.62 % of carbon was present, as well as 5.08 % of hydrogen and 0.88 % of nitrogen. The hydrogen content is too high and the carbon content is too low based on the expected values. Again, the nitrogen content can be explained by trapped nitrogen from the gas sorption measurements or from bipyridyl used in the reaction. A missing mass of 6.42 % can be calculated which would be due to unreacted bromine end groups. When looking at the network which could have formed, it becomes clear that the network could not have coupled at all four positions of the tetrabromobenzene due to steric hindrance.[31] Analysing this conformation of the network shows that the microanalysis almost matches the experimental results found. All values are within a 0.5 % range. From this it

becomes likely that hydrodehalogenation must occur in order for the hydrogen content to be so high.

Figure 42 below shows the reaction scheme for the synthesis of a polyphenylene network from tetrakis(4-bromophenyl) adamantane and dibromobenzene. The network exhibits an apparent BET surface area of 2700 m^2/g. This surface area is approximately 1000 m^2/g lower than for the homo-coupled adamantane network. Based on the CMP work carried out previously in our labs, it was not surprising that with an increasing strut length the surface area decreases.[32]

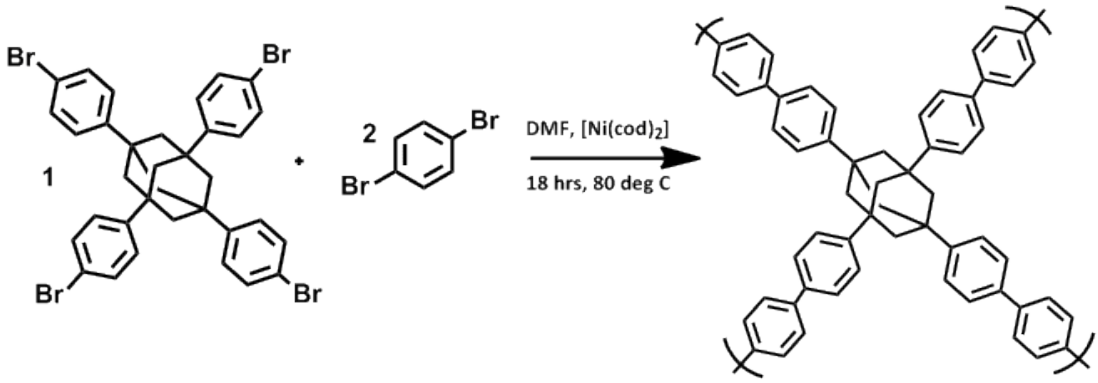

Figure 42: reaction scheme for the reaction between 1,3,5,7-tetrakis(4-bromophenyl) adamantane and 1,4-dibromobenzene

Looking at the TGA data (Figure 43) for this material one can observe a step-wise decomposition as seen before in the material synthesised from tetrakis(4-bromophenyl) methane and 1,4-dibromobenzene (Figure 46) . The initial weight loss of 2 % can be accounted for by the presence of methanol again from the extraction step. The next step, where a further 4.5 % of weight is lost, can be attributed to some unreacted 1,4-dibromobenzene monomer, which was trapped in the pores of the material. The decomposition of the network started from about 440 °C onwards, initially losing a further 20 % of weight and then gradually coming to a

total weight loss of 45 % when reaching 1000 °C. A further weight loss of 10 % was observed when holding the temperature at 1000 °C for 30 minutes. As seen before, the material decomposed completely when switching from inert conditions to a flow of air.

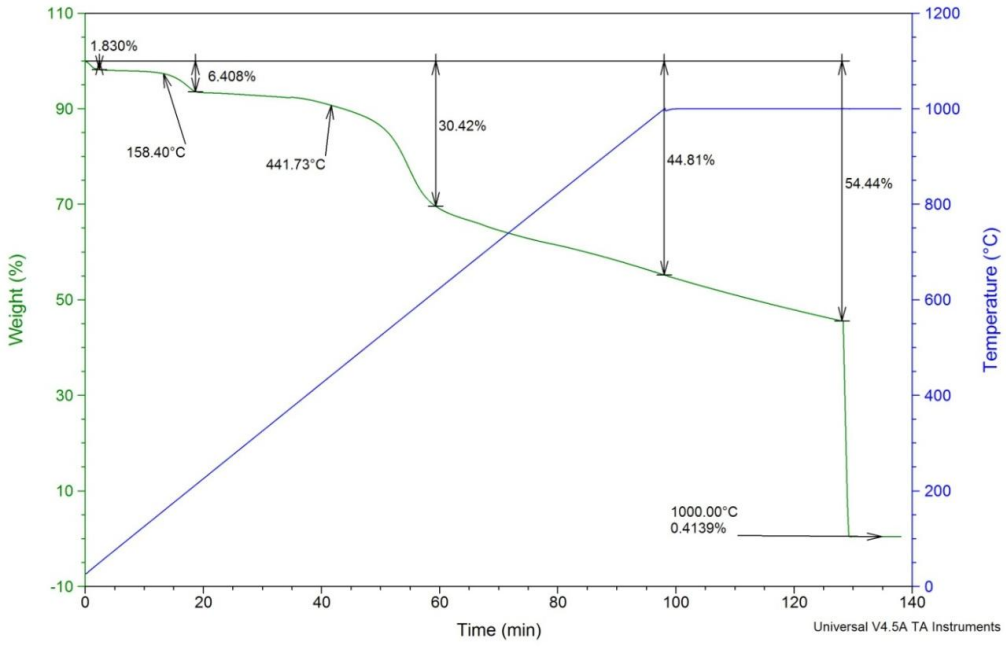

Figure 43: TGA of the polyphenylene network synthesised by cross-coupling reaction of tetrakis(4-bromophenyl) adamantane and 1,4-dibromobenzene, ramp to 1000 °C at 10 °C/min under N_2, 50 ml/min, switching to compressed air after holding temperature at 1000 °C for 30 minutes

The microanalysis for this material resulted in a carbon and hydrogen content of 87.39 % and 6.05 % respectively. A 0.72 % content of nitrogen was also detected. The theoretical values for carbon and hydrogen content were calculated to be 94.01 % and 5.99 %. A missing mass of 5.84 % can be calculated from this, which is most likely due to unreacted bromine end groups. This would translate to two bromine end groups per every four repeating units with only a very small amount of hydrodehalogenation occurring compared to the previous networks. Again, the nitrogen might be accounted for by trapped nitrogen in the material

after gas sorption measurements, as the materials are not additionally evacuated post-measurement.

Figure 44 below shows the reaction scheme for the cross coupling reaction of TPA-Br and tribromobenzene. The network formed was found to have an apparent BET surface area of 3300 m^2/g. This surface area is only 400 m^2/g lower than the surface area of the homo-coupled TPA network and approx 600 m^2/g higher than for the cross-coupled network of tetrakis(4-bromophenyl) methane with 1,4-dibromobenzene. The porosity and gas sorption of these networks will be discussed in Chapter 5.

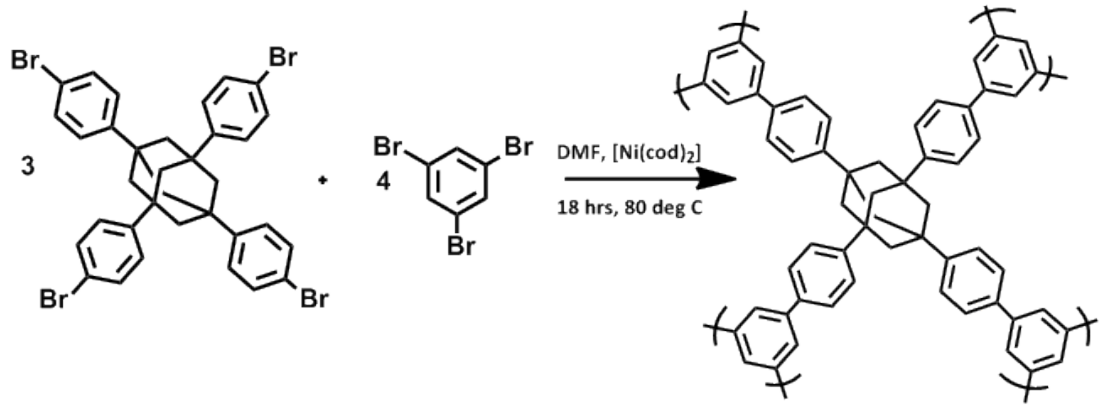

Figure 44: reaction scheme for the reaction between tetrakis(4-bromphenyl) adamantane and 1,3,5-tribromobenzene

Looking at the TGA data for this material (Figure 45) one can observe some steps in the decomposition of the network, as seen before. There was no initial weight loss at low temperatures indicating an absence of trapped solvent. The first step of decomposition can be observed form 150 °C onwards with a weight loss of 8 %. This can assigned to some trapped 1,3,5-tribromobenzene in the network. The decomposition of the network starts at 420 °C, initially losing 18 % of weight and

then a further 30 % before reaching the target temperature of 1000 °C. On holding the temperature for a further 30 minutes, an additional 20 % of weight was lost before switching from inert conditions to air and total decomposition of the material. A negligible amount of remaining mass is present after total decomposition, indicating that a small amount of catalyst remained in the network.

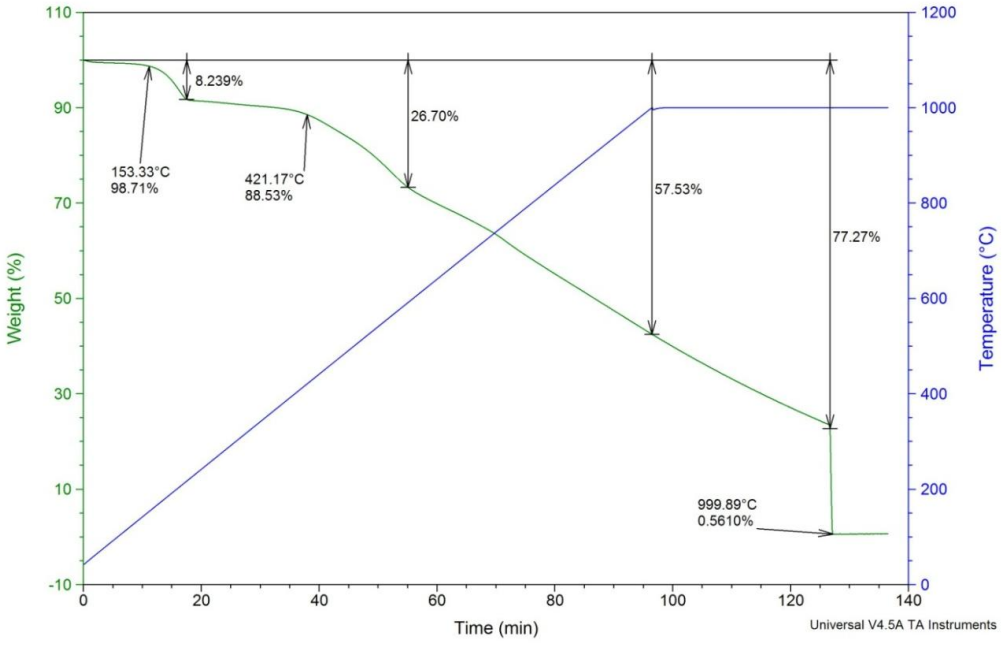

Figure 45: TGA of the polyphenylene network synthesised by cross-coupling reaction of tetrakis(4-bromophenyl) adamantane and 1,3,5-tribromobenzene, ramp to 1000 °C at 10 °C/min under N_2, 50 ml/min, switching to compressed air after holding temperature at 1000 °C for 30 minutes

From looking at the TGA data one can assume that the network has formed as suspected or in a similar way, without large amounts of unreacted monomers present. The TGA data however, does not show if the network is highly condensed or not. It can only be said that the network has a high thermal stability with a weight loss of 55 % when reaching 1000 °C.

The CHN analysis gave measurements for carbon and hydrogen content of 68.35 % and 6.85 % respectively. A nitrogen content of 3.71 % was also detected. In

theory, 94.55 % of carbon content should have been measured and 5.47 % of hydrogen. The large deviation between the experimental and the calculated content of carbon and nitrogen can be explained if assuming that unreacted bromine end groups are present within a repeating unit and hydrodehalogenation occurs. The missing mass of 21.09 % was assigned to unreacted bromine end groups. This means that eight unreacted bromines are present per repeating unit, meaning that this network has a very low polycondensation and therefore does most likely not exhibit its highest surface area. A repeating unit consists of four tetrahedral units and six tri-functional benzene units. The amount of unreacted bromines and hydrodehalogenation also means that this network is most likely not microporous anymore. Gas sorption properties and porosity will be discussed in Chapter 5.

Figure 46 below shows the reaction scheme for the final cross-coupling reaction in this series. The network was synthesised by coupling of 1,3,5,7-tetrakis(4-bromophenyl) adamantane and 1,2,4,5-tetrabromobenzene, applying Yamamoto coupling conditions. This network had an apparent BET surface area of 1800 m^2/g. This surface area was significantly lower than the surface are of the two previous adamantane cross-coupled networks and the adamantane homo-coupled network. This trend is opposite to the carbon centred cross-coupled networks. In the carbon-centred cross-coupled reactions, the network formed with the tetrabromobenzene showed the highest surface area of the three cross-coupling reactions.

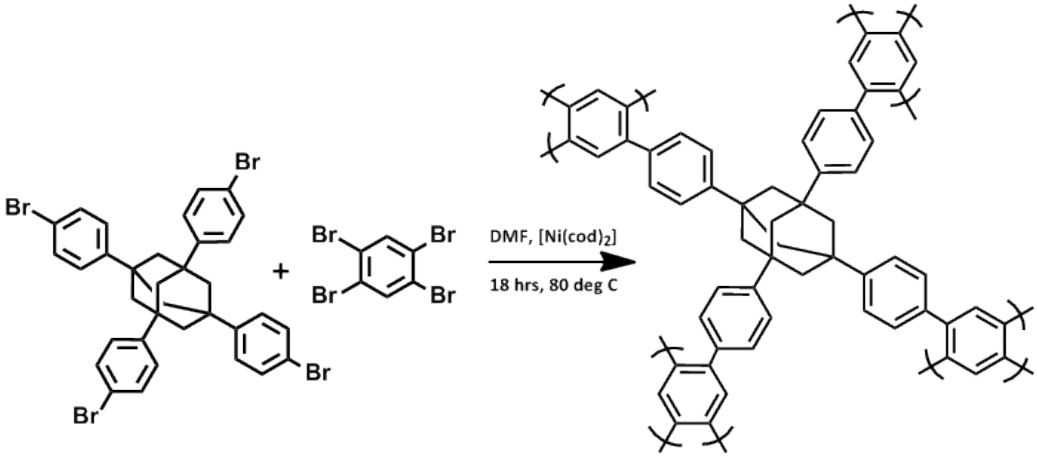

Figure 46: reaction scheme for the reaction between TPA-Br and TetBrB

Looking at the TGA data for this network (Figure 47) a decomposition occurring in steps was observed. The initial weight loss at 150 °C of 6 % was assigned to remaining tetrabromobenzene monomer in the network. The decomposition of the network started from about 380 °C onwards, losing initially 30 % of the total mass. A very small step was observed in the decomposition here, with a change in rate of decomposition from about 700 °C again. This network seems to decompose almost completely on reaching the maximum temperature of 1000 °C, losing 90 % of the total mass. This suggest that the network is not a network but perhaps only an oligomer. The oligomer decomposes almost completely before switching from inert conditions to air. The weight increase after switching to air can be explained by oxidation of the remaining catalyst. Although this has not been observed before, this is the only explanation for a weight increase after switching to air.

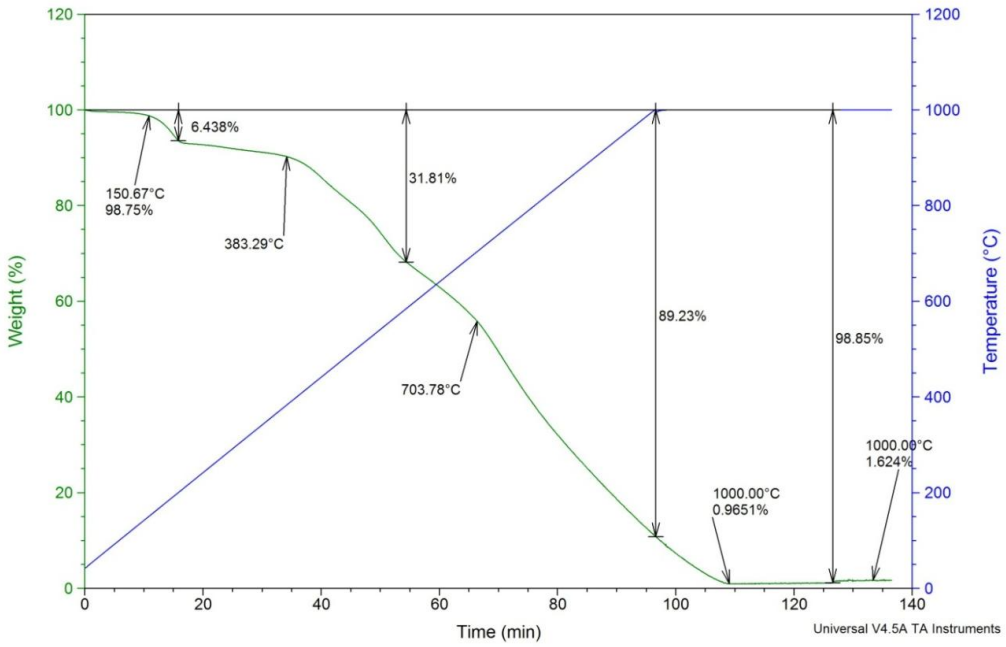

Figure 47: TGA of the polyphenylene network synthesised by cross-coupling reaction of tetrakis(4-bromophenyl) adamantane and 1,2,4,5-tetrabromobenzene, ramp to 1000 °C at 10 °C/min under N_2, 50 ml/min, switching to compressed air after holding temperature at 1000 °C for 30 minutes

Analysing the CHN data for this network confirmed that an oligomer was formed rather than a network. The carbon and hydrogen content were measured to be 79.72 % and 5.95 % respectively. A nitrogen content of 2.01 % was also detected. The theoretical values for a completely condensed network are 95.05 % for carbon and 4.95 % for hydrogen. The missing mass of 12.32 % was assigned to unreacted bromine end groups. Taking these values into account, an oligomer consisting of three adamantane units and three tetra-functional benzene units, can be constructed giving similar theoretical values for the CHN analysis as the actual measured values. This is the first time an 'oligomer' formation rather than a network formation could be observed for this type of chemistry.

3.3 Conclusion

In conclusion, although the high surface area of 5600 m^2/g as published by Ben *et.al.*[10] could not be achieved or increased further, a range of interesting networks was synthesised with very high surface areas and high thermal stabilities. Indeed, several of these materials are more porous than 95 % + of structures in the literature, and the solids have very good thermal stability. The cross-coupling reactions in particular are interesting as they form novel networks with high surface areas. Unfortunately at this moment we cannot confirm 100 % if the networks cross-couple in the proposed manner. Further investigation into this is necessary, possibly by solid state NMR spectroscopy. With materials such as the ones discussed here, it is difficult to determine the exact structure even when solid state NMR spectroscopy, CHN analysis, halogen analysis, TGA and gas sorption measurements are all present. The porosity and gas sorption properties of the networks will be discussed in Chapter 5.

3.4 References

[1] Schmidt, J., *et al., Macro.*, **2009**, 42, 4426

[2] Jahveri, S. B., *et al., Chem. Eur. J.*, **2008**, 6845

[3] Murakami, Y., Yamamoto, T., *Macro.*, **2002**, *35*, 1988

[4] Kim, Y.-J., *et al., J. Chem. Soc. Dalton Trans.,* **1994,** 943

[5] Murakami, Y., Yamamoto, T., *Inorg. Chem.*, **1997**, *36*, 5682

[6] Yamamoto, T., Abla, M., *J. Organomet. Chem.,* **1997**, *535*, 209

[7] Zhou, Z.-H., Yamamoto, T., *J. Organomet. Chem.*, **1991,** *414,* 119

[8] Yamamoto, T., *et al., J. Am. Chem. Soc.,* **1994**, *116*, 4832

[9] Yamamoto, T., Wakabayashi, S., Osakada, K., *J. Organomet. Chem.*, **1992,** *428,* 223

[10] Ben, T., *et al., Angew. Chem. Int. Ed.*, **2009**, *48*, 9457

[11] Eddaoudi, M., *et al., Acc. Chem. Res.*, **2001**, 34, 319

[12] Chae, H. K., *et al., Nature,* **2004**, *427*, 523 (MOF-177)

[13] Wong-Foy, A. G., *et al., J. Am. Chem. Soc.,* **2006**, *128*, 3494 (MOF-177, H2)

[14] Millward, A. R., Yaghi, O. M., *J. Am. Chem. Soc.,* **2005**, *127*, 17998 (MOF-177, CO2)

[15] El-Kaderi, H. M, *et al., Science,* **2007**, *316*, 268

[16] Koh, K, Wong-Foy, A. G., Matzger, A. J, *J. Am. Chem. Soc.,* **2009**, *131*, 4184

[17] Pal, M., *et al., Synlet*., **2004**, 1965

[18] Hong, K. B., *et al., Tet*. *Lett*., **2004**, 45, 693

[19] Yao, T., Larock, R. C., *J. Org. Chem*., **2005**, 70, 1432

[20] Yamamoto, T., *et al., J. Orgmet. Chem*., **1992**, 428, 223

[21] Reichert, V. R., Mathias, L. J., *Macro.*, **1994**, *27*, 7015

[22] Rathore, R., *et.al.*, *J.Org.Chem.*, **2004**, 69, 1524

[23] Reichert, V. R., Mathias, L. J., *Macro.,* **1994**, 27, 7015

[24] Stöckel, E., *et al., Chem. Commun.*, **2009**, 212

[25] Yamamoto, T., Wakabayashi, S., Osakada, K., *J. Orgmet. Chem.*, **1992**, 428, 223

[26] Selvam, P., *et al., App. Cat. B: Environ.,* **2004,** 49**,** *251*

[27] Xia, C., *et al*., *Catalysis Communications,* **2004,** 5, 383

[28] Cannon, K. A., *et al., Organomet.*, **2011**, 30 (15), 4067

[29] Zheng, F., *et al., J. Chem. Phys*., **2009**, 130, 204701

[30] Beyler, C. L., Hirschler, M. M., SFPE Handbook 3, Chapter 7, 110 – 131

[31] Weinhold, F., *Nature,* **2001**, 411, 539

[32] Jiang, J., *et al., J. Am. Chem. Soc*., **2008**, *130*, 7710

Chapter 4

Importance of solvent and solvent concentration in Sonogashira cross coupling reactions

4.1 Introduction

In the previous chapters, we discussed attempts at increasing the surface area of CMPs via different coupling reactions and by using tetrahedral monomers in the reactions. During this work, it was also discovered that the solvent has an influence. Dawson *et al.* published their findings on the strong influence of solvents on the surface area of CMPs.[1] That publication discusses the importance of choosing the correct solvent to form high surface area materials.

Based on the results published by Dawson, it was decided to return to the Sonogashira coupling reactions (Chapter 2) to see if a change of solvent as well as the usage of templating agents would improve the surface areas. Templating agents have been used in materials chemistry to 'force' networks to obtain a defined framework.[2] It can be said that the templating agent forms a scaffold for the network to 'grow' around and which can be removed post synthesis.[3] Templating agents are also used to make inherently non-porous materials porous.[4] Low molecular weight polyethyleneglycols (PEGs) were evaluated as templating agents in this work. PEGs are commonly used to increase the porosity of materials with low or no porosity.[5-7] The advantage being that monomers can be in a orientation to one another which is favourable for the coupling reaction, meaning that the network 'grows' in a more ordered fashion, causing a higher degree of polycondensation. As an alternative, 'bulky' solvents can also be used instead of PEG. A bulky solvent acts like a templating agent, but has the advantage that it can be used as a solvent at the same time.[1, 8-10] In the case of PAF-1, for example,[11] DMF is used as the solvent which can improve surface area by improved dilution of the monomers as discussed by Dawson[1] before and has shown to act as a template.[12]

When using DMF as a solvent for the Sonogashira coupling reaction, it was observed that an increased surface area could be measured.[1] In some cases formerly non-porous materials or materials with low surface areas, became porous with surface areas of up to 1200 m^2/g.[1]

In this Chapter, a series of reaction are discussed where various ratios of solvent to template were investigated. The templating agent used was polyethylene glycol (PEG) with an average molecular weight of 300 g/mol or 500 g/mol (PEG300 or PEG500 respectively). The aim of this work was to increase the surface area of previously discussed Sonogashira networks (Chapter 2) from 1200 m^2/g.

4.2 Results and Discussion

The following figures show the reactions carried out applying Sonogashira coupling reactions with DMF as solvent and PEG as templating agent. The networks are the same networks synthesised previously by this route (Chapter 2). A direct comparison of surface areas can therefore be drawn. An indication of the different reactivity in the different solvent systems and of the degrees of polycondensation of the networks formed can also be drawn, as only the solvent system has been changed. A complete comparison between the networks discussed in Chapter 2 and in this chapter can be made.

4.2.1 Influence of templating agents on the surface area of the E-1 network

Following the findings of Dawson *et al.,* it was decided to repeat the previously synthesised tetrahedral CMP networks by Sonogashira coupling reactions. Figure 48 shows the first of these reactions.

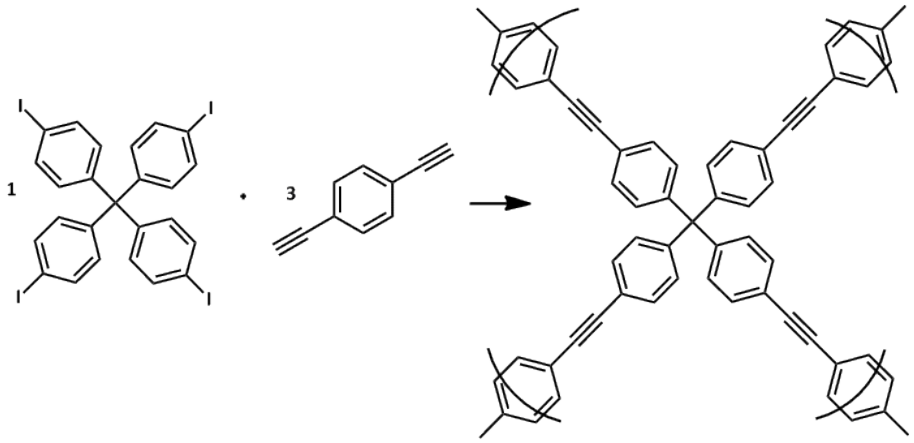

Figure 48: reaction scheme for the synthesis of E-1 network by Sonogashira cross-coupling reaction between tetrakis(4-iodophenyl) methane and 1,4-diethynylbenzene

The network was formed by the palladium catalysed Sonogashira coupling reaction of tetrakis(4-iodophenyl) methane and 1,4-diethynylbenzene in a 1 to 1.5 functional group ratio. The 1 to 1.5 functional group ratio of halogen to ethyl group was shown to minimise homo-coupling and hence maximise cross-coupling by Jiang.[13] PEG300 was chosen as the templating agent for this set of reactions. Different ratios between PEG and DMF were applied to see if the solvent (DMF) or the template (PEG300) has a bigger influence on the surface area. Table 1 shows the results for this set of reactions. The original network, called E-1, was synthesised in toluene with diisopropylamine as the base (see Experimental Chapter for full details and Chapter 2 for previous discussions) and had an apparent BET surface area of 1200 m^2/g. The reactions discussed here were carried out under the hypothesis that the surface area would increase if the better solvent, DMF, was used. It was also hypothesised that the use of a bulky templating agent might have a positive influence on the surface area,[14] i.e. increase the surface area from the previously published 1200 m^2/g.[15]

Looking at the results presented in Table 1, we can see that changing the solvent to DMF did not increase the surface area. In fact, the surface area for this reaction was slightly reduced to 1127 m^2/g. Across all results, only a 75 / 25 mixture of DMF and PEG300 gave a small increase in surface area to 1330 m^2/g from a former 1200 m^2/g. The maximum error bar usually considered for surface area measurements is ± 100 m^2/g[16] and the error usually is smaller than this. The increase is in surface area for the 75 / 25 mix of DMF and PEG300 is therefore (just) outside this error bar, and considered to be a true increase in surface area.

Table 8: composition of E-1 synthesis with additional templating agent, surface area calculated from BET model, colours respond to colouring in TGA data

	DMF (mL)	PEG300 (mL)	Surface Area (m^2/g)
original E1			1213 [15]
E1-DMF	5	0	1130
E1-DMF/PEG300 (75/25)	3.75	1.25	1330
E1-DMF/PEG300 (50/50)	2.5	2.5	1100
E1-DMF/PEG300 (25/75)	1.25	3.75	820
E1-DMF/PEG300 (10/90)	1	4	1050
E1-PEG300	0	5	880

Since the reaction carried out exclusively in DMF did not give an increase in surface area, it can be assumed that the increase in the surface area in the 75 / 25 mix of DMF / PEG300 is due to the templating agent PEG300, and not due to the change in solvent. DMF and PEG300 were completely miscible.

Looking at the TGA data for this set of reactions (Figure 49), it can be seen that the materials again had a high thermal stability. The networks started to decompose from about 400 °C onwards, apart from the material synthesised in 100 % PEG300, which started to decompose from 330 °C onwards. The network synthesised in DMF only (green) gave rise to the highest thermal stability, losing only 30 % of its mass when heating to 1000 °C under inert conditions. The next most thermally stable network was the network synthesised in 75/25 DMF/PEG. It lost 50 % of its mass under inert conditions. The network synthesised with 10/90 DMF/PEG300 lost 80 % of its mass when heated to 1000 °C under inert conditions, making it still reasonably thermally stable. The other three networks, synthesised in 50/50, 0/100, and 25/75 DMF/PEG300, were the least thermally stable networks. They decompose almost completely, losing approximately 94 % of their mass.

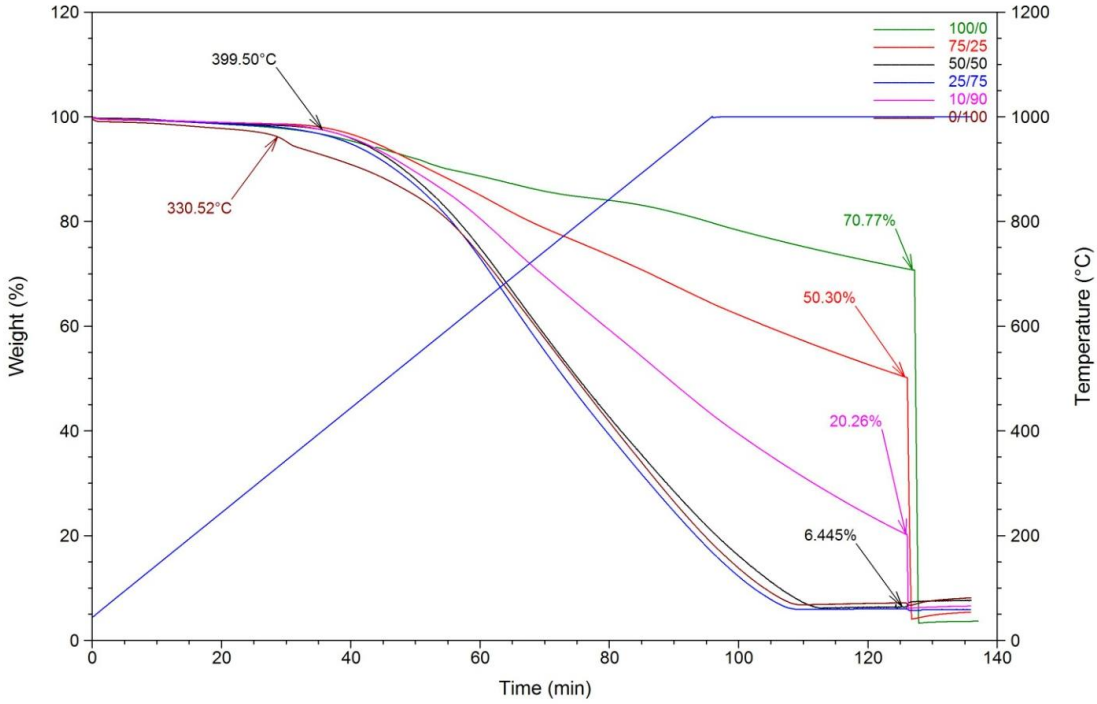

Figure 49: TGA data for E-1 network synthesied with PEG300 as templating agent, heating rate of 10 °C per minute till 1000 °C, holding at temperature for 30 minutes, all under nitrogen, switching to air after 30 minutes and holding for a further 10 minutes

In general, the materials with the surface areas above 1000 m^2/g are somewhat more thermally stable than the ones with surface areas below 1000 m^2/g.

From the TGA data for these networks (Figure 49), it can be seen that no remaining PEG300 is present in the networks. If some PEG were present, a step before 200 °C would have been observed where the PEG would have decomposed, as PEG300 has a boiling point above 200 °C. As such a step is not present, it can be confirmed that all of the PEG was washed out in the extraction step (see Experimental Chapter for details).

Further confirmation of the absence of PEG was given by infrared (IR) spectroscopy for the networks (Figure 50). The IR spectra confirm that no vibrations attributed with PEG were present. PEG would give rise to vibrations at 2900, 1500,

1300, 1250 and 1100 cm^{-1} (see Appendix for IR spectra of PEG400 taken from Sigma Aldrich), and the most significant of these vibrations being the vibration occurring at 2900 cm^{-1}. The vibrations at lower cm^{-1} would overlap with vibrations from the network itself.

From the IR spectrum (Figure 50) it can be observed that all networks are very similar. They all show the same vibrations, although intensities are different, which is due to the loading of the samples. The IR is run in transmission mode using a high throughput method and not KBr discs. It can be observed that only a small vibration at 2900 cm^{-1} was present. If PEG were still present in the samples, the vibration would be stronger. This vibration is therefore due to the aromatic units in the network and not due to PEG trapped in the network. The materials therefore had essentially no remaining PEG300 trapped in the pores.

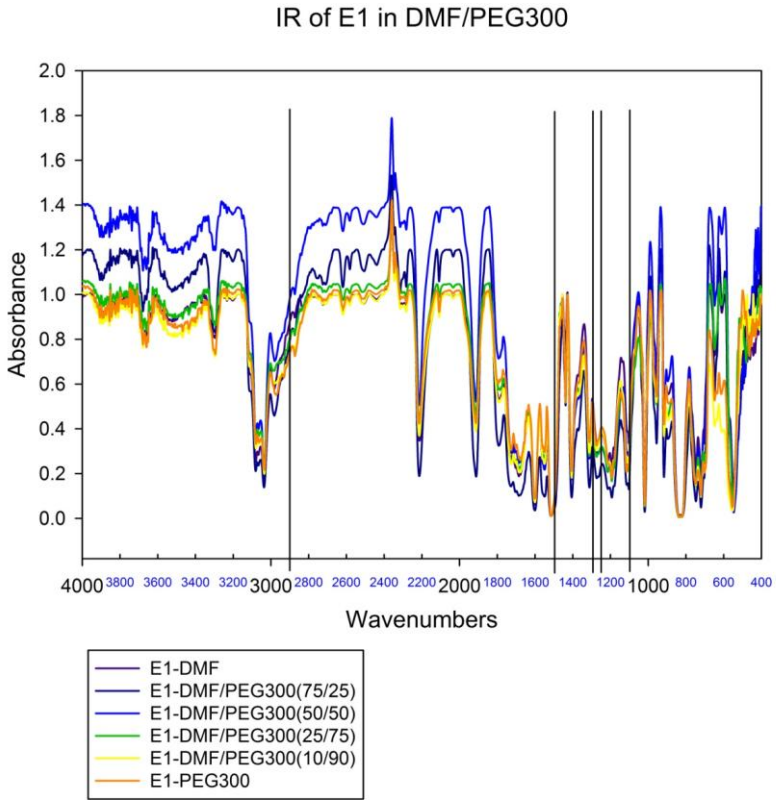

Figure 50: IR of E-1 network synthesised with PEG300 as template, showing that no PEG is present, black lines represent characteristic PEG300 vibrations

As PEG300 did not influence the surface area greatly, it was decided to repeat the reactions and increase the molecular weight of the template. By increasing the molecular weight it was hypothesised that the particle size of the PEG in solvent would be increased.[17] PEG550 was the new chosen templating agent.

Table 9 below shows the results for the surface area measurements carried out on these samples. As can be seen, the surface area was increased slightly in the majority of samples to an average of 1325 m^2/g. The highest surface was achieved when carrying out the reaction in a 75/25 mix of DMF/PEG550, reaching 1350 m^2/g. Although this is a relatively small increase in surface area, it shows that the surface area can be increased through tuning the parameters of the reaction by introducing a templating agent. We believe that the consistent rise in surface area across these samples validate our templating concept.

Table 9: composition of E-1 synthesis with additional templating agent PEG550, surface area calculated from BET model, colours respond to colouring in TGA data

	DMF (mL)	PEG550 (mL)	Surface Area (m^2/g)
original E1			1213 [15]
E1-DMF/PEG 550 (90/10)	4	1	1328
E1-DMF/PEG 550 (75/25)	3.75	1.25	1348
E1-DMF/PEG 550 (50/50)	2.5	2.5	1314
E1-DMF/PEG 550 (25/75)	1.25	3.75	1300
E1-DMF/PEG 550 (10/90)	1	4	1115
E1-PEG 550	0	5	1208

The lowest surface areas for this set of reactions occurred, when using high concentrations of PEG, i.e. when using 90 % of PEG in the solvent mixture the surface area is decreased. The decrease was, however, not as significant as when using PEG300 as the template, thus showing that the higher molecular weight PEG had a generally positive influence on the surface area. This means that when using

the higher molecular weight PEG as a template, the surface area was not decreased as far as for the same reaction when using PEG300.

Comparing the highest surface areas for both sets of templating attempts, it can be seen that the surface area in both cases was highest when using a 75/25 mixture of DMF and PEG. When using PEG300 (Table 8), the surface area was 1330 m^2/g and, when using PEG550 (Table 9), the surface area was 1348 m^2/g. The very similar surface areas indicate that the materials are comparable. It shows that, even when changing the template, the networks are formed in the same way.

Looking at the trends in both series (black lines, Graph 5), it can be observed that with increasing amount of PEG in the reaction the surface area decreases. However, the higher molecular weight PEG, in general, gives rise to higher surface areas in the material than without templating agents in the reaction.

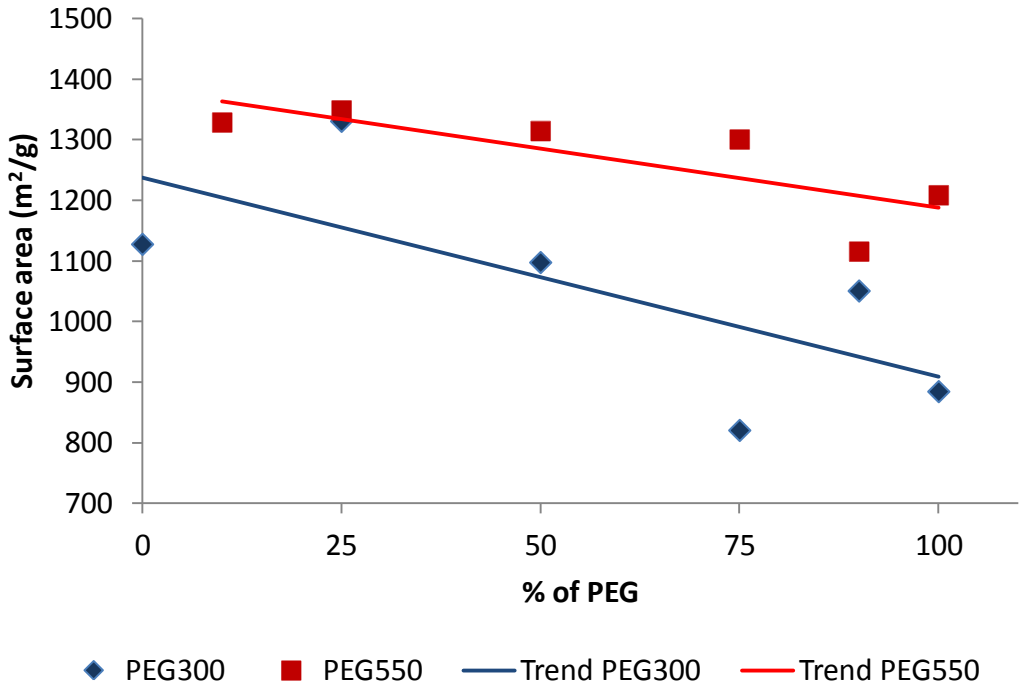

Graph 5: surface area trend (black lines) compared between PEG300 templated and PEG550 templated E-1 networks

The TGA data for this series of samples is presented in Figure 51. All networks were highly thermally stable and only started to decompose from around 370 °C. From the TGA data, it can be observed that the most thermally stable network was the material synthesised in 25/75 DMF/PEG550 (red). At the maximum temperature of 1000 °C, the material still had 66 % of its mass remaining and only decomposed completely when switching to air from inert conditions. The next most thermally stable materials were the networks synthesised in 50/50 DMF/PEG (black) showing a weight loss of 45 %. The two networks having a remaining mass of 47 % and 43 % were synthesised in 25/75 (blue) and 10/90 (pink) DMF/PEG. The two networks with the least thermal stability had a remaining mass of 20 % and 15 % and were synthesised in 0/100 (maroon) and 90/10 (green) DMF/PEG respectively. All networks decomposed completely when switching from inert conditions to air, with remaining masses between 6 % and 2.5 %, which can be accounted for by remaining catalyst in the networks.

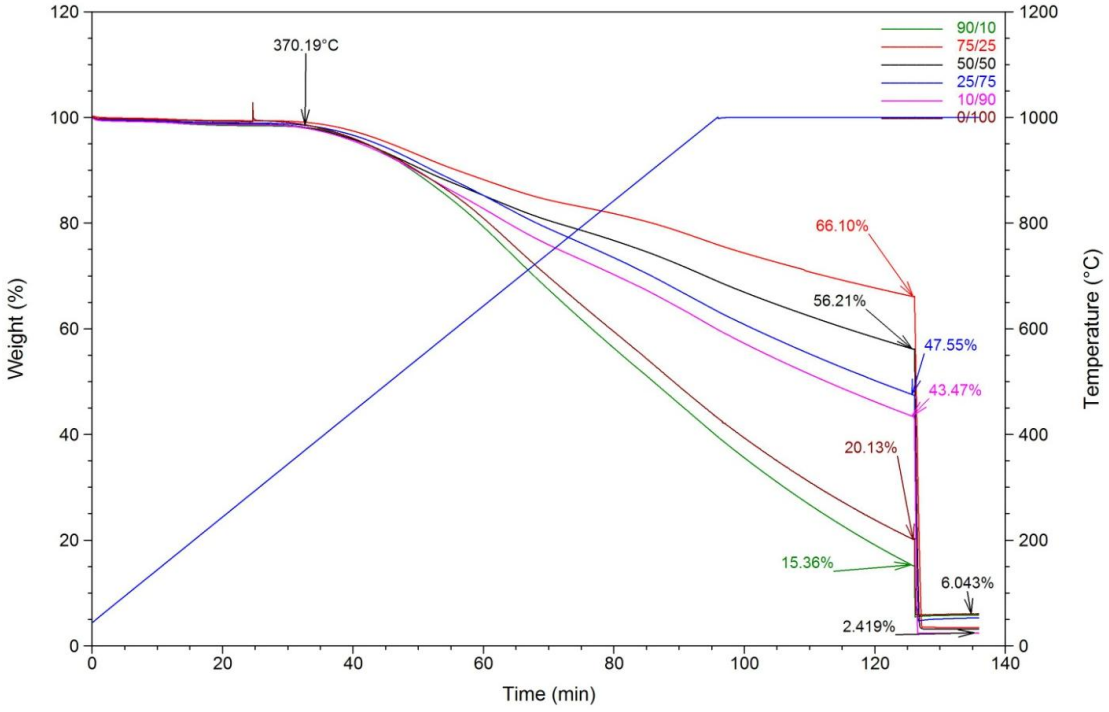

Figure 51: TGA data for E-1 network synthesied with PEG550 as templating agent, heating rate of 10 °C per minute till 1000 °C, holding at temperature for 30 minutes, all under nitrogen, switching to air after 30 minutes and holding for a further 10 minutes

Comparing the IR spectra for the networks synthesised here (Figure 52) it can be seen that no PEG550 is detectable in the network. As before, the characteristic vibration for PEG at 2900 cm^{-1} was not present. It would be expected to be a strong signal if significant amounts of PEG remained in the networks. In this case, it was only a weak signal, and can therefore, be assigned to the aromatic stretching which occurs in the network itself.

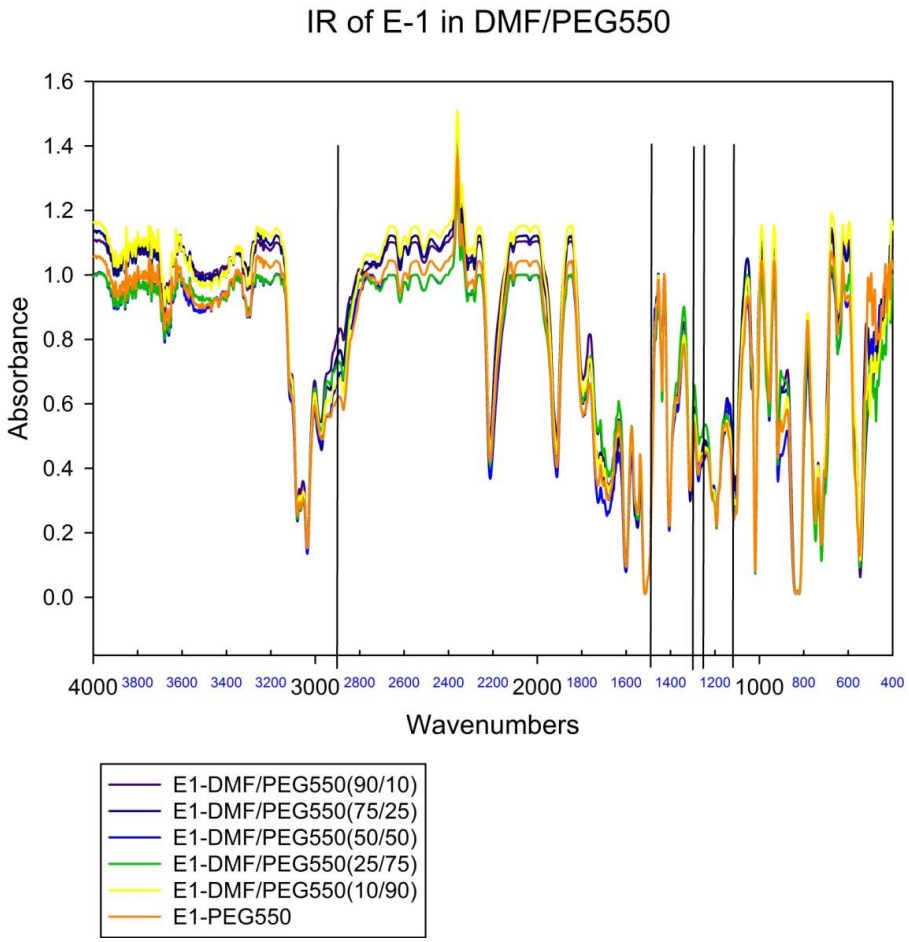

Figure 52: IR of E-1 network synthesised with PEG550 as template, showing that no PEG is present, black lines represent characteristic PEG vibrations

The IR spectra (Figure 52) also show us that, as before, all networks are very similar, with the same IR vibrations, showing that the synthesis of these networks is reproducible even when changing the solvent system or introducing templating agents.

4.2.2 Solvent concentration effect on the surface area of the E-1 network

Based on the results from the templating series with PEG300 and PEG550 and on the fact that previous reactions for the Yamamoto coupling reactions (Chapter 3) are carried out at lower concentrations than the Sonogashira coupling reactions, a concentration study in DMF and DMF / PEG550 mixtures was carried out.

First, the effect of the concentration of the reaction was examined for the already well-established network, E-1 (Figure 48). The molar ratios of the reagents were kept the same (see Experimental Chapter for details) including the amount of base.

Table 10 below shows the results and solvent concentration for the first series. The original surface area for the E-1 network synthesised at 'high' concentration in toluene was 1200 m^2/g. Looking at the results when only DMF was used as the solvent and the concentration was lowered, it can be seen that the surface area did not increase. A similar surface area to the original network was achieved when carrying out the reaction in 50 mL of DMF. The higher dilution reaction, where 100 mL of DMF were used, resulted in a surface area that was 200 m^2/g lower than the original surface area. This showed that for Sonogashira coupling reactions the lower dilution, i.e. higher concentration, was necessary to form a network with the highest surface area possible.

Table 10: E1 network concentration study (a) BET surface area, colours coordinated with TGA data

	Volume DMF (mL)	Volume PEG550 (mL)	Surface Area (m^2/g)[a]
1	25	0	1130
2	50	0	1210
3	100	0	1020
4	12.5	12.5	860
5	25	25	970
6	50	50	1000

Considering the part of the concentration study where PEG550 was used as a templating agent in addition to the solvent (Table 10), it can be seen that the surface areas are also decreased compared to the original surface area of 1200 m^2/g for the network synthesised in toluene. Considering the PEG550 concentration series, it can be observed that the surface areas increase steadily from 855 m^2/g to 1000 m^2/g. This increase in surface area can be attributed to the solvent, rather than the PEG. As could be seen before (Table 9 and 10), the PEG does not have an influence on the surface area. If anything, a large amount of PEG in the reaction seems to hinder an increase in surface area.

Looking at the TGA data for this series, few of the materials showed a high thermal stability under inert conditions (Figure 53). The materials with the highest thermal stability were the first two networks synthesised in DMF only (green and red, Figure 57) and the first two networks synthesised in DMF with PEG550 (blue and pink). On reaching the highest temperature of 1000 °C and holding for 30 minutes these four networks had a remaining mass of 70 to 65 %. The network synthesised in 50 mL DMF and 50 mL PEG550 had a weight decrease of 70 % on

heating to 1000 °C under inert conditions and holding for 30 minutes (maroon). The least thermally stable network is the material synthesised in 100 mL pure DMF (black). It lost over 90 % of its weight on heating. This somewhat confirms the theory of the least concentrated reaction not forming full networks but only oligomers. Oligomers would decompose more easily on heating. All materials decomposed completely when switching from inert conditions to air, leaving a negligible amount of 1.5 % of mass. The network synthesised in 50 mL DMF and 50 mL PEG550 (maroon) showed an initial step in its weight loss. The initial weight loss up until 110 °C can be attributed to the decomposition of trapped solvent in the pores of the network.

All networks started to decompose at around 330 °C with exception of the networks synthesised in 25 mL and 50 mL of DMF, which started to decompose from about 380 °C. This shows that all networks have a high thermal stability.

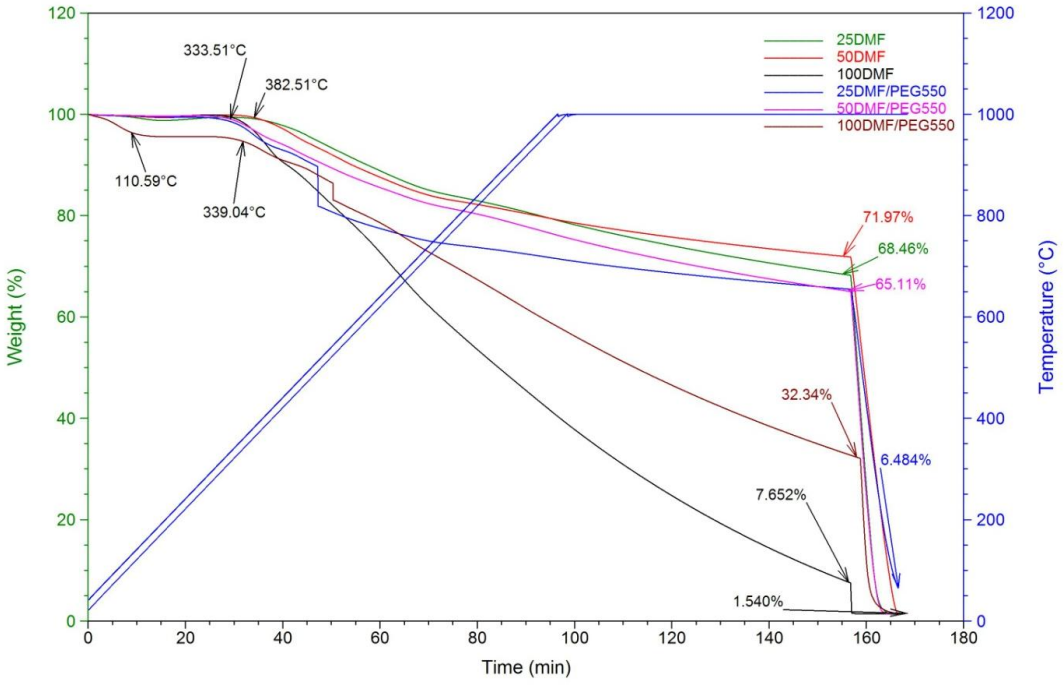

Figure 53: TGA data for E-1 network synthesised with PEG550 as templating agent and at different concentrations, heating rate of 10 °C per minute till 1000 °C, holding at temperature for 30 minutes, all under nitrogen, switching to air after 30 minutes and holding for a further 10 minutes

4.2.3 Effect of templates on the surface area of the E-2 network

Although the results discussed previously in this chapter showed no significant improvement, additional reactions were carried out on a network with a known low surface area to prove or disprove that the concentration and / or the introduction of a templating agent in the reaction does influence the surface area. The E-2 network[15] was originally synthesised by Sonogashira coupling reaction between tetrakis(4-iodophenyl) methane and 1,3,5-triethynylbenzene (Figure 54) in toluene resulting in a material with a surface area of 500 m^2/g. The low surface area of this network was explained by the network 'collapsing on itself' or by interpenetration and thus blocking pores. The introduction of a templating agent might therefore in principle stop the network from collapsing or any interpenetration and hence increase the surface area.

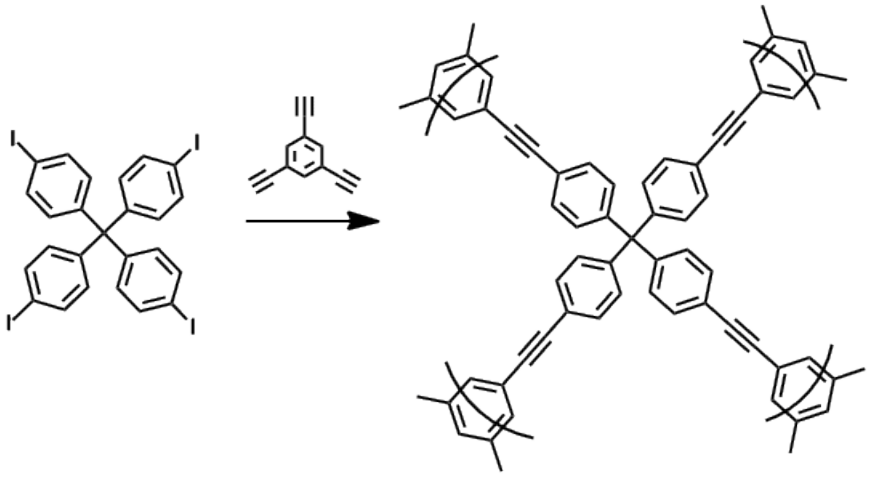

Figure 54: reaction scheme for the synthesis of E-2 network by Sonogashira cross-coupling reaction between tetrakis(4-iodophenyl) methane and 1,3,5-triethynylbenzene

The study for the E-2 network was carried out as before for the E-1 network (Table 10), varying the dilution of the reaction mixture and combining the solvent system with a templating agent, PEG550. PEG550 was chosen as the templating agent as it showed an improvement in surface area for the E-1 network. From the measured surface areas, it was clear that, in this case, the change in solvent had a great influence on the network formation. The surface area was quadrupled to 1900 m^2/g from the original 500 m^2/g. These results confirmed the theory that DMF was the better solvent for this type of reaction. In this case, it apparently stopped the network from 'collapsing', therefore helped the network to become more poly-condensed, and thus increased the surface area. The templating agent, PEG550, on the contrary had a negative influence on the network formation, decreasing the surface area again to around 1325 m^2/g.

Table 11: E-2 network concentration study (a) BET surface area, Langmuir surface area given in parentheses, colours coordinated with TGA data

	Volume DMF (mL)	Volume PEG550 (mL)	Surface Area (m^2/g)
1	25	0	1900
2	50	0	1750
3	100	0	1810
4	12.5	12.5	1330
5	25	25	1300
6	50	50	1350

From this series, it also was clear that the concentration influenced the surface area of a network. By diluting the reaction mixture by a factor of five, the surface area was increased almost by a factor of four, from 500 m^2/g to 1900 m^2/g.

Although this increase was not the case for the E-1 network, which had an initial high surface area, it was true for a material with a low surface area.

The TGA data (Figure 55) showed that no PEG remained in the material. No additional step was observed in the region of up to 200 °C, which is the temperature when PEG would start boil, as it has a boiling point of 200 °C. All materials showed again a very high thermal stability under inert conditions.

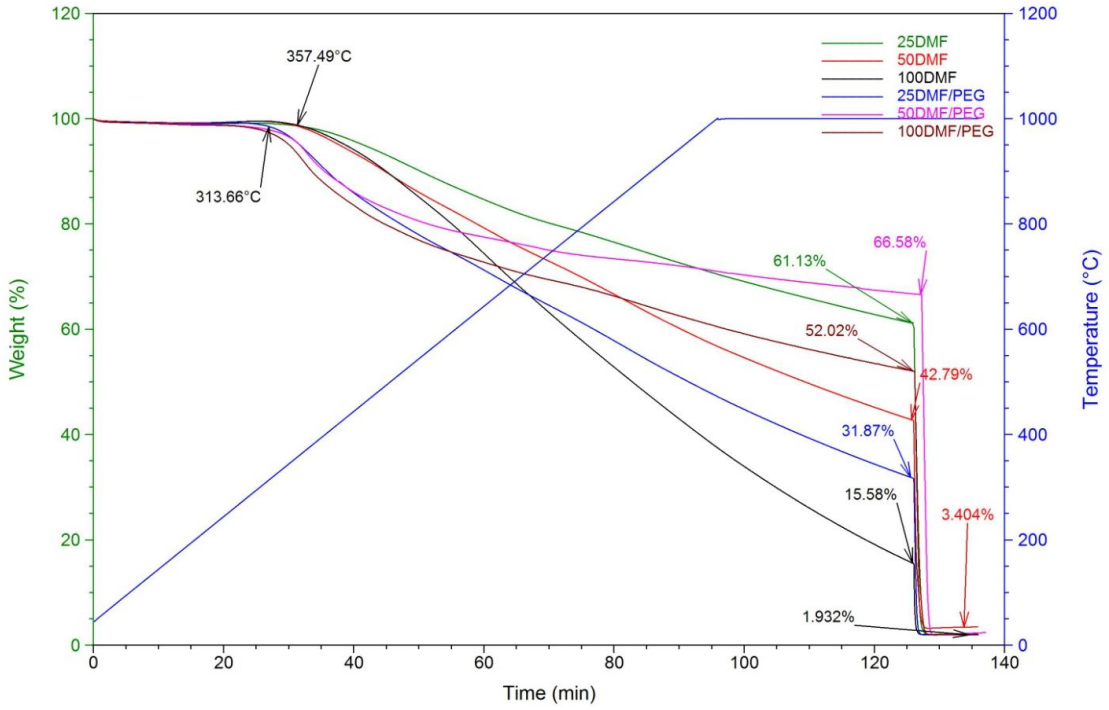

Figure 55: TGA data for E-2 network synthesised with PEG550 as templating agent and at different concentrations, heating rate of 10 °C per minute till 1000 °C, holding at temperature for 30 minutes, all under nitrogen, switching to air after 30 minutes and holding for a further 10 minutes

The networks started to decompose at around 310 °C for the materials synthesised in 12.5 mL PEG and 12.5 mL DMF (blue, Figure 55), 25 mL PEG and 25 mL DMF (pink, Figure 59) and 50 mL PEG and 50 mL DMF (maroon, Figure 55), and at around 355 °C for the materials synthesised in DMF only (green, red and black, Figure 55). Although the networks started to decompose in two sets, according to

whether they have templating agent present or not, they do not keep the same trend and decompose at very different rates. The most stable network was the network synthesised in 25 mL PEG and 25 mL PEG, giving a remaining mass of 66 % under inert conditions. The next most thermally stable network was the material synthesised in 25 mL DMF only. It had a remaining mass of 61 % before switching from inert conditions to air. With 52 % remaining mass the next most thermally stable material was the one synthesised in 50 mL PEG and 50 mL DMF. The three least thermally stable materials were synthesised in 50 mL DMF (red), in 12.5 mL DMF and 12.5 mL PEG (blue), and in 100 mL DMF (black), having remaining masses of 42 %, 32 % and 15.5 % respectively. The order of thermally stability under inert conditions for the six materials was therefore as follows: 5 > 1 > 6 > 2 > 4 > 3 (Table 12). Material 5 being the most thermally stable and material three is the least thermally stable. This thermal stability does not correlate with the surface area. When ordering the materials by thermal stability (Table 5) the only correlation that could be made was based on the reaction system. The most thermally stable network, material 5 (pink), is synthesised in 25 mL DMF and 25 mL PEG. The same reaction synthesised without PEG, i.e. in 25 mL DMF (green) is the next most thermally stable network. This indicated that the templating agent increased the thermal stability of the network but at the same time decreased the surface area.

Table 12: E-2 network concentration study in order of thermal stability, most thermally stable network at top, least thermally stable network at bottom

	Volume DMF (mL)	Volume PEG550 (mL)	Surface Area (m^2/g)
5	25	25	1300
1	25	0	1900
6	50	50	1350
2	50	0	1750
4	12.5	12.5	1320
3	100	0	1800

Comparing the networks by decreasing thermal stability, it can be seen that the networks with added templating agent were thermally more stable compared to the networks synthesised in the same amount of DMF without added PEG550. This indicates that either some PEG was incorporated in the network, increasing its thermal stability that way or that the network formed was more flexible and hence bonds could break more easily, decreasing its thermal stability. The change of solvent had the largest influence on the flexibility of the network, decreasing its thermal stability while increasing the surface areas. All materials decomposed completely when switching from inert conditions to air.

4.3 Conclusion

In conclusion, we can say that for high surface area materials, templating can influence the surface area in some but not all cases. Templates have been used in the synthesis of MOFs and have been shown to increase the surface area.[18] In the case of the E-1 network discussed here, the template seems to decrease the surface area. In addition, the change in solvent from toluene to DMF does make only little difference to the surface area for networks with high surface areas (E-1 networks).

Materials with low surface areas, however, can benefit from the change in solvent. In one case, the surface areas have been quadrupled. The template again does not increase but diminish the surface area.

4.4 References

[1] R. Dawson, *et al., Macromolecules*, 2010, *43*, 8524-8530

[2] Imhof, A. Pine, D. J., *Nature*, **1997**, 387, 948-950

[3] Park, M., Komarneni, S., *Microporous and Mesoporous Materials,* **1998**, 25 (1-3), 75-80

[4] Jiao, J., *et al., Colloid and Interface Science,* **2007**, 316 (2), 596-603

[5] Tan, R., *et al., Journal of Materials Science*, 38 (19), 3973-3978

[6] Liu, Z., *Materials Letters,* **2005**, 59 (28), 2005, 3620-3625

[7] Sun, Q., *et al., J. Phys. Chem. B*, **2002**, 106 (44), 11539–11548

[8] de A. A. Soler-Illia, G. A., *et al., Chem. Rev.*, **2002**, 102 (11), 4093–4138

[9] Khushalani, D., *et al., J. Mater. Chem.,* **1999**, *9*, 1500.

[10] de A. A. Soler-Illia, G. A., *et al., Chem. Mater.*, **2002**, *14*, 750.

[11] Ben, T., *et al., Angew. Chem. Int. Ed.*, **2009**, *48*, 9457 –9460

[12] Vidal, L., *et al., Microp. Mesop. Mat.,* **1998**, 24 (4-6), 189-197

[13] Jiang, J., *et al., Angew. Chem. Int. Ed*., **2007**, 46, 8574-8578

[14] Zhang, L., *et al., Applied Catalysis B: Environmental*, **2003**, 40 (4), 287-292

[15] E. Stöckel, *et al., Chem. Commun*., **2009**, 212-214

[16] Hodson, M. E., *Journal of Geochemical Exploration,* **2006**, 88 (1-3) 288-291

[18] Collins, D. J., Zhou, H.-C., *J. Mater. Chem.*, **2007**, 17, 3154-3160

4.5 Appendix (IR of PEG300, taken from Sigma Aldrich website)

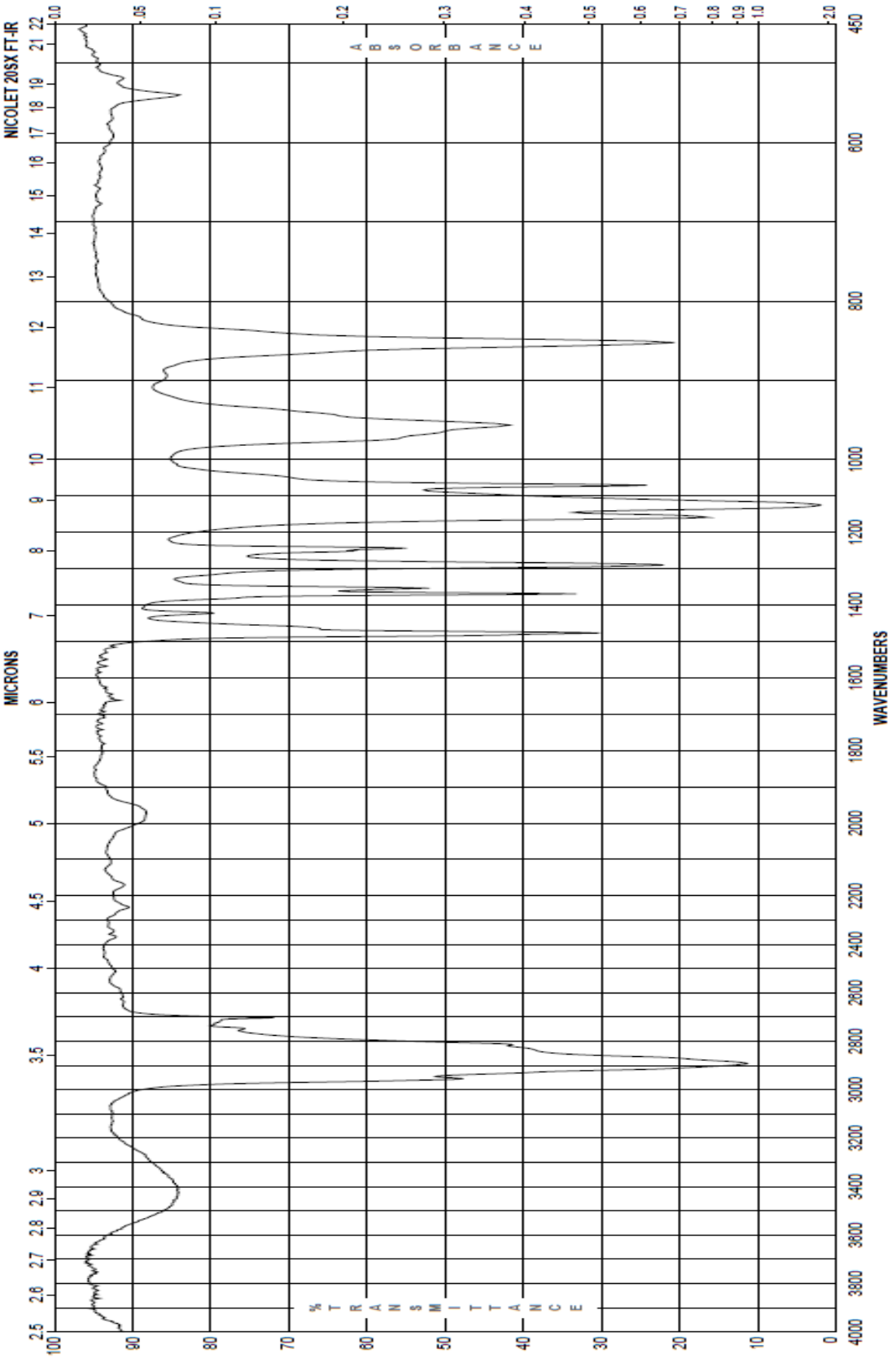

Chapter 5:

Gas sorption in Sonogashira- and Yamamoto-coupled CMPs

5.1 Introduction

Gas sorption is a very important part of the physical characterisation for insoluble porous polymer networks. All CMPs and PAFs synthesised here by either Sonogashira (Chapter 2) or Yamamoto (Chapter 3) coupling reaction are completely insoluble in any solvents. The gas sorption measurements therefore form a major part of the analysis for these networks. The gas sorption analysis also gives an indication of how applicable the materials are for hydrogen storage,[1] carbon dioxide capture[2] and methane storage.[3] Solid state NMR (ssNMR) spectroscopy is also important. The experiments and analysis for ssNMR are, however, time-consuming[4] and thus only the most promising materials, in terms of gas sorption, are analysed by ssNMR.[5, 6]

Gas sorption measurements show if the materials might in principle have an application outside of the research laboratory. The focus on gas storage in porous materials has shifted somewhat in the last 10 years.[7] Where at first researchers focused on hydrogen storage, there is now a growing emphasis on materials which are good at capturing carbon dioxide pre-[9] and post-combustion.[10] The best material to date for carbon dioxide capture is COF-102 with an uptake of 27.3 mmol/g at 35 bar and 298 K.[11] The safe storage of methane has been a focus, too.[12] As methane is a highly explosive gas,[13] it is important to find a solution to the safer storage of methane in the context of natural gas powered vehicles.

5.2 Results and Discussion

5.2.1 Catalyst Study (Chapter 2)

The following figures summarise the results for the gas sorption measurements of the previously discussed Sonogashira and Yamamoto coupled networks. All data were recorded on a Micromeretics 2420 or 2020 gas sorption instruments. Nitrogen and hydrogen isotherms were collected at liquid nitrogen temperatures (77 K) and CO_2 and CH_4 isotherms were collected at 298 K. The surface areas were calculated by calculation of the BET theory in the pressure range used mainly for microporous materials, 0.01 – 0.1 p/p_0. The pressure range applied for the BET calculations influences the surface areas of the networks. (See later discussions on the example of the Yamamoto coupled networks.) For the Sonogashira-coupled networks, the pressure range traditionally used in our group for microporous materials was applied in the BET calculations (0.01 – 0.1 p/p_0) paying attention that the C-value for the measurement is positive, otherwise the surface area would not be valid.

Figure 57 shows the nitrogen sorption isotherms for the first part of the catalyst study discussed in Chapter 2 (section 2.1). The isotherms on the left are the isotherms recorded from the networks synthesised by Sonogashira cross-coupling reaction between 1, 4-diethynylbenzene (DEB) and tetrakis (4-iodophenyl) methane (TPM-I) (Figure 56) using diisopropylamine as the base. The isotherms on the right show the adsorptions of the networks synthesised using triethylamine as the base.

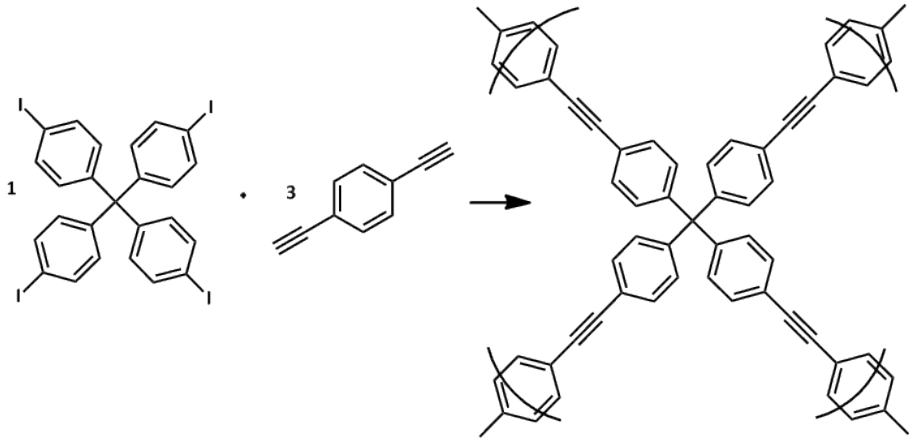

Figure 56: reaction scheme for the synthesis of E-1 network by Sonogashira cross-coupling reaction between tetrakis(4-iodophenyl) methane and 1,4-diethynylbenzene

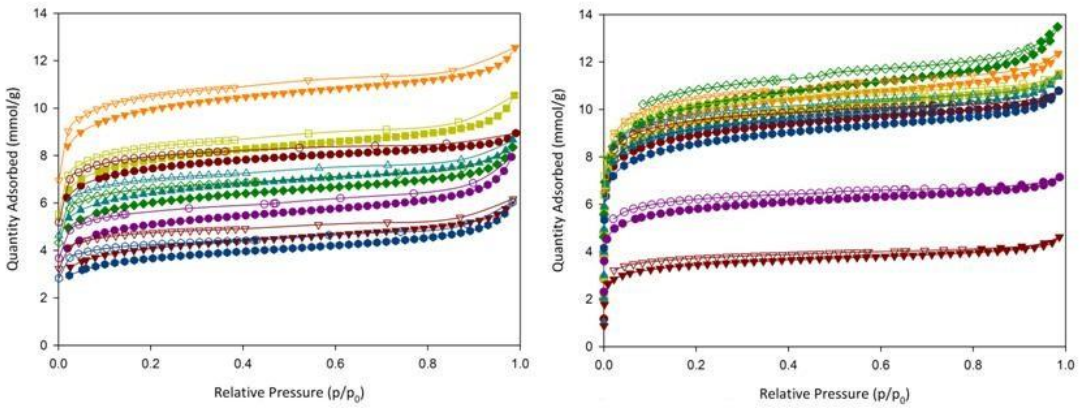

Figure 57: Nitrogen isotherms for first part of the catalyst study (see Table 1 Chapter 2, reaction 1 in red (circle), 2 in orange (triangle down), 3 in yellow (square), 4 in green (diamond), 5 in turquoise (triangle up), 6 in blue (circle), 7 in purple (circle), 8 in maroon(triangle down)) comparing the isotherms for networks synthesised where diisopropylamine was used as the base (left) and where triethylamine was used as the base (right, denoted with 'a' in Table 1, Chapter 2), filled symbols mark the adsorption and empty symbols the desorption,

Comparing the sorption isotherms of the two set of networks, it can be seen that the shape of all isotherms are broadly the same. All isotherms exhibit a type I character, meaning that the polymers are microporous. Comparing the isotherms more closely, it can be seen, as discussed before in Chapter 2 that the porosity changes dramatically between the two set of networks. Looking at the isotherms for the set of networks synthesised using diisopropylamine as the base, the most

porous network is the network formed under reaction 2 (80 mg Pd(II), blue triangles, down) or reaction 4a (40 mg Pd(0), green, squares) in the case where triethylamine was used as the base. The least porous of the networks synthesised with diisopropylamine as the base is number 6 (orange, circles). When using the same reaction conditions as for number 6, but changing the base to triethylamine (6a, orange, circles), it becomes more porous.

Looking at the pore size distribution (Figure 58), it can be seen that all networks have the majority of their pore sizes in the range < 2 nm. The pore sizes were calculated using the non-local density function (NLDFT) for pillard clay with cylindrical pore geometries found within the Micromeritics ASAP software. The networks synthesised with diisopropylamine as the base have pore sizes of 10 to 26 Å making them mainly, but not exclusively, microporous. All networks have similar pore size distributions, showing that the amount of catalyst used does not influence the pore sizes greatly. The surface area is influenced by the amount of catalyst used, but it does not strongly influence the pore sizes in the networks. Previous research by the Cooper group has shown that the strut length influences the pore size distribution as well as the surface area.[14] The pore size distribution broadens and the surface area decreases with increasing strut length.

When comparing the pore size distributions (Figure 58) of the networks synthesised using diisopropylamine as the base (left) with the networks synthesised where triethylamine was used (right), it can be seen that the pore size of the networks shifts slightly to a smaller pore size. The networks now have an average

pore size of 10 to 20 Å, and not up to 28 Å as for the networks synthesised with diisopropylamine as the base.

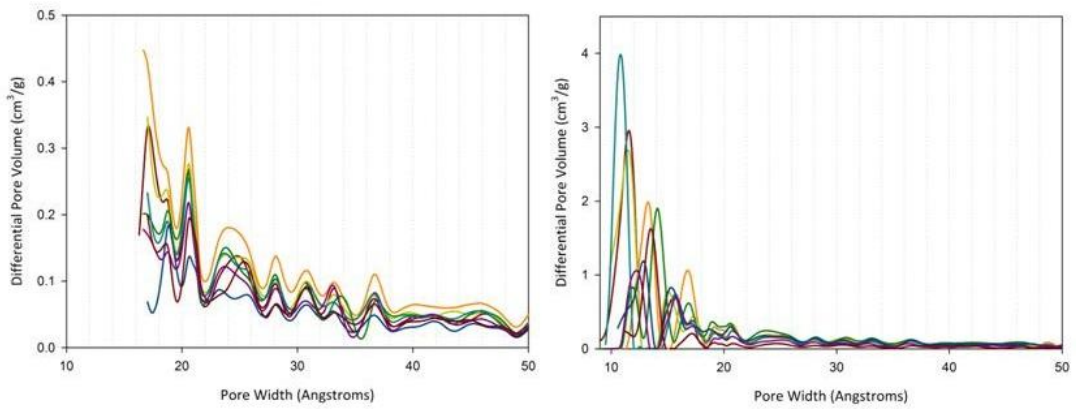

Figure 58: Differential Pore Size Distribution of Sonogashira coupled networks, first part of catalyst study (see Table 1, Chapter 2, reaction 1 in red, 2 in orange, 3 in yellow, 4 in green, 5 in turquoise, 6 in blue, 7 in purple, 8 in maroon), synthesized using diisopropylamine as the base (left) and triethylamine as the base (right)

The networks synthesised with triethylamine as the base are more micro porous than the networks synthesised with diisopropylamine as the base. Analysing these micropore volumes more closely (Figure 59), one can see that, although the general pore volume is the same for all networks, some very well-defined maximum volumes in different pore size ranges can be identified for individual networks.

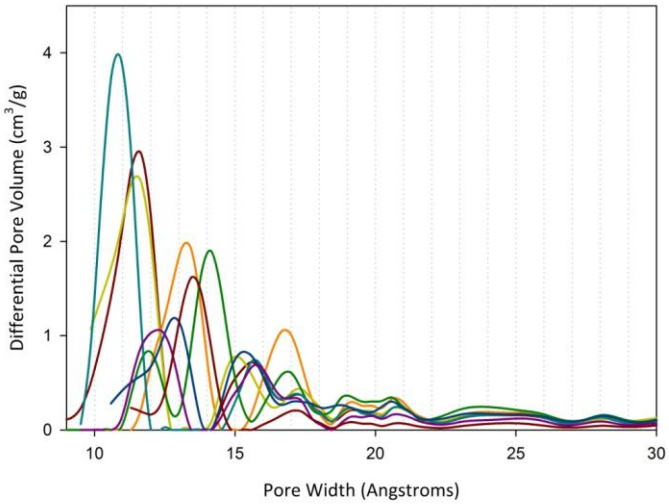

Figure 59: zoom of Differential Pore Size Distribution of Sonogashira coupled networks, first part of catalyst study (see Table 1, Chapter 2, reaction 1 in red, 2 in orange, 3 in yellow, 4 in green, 5 in turquoise, 6 in blue, 7 in purple, 8 in maroon), synthesized using and triethylamine as the base

Number **5a** (blue) is the most microporous network with a maximum pore volume at 18 Å. The next two networks with the highest pore volumes are **1a** and **3a** (black and green), with peaks showing the maximum pore volume at 12 Å and with additional peaks at 15 and 15.2 Å, respectively. Network number **2a** (red) shows peaks at 13 and 17 Å and network **8a** (grey) has a peak at 13.5 Å. The network with the most number of peaks and hence with the most amount of different pore sizes is network number **4a** (yellow) with peaks at 12, 14 and at 17 Å. The networks with the lowest pore volume are networks **6a** and **7a** (purple and aqua) with pore sizes of 15 and 12 Å each. This shows that all networks are highly microporous with well defined and in most cases very narrow pore size distributions of 10 to 20 Å.

Although the pore size distributions were not as similar as expected, as they were all the same networks, the pore size distributions should have been the same, maybe with a change in amounts of pores rather than a shift in pores sizes. They were still very similar and had the same range of pores. However, the difference between the distributions showed that the reaction cannot be simply predicted on paper but can have slight variation each time they are run. These variations could not influence the surface area or other gas sorption properties and can only be detected when comparing the pore size distributions. Repeating reactions, which form the same network, were broadly consistent in terms of gas sorption properties. This has been proven in our research group by repeating for example CMP-1 several times, always with similar surface areas and gas uptakes.

Figure 61 below shows the nitrogen isotherms for the second part of the catalyst study, the reaction between tetarkis(4-iodophenyl) methane and 1,3,5-triethynylbenzene (Figure 60). The isotherms on the left show the isotherms for the synthesised networks where diisopropylamine was used as the base, and the ones on the right the networks synthesised with triethylamine as the base. The networks were synthesised by Sonogashira cross-coupling reaction between 1,3,5-triethynylbenzene and tetrakis(4-iodophenyl) methane (Figure 64 and Table 2, Chapter 2).

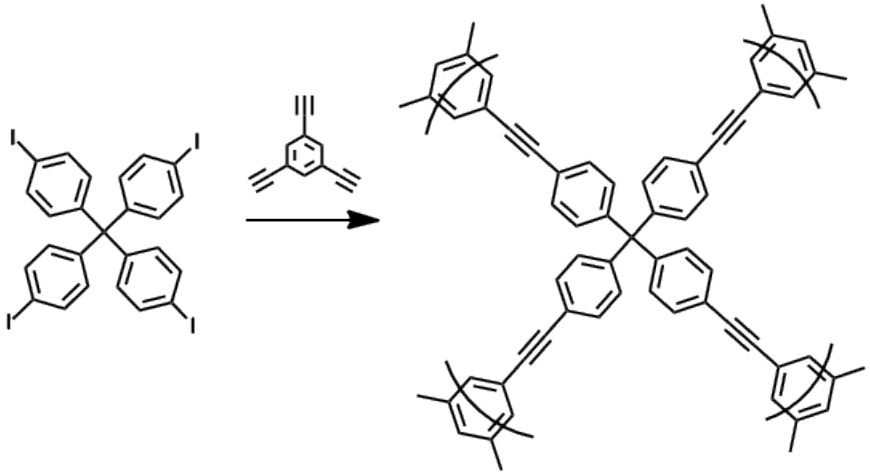

Figure 60: reaction scheme for the synthesis of E-2 network by Sonogashira cross-coupling reaction between tetrakis(4-iodophenyl) methane and 1,3,5-triethynylbenzene

Comparing the isotherm shape of all networks, it was observed that all networks exhibit a Type I isotherm, which makes all the networks microporous. The isotherms for reaction number **10** and number **10a** show a small amount of Type II character but are still mainly Type I isotherms.

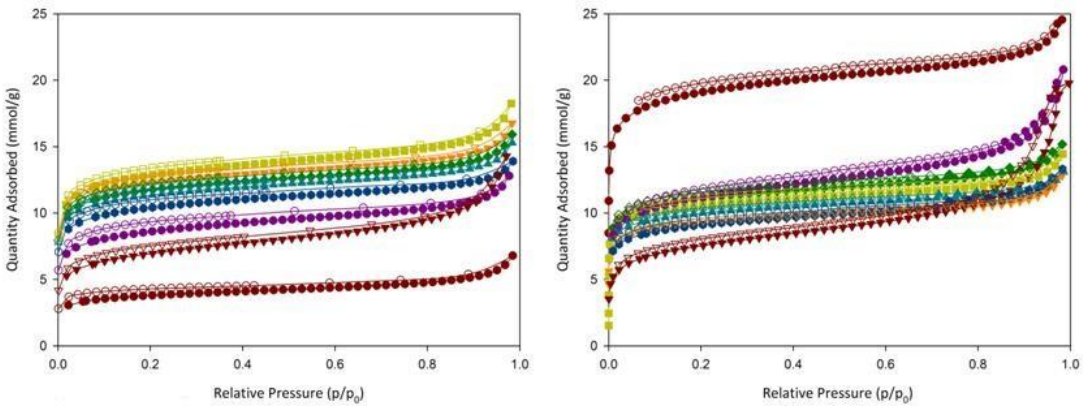

Figure 61: Nitrogen isotherms for second part of the Catalyst Study (see Table 2 Chapter 2, reaction 9 in red (circle), 10 in orange (triangle down), 11 in yellow (square), 12 in green (diamond), 13 in turquoise (triangle up), 14 in blue (circle), 15 in purple (circle), 16 in maroon(triangle down)) comparing the isotherms for networks synthesised where diisopropylamine was used as the base (left) and where triethylamine was used as the base (right), filled symbols mark the adsorption and empty symbols the desorption

The most noticeable difference can be seen between networks **9** and **9a**. The network synthesised in diisopropylamine (number **9**, maroon circles, left) was the least porous network out of the series of networks synthesised with diisopropylamine as the base. On switching the base to triethylamine, it became the most porous network in the series (number **9a**, purple circles, right). This observation is in agreement with the discussion in Chapter 2. The surface area for reaction number **9** was increased by a factor of five when changing the base from diisopropylamine to triethylamine. The remaining networks showed some differences in porosity, but were generally very similar to one another.

Figure 62 below showed the comparison of pore size distributions between the set of networks synthesised using diisopropylamine (left) and triethylamine (right) as the base. The networks showed pore size distributions of 10 to 26 Å approximately. The majority of the pores were between 10 and 20 Å with narrow distributions, making all networks highly microporous.

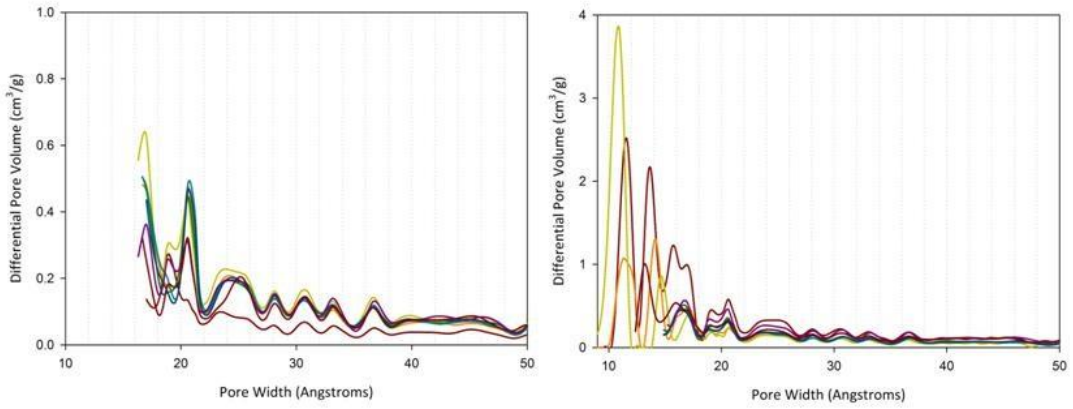

Figure 62: Differential Pore Size Distribution of Sonogashira coupled networks, first part of catalyst study (see Table 2, Chapter 2, , reaction 9 in red, 10 in orange, 11 in yellow, 12 in green, 13 in turquoise, 14 in blue, 15 in purple, 16 in maroon), synthesized using diisopropylamine as the base (left) and triethylamine as the base (right)

The pore size distributions for the networks synthesised with diisopropylamine as the base (left) showed that all networks are formed with similar pore sizes, meaning that the amount of catalyst did not have an influence on the pore sizes within the network. The pore sizes were potentially predefined due to the choice of monomers and form the same kind of network with different amounts of catalyst present. Taking into account bond length and bond angles it can be predicted with the help of atomistic simulations, it can be predicted that pore sizes of 13 to 26 Å could be expected. The pore sizes vary due to twisting within the structure. However, the reaction and mainly the obstruction of reactive sites by catalyst and / or ligands will influence this 'predefined' structure. This is why differences in the pore size distributions can be observed. Although this would indicate that the reactions are not repeatable, the gas sorption properties do not normally vary between repeat reactions, as from experience in our laboratories.

The pore size distribution of the networks synthesised using triethylamine as the base (right) show slightly different pore sizes between the networks were found. In general, the pore size distributions were very similar and one can say that the argument above was also applicable. Network **11a** (green), for example, has the most defined pore size distribution of the series with pore almost exclusively present at 11 Å. The network synthesised with the highest amount of catalyst, number **9a** (black), showed that three different kinds of pore sizes were present at 12, 14 and 16 Å. The remaining networks had similar pore size distributions to number **9a,** alas with lower volumes of pores. This showed that reaction **11a** was carried out under the optimum catalyst conditions resulting in a very narrow pore size distribution. The other networks, while still having very narrow pore size

distributions, were not formed at optimum conditions, either through a lack of catalyst and, hence, a large number of unreacted end groups, or due to too much catalyst being present, which could block reactive sites and hence increased the number of larger pores.

Figure 64 shows the comparison of nitrogen isotherms synthesised by Sonogashira cross coupling reaction between 1,4-diethynylbenzene and tetrakis(4-iodophenyl) methane (Figure 63) using palladium (0) as the catalyst with diisopropylamine (left) and triethylamine (right) as the base.

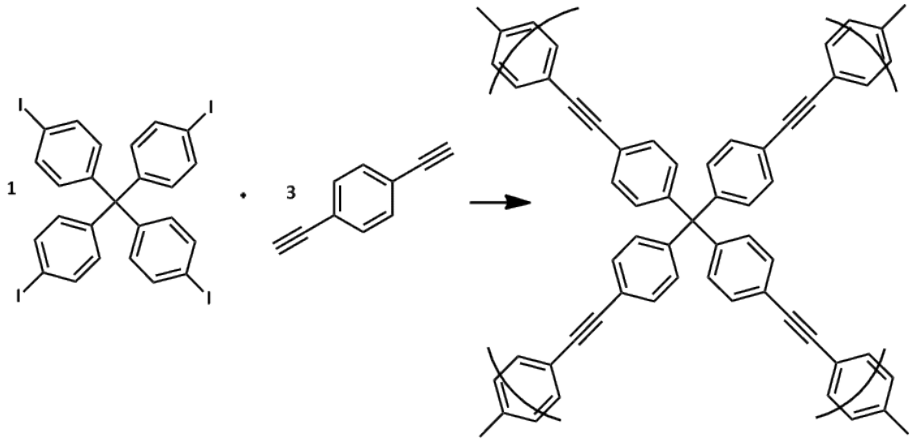

Figure 63: reaction scheme for the synthesis of E-1 network by Sonogashira cross-coupling reaction between tetrakis(4-iodophenyl) methane and 1,4-diethynylbenzene

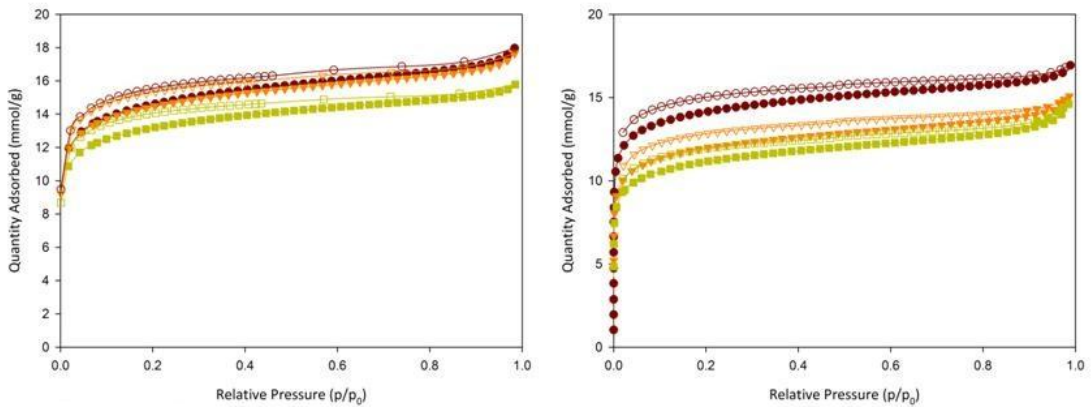

Figure 64: Nitrogen isotherms for second part of the Catalyst Study (see Table 3 Chapter 2, reaction 17 in red (circle), 18 in orange (triangle down), 19 in yellow (square)) comparing the isotherms for networks synthesised where diisopropylamine was used as the base (left) and where triethylamine was used as the base (right), filled symbols mark the adsorption and empty symbols the desorption

From the isotherms, it was observed that the differences in porosity were very subtle between the two sets of networks. All networks had a Type I shape isotherm, making them microporous. The networks synthesised with diisopropylamine as the base were a little more porous than the ones synthesised with triethylamine as the base, giving slightly higher surface areas. All networks had surface areas ranging from 930 m^2/g (reaction **19a**) to 1230 m^2/g (reaction **17**). Both sets of networks followed the same trend of surface area. Number **17(a)** had the highest surface area, 1230 m^2/g, and number **19(a)** had the lowest surface area, 930 m^2/g.

Figure 65 below shows the pore size distribution of the two sets of networks. The pore size distribution for the networks synthesised with diisopropylamine as the base (left) were almost identical, showing that the network was formed in exactly the same way independent of the base or the amount of catalyst used.

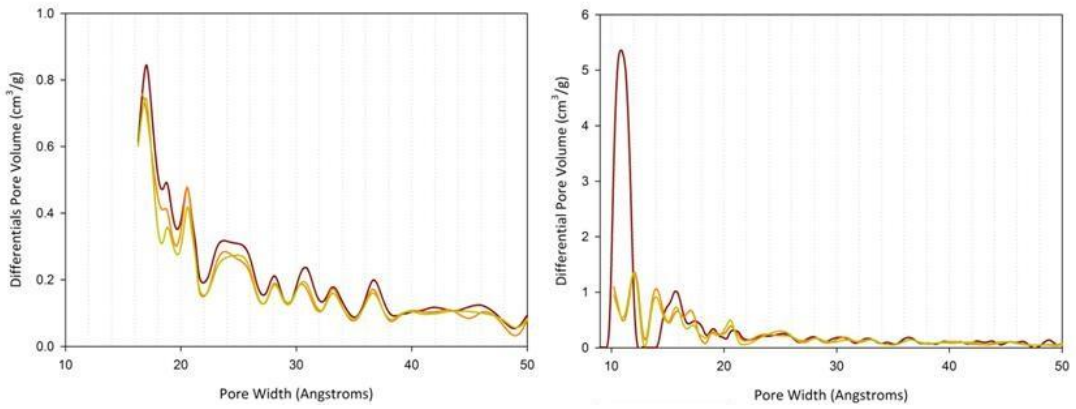

Figure 65: Differential Pore Size Distribution of Sonogashira coupled networks, third part of catalyst study (see Table 3, Chapter 2, reaction 17 in red, 18 in orange, 19 in yellow), synthesized using diisopropylamine as the base (left) and triethylamine as the base (right)

Looking at the pore size distributions of the networks synthesised with triethylamine it was seen that two of the three networks, numbers **18a** and **19a**,

had exactly the same pore size distribution, showing that the amount of catalyst for these two reactions did not influence the porosity in the network. However, network number **17a** showed that the majority of the pores present were uniform with a pore size of 11 Å. This showed that for the reactions where triethylamine was used the amount of catalyst, palladium (0) in this case, was important, making the conditions for reaction **17a** (see Table 3, Chapter 2 or Chapter 6 for details) the optimum conditions for this set of reactions.

Figure 67 below shows the nitrogen adsorption isotherms for the networks synthesised by Sonogashira cross-coupling reaction between 1,3,5-triethynylbenzene and tetrakis(4-iodophenyl) methane (Figure 66) using palladium (0) as the catalyst and diisopropylamine (left) or triethylamine (right) as the base.

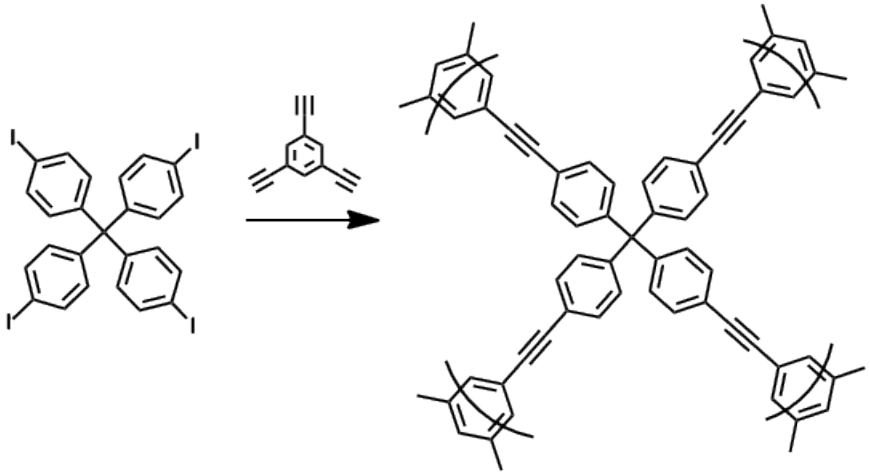

Figure 66: reaction scheme for the synthesis of E-2 network by Sonogashira cross-coupling reaction between tetrakis(4-iodophenyl) methane and 1,3,5-triethynylbenzene

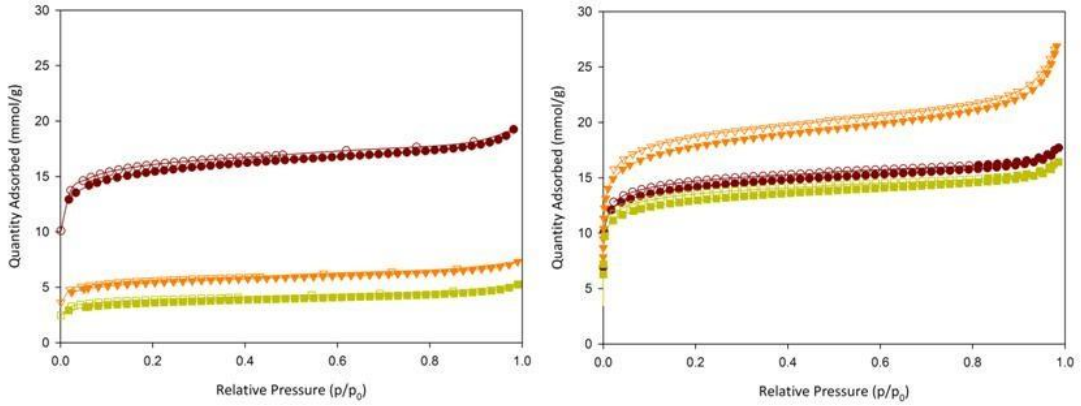

Figure 67: Nitrogen isotherms for second part of the Catalyst Study (see Table 4, Chapter 2, reaction 20 in red (circle), 21 in orange (triangle down), 22 in yellow (square)) comparing the isotherms for networks synthesised where diisopropylamine was used as the base (left) and where triethylamine was used as the base (right), filled symbols mark the adsorption and empty symbols the desorption

Comparing the two sets of networks it was seen that the networks were quite different from one another, in terms of porosity. The networks synthesised with diisopropylamine as the base were less porous with lower surface areas than the networks synthesised with triethylamine as the base.

Network number **20** (black circles) was the most porous of the series of networks synthesised with diisopropylamine as the base. Its porosity did not change much when changing the base to triethylamine (number **20a**) which showed that this reaction did not depend on the base used. However, comparing reaction **21** with **21a** (red triangles) and **22** with **22a** (green squares) it can be seen that by changing the base to triethylamine from diisopropylamine the porosity was increased significantly.

Figure 68 below shows the pore size distribution for these networks. Comparing the pore size distributions for the networks it was seen that all networks had a similar distribution, meaning that the catalyst concentration has only a mild influence on the pore sizes.

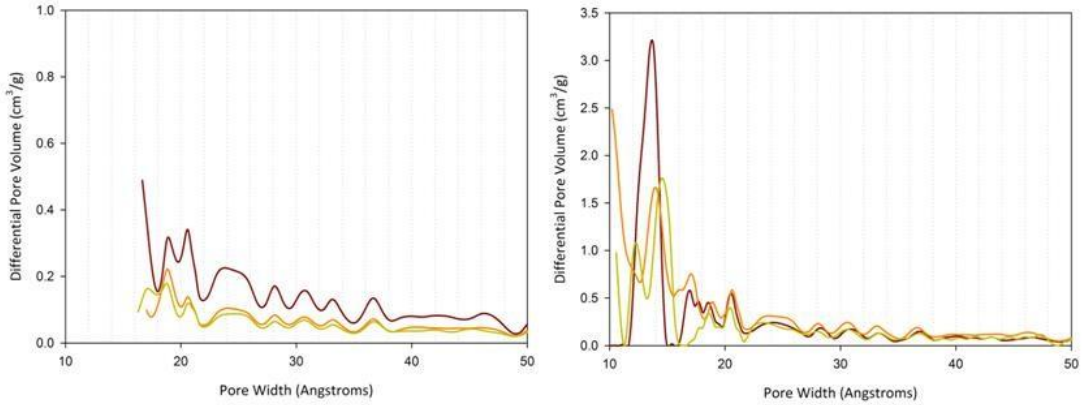

Figure 68: Differential Pore Size Distribution of Sonogashira coupled networks, first part of catalyst study (see Table 4, Chapter 2, reaction 20 in red, 21 in orange, 22 in yellow), synthesized using diisopropylamine as the base (left) and triethylamine as the base (right)

For the networks synthesised with diisopropylamine as the base, it was noticed that network number **20** (black) gives rise to highest volume of pores in general. The network had pore sizes of 10 to 25 Å at various different amounts. The majority of the pores will most likely be at around 10 Å although these pore sizes were not measured, due to quick measurements carried out rather than complete isotherms. Overall the higher volume of pores explained the higher porosity, i.e. the higher surface area compared to the other two networks, number **21** and **22** (red and green respectively). This showed that all networks had the same composition but with a lower number of repeating units, hence the lower volume of pores in networks **21** and **22**.

Comparing the distribution of pores for the networks synthesised with triethylamine as the base (right) it can be observed that again the majority of the pores, but not exclusively all pores, were between 10 Å and 20 Å. Network **20a** (black) has the narrowest distribution with almost exclusively pores at around 12 Å.

All distributions again show a similar range of pore sizes showing that the amount of catalyst did not influence the pore sizes but only the volume of pores.

Figure 70 shows the nitrogen adsorption isotherms for the control experiments of the catalyst study discussed in Chapter 2. The networks were synthesised by Sonogashira cross-coupling reaction between 1,3,5-triethynylbenzene and 1,4-diiodobenzene (Figure 69) using palladium (0), **23(a)** and **25(a)**, or palladium (II), **24(a)** and **26(a)**, as the catalyst and diisopropylamine or triethylamine, denoted with '**a**', as the base (see Chapter 2 and Chapter 6 for details).

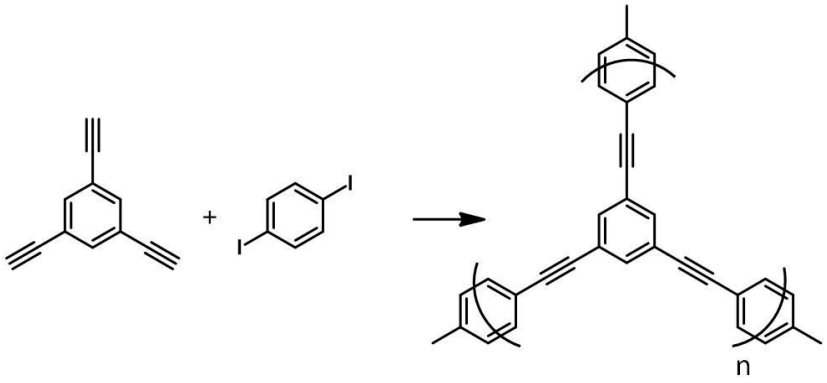

Figure 69: Schematic view of the reaction between TEB and DIB to form ideal CMP network

All networks show a Type I isotherm, with a negligible Type IV characteristic at the highest pressures. All networks are therefore again predominantly microporous.

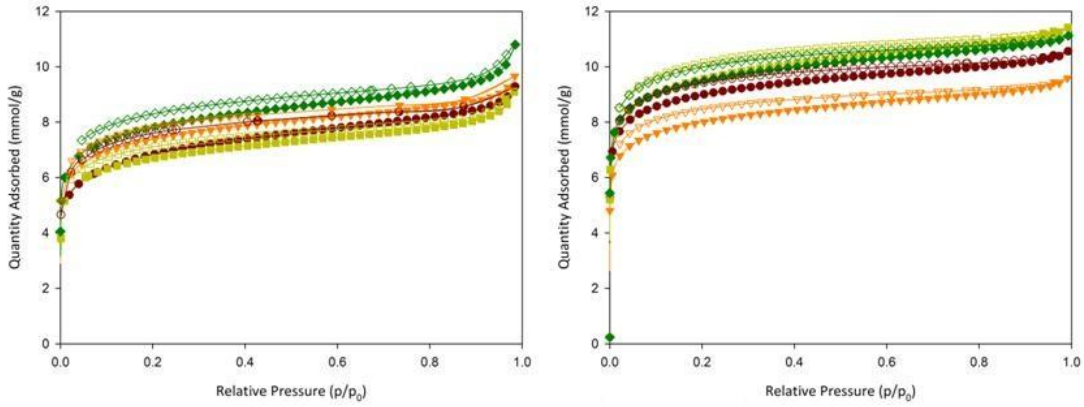

Figure 70: Nitrogen isotherms for second part of the Catalyst Study (see Table 5, Chapter 2, reaction 23 in red (circle), 24 in orange (triangle down), 25 in yellow (square), 26 in green (diamond)) comparing the isotherms for networks synthesised where diisopropylamine was used as the base (left) and where triethylamine was used as the base (right), filled symbols mark the adsorption and empty symbols the desorption

Comparing the isotherms, it was observed that not a very large difference in porosity is evident. The networks were almost identical, with only slight differences in shape and magnitude. Neither the oxidation state of the catalyst nor the type of base used for these reactions, influenced the porosity of these networks significantly. The networks synthesised with triethylamine as the base were slightly more porous than the networks synthesised with diisopropylamine as the base. The total quantity adsorbed is higher in the networks synthesised with triethylamine (right) as the base compared to the networks synthesised with diisopropylamine (left).

The networks synthesised with palladium (0) and diisopropylamine (left, **23** and **25**) resulted in a more porous network when switching to triethylamine as the base (right, **23a** and **25a**). Hence, the base influenced the surface area of these

networks. The difference in porosity was not very large, but still significant. The same was true for the networks synthesised with palladium (II) as the catalyst.

Figure 71 below shows the pore size distributions of the networks. Again, it was seen that the networks had mainly pores in the region of 10 Å to 20 Å. All networks were therefore highly microporous with narrow pore size distributions.

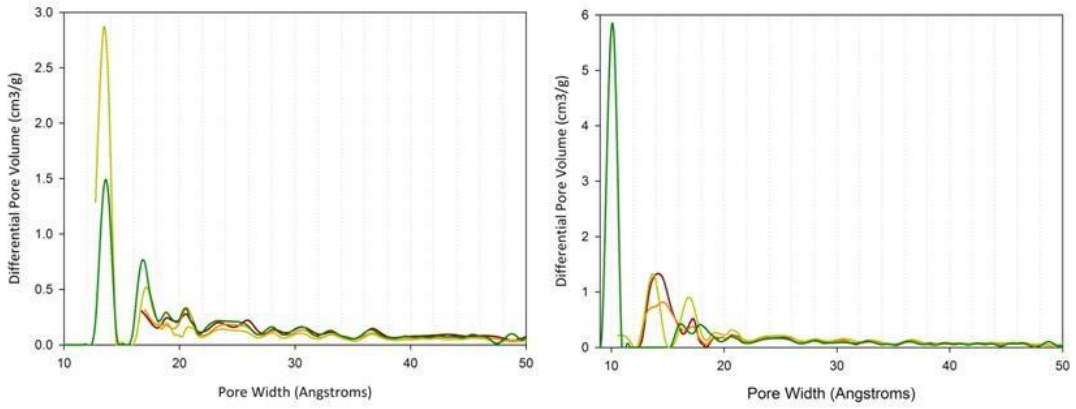

Figure 71: Pore Size Distribution of Sonogashira coupled networks, fifth part of catalyst study (see Table 5, Chapter 2, reaction 23 in red, 24 in orange, 25 in yellow, 26 in green), synthesized using diisopropylamine as the base (left) and triethylamine as the base (right)

The distribution of the different pore sizes was very similar between the networks, showing that the reactions are reproducible, to an extent, and that the amount of catalyst had no significant influence on the pore sizes, but only on the volume of the pores at certain sizes. When comparing the pore size distributions between the two different bases used, it was noticed that a small shift to smaller pore sizes occurred when using triethylamine as the base. Network number **26a** (right, green) had, almost exclusively, a pore size of 10 Å. Whereas the same network (**26**, left, green) synthesised with diisopropylamine as the base had a pore size of 14 Å at a much lower volume. This showed that, in this case, the base had an influence on the pore sizes of the network.

5.2.2 Yamamoto coupled CMPs (Chapter 3)

Table 13 below shows a summary of the surface areas, pore widths, and gas uptakes for the homo-coupled networks synthesised by Yamamoto coupling reaction discussed in Chapter 3 (monomers used in Yamamoto couplings shown in Figure 72). The surface areas within two different pressure ranges were compared. Namely, the pressure range published for the high surface area PAF-1 network, 0.05 – 0.2 p/p_0, and the pressure range used mainly in our group for microporous materials, 0.01 – 0.1 p/p_0.

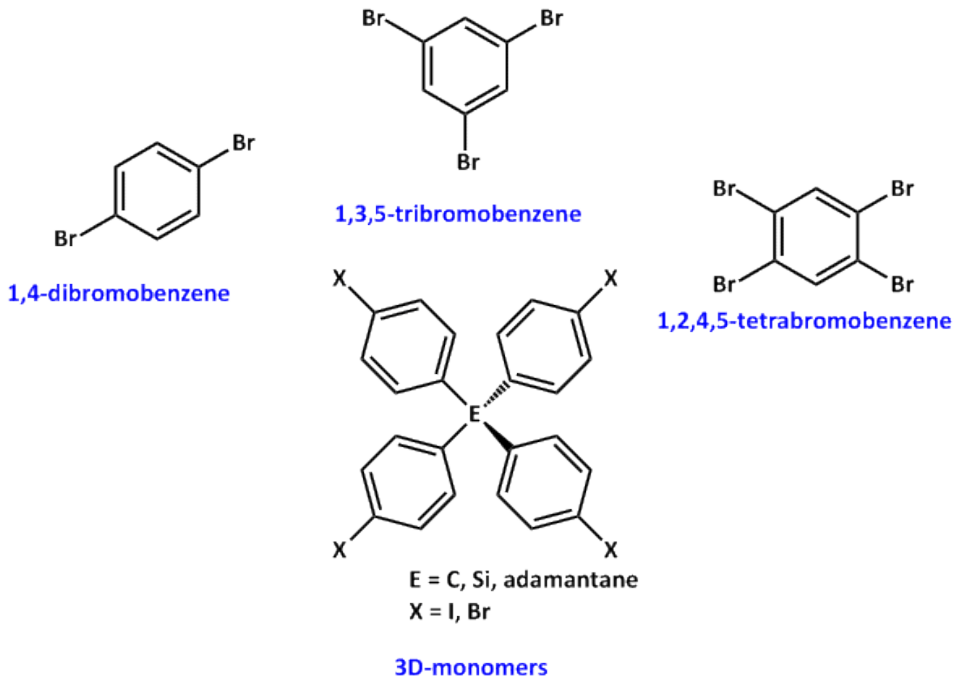

Figure 72: monomers used for Yamamoto coupling reactions

The pressure range applied for the BET calculations influences the surface areas of the networks. It also changes the C-value, which needs to be positive for a valid surface area. As can be seen from the Table 13 below, not all networks have a positive C-value using both pressure ranges. In general, the lower pressure range of

0.01 – 0.1 p/p_0 is a good basis for BET calculations of the surface areas. The higher pressure range, applied for the original PAF-1 network, does not apply for the silicon centred network or the PAF-1 network synthesised from the iodo monomer. Negative C-values mean that the surface area is not calculated correctly for these two networks.

Table13: comparison of surface areas (at different pressure ranges) and gas uptake of PAF-1 type polymer networks

Sample	Pressure range (P/P_0)	BET SA (m^2/g)	Average pore width (Å)	C value	H_2 (mmol/g @ 1.12 bar, 77 K)	CO_2 (mmol/g @ 1.12 bar, 300 K)	CH_4 (mmol/g @ 1 bar, 303 K)
poly-TPM-Br	0.05 – 0.2	3600	42.8	+	8.5	1.16	0.44
poly-TPM-Br	0.01 – 0.1	3910		+			
poly-TPA-Br	0.05 – 0.2	3530	40.7	+	11.5	1.81	0.63
poly-TPA-Br	0.01 – 0.1	3700		+			
poly-TPS-Br	0.05 – 0.2	---	46.0	-	5	0.91	0.25
poly-TPS-Br	0.01 – 0.1	1100		+			
poly-TPM-I	0.05 – 0.2	---	43.4	-	10.5	1.49	0.56
poly-TPM-I	0.01 – 0.1	3610		+			

The isotherms for the PAF-1 type networks are shown below (Figure 73). This Figure also incorporates a PAF-1 network synthesised by Arne Thomas' group in Berlin (maroon circles). As can be seen by comparing all four networks, the isotherm did not change significantly and showed that the reactions are repeatable. All networks exhibit a Type I isotherm by IUPAC definition with some Type IV characteristics, making them predominantly microporous. The network was Soxhlet extracted after the reaction and remeasured (orange triangles). As was seen the porosity increased slightly after Soxhlet extraction. This means that a small amount of unreacted monomer and / or catalyst was still present in the network and was successfully removed by Soxhlet extraction.

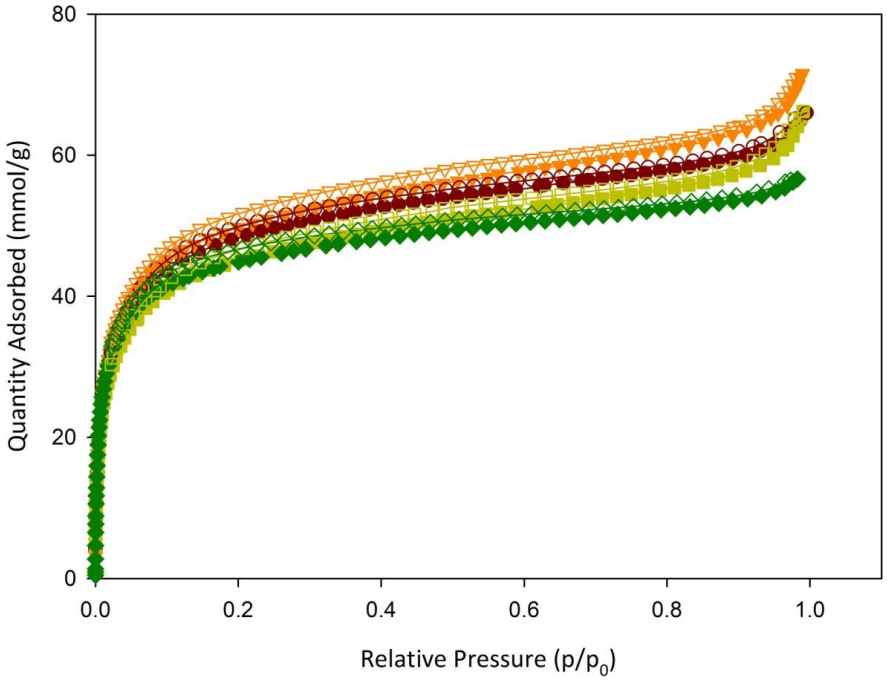

Figure 73: Nitrogen isotherms for PAF-1 networks (Arne Thomas' PAF from Berlin (maroon circles), PAF-1 after soxhlet extraction (orange triangles down) PAF-1 attempt 2 (yellow squares), PAF-1 attempt 3 (green diamonds)) filled symbols mark the adsorption and empty symbols the desorption

Comparing the pore size distributions between the PAF-type networks (Figure 74) it can be seen that all networks have the same pore size distribution with the main peak of the pores being between 10 and 20 Å and an average pore width of 40 to 45 Å (Table 13).

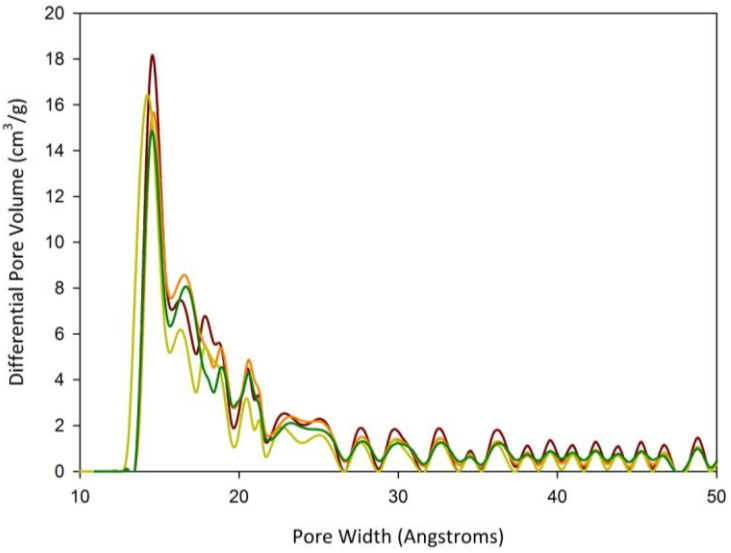

Figure 74: Pore Size Distributions of Yamamoto coupled Paf-1 type networks (Arne Thomas' PAF from Berlin (maroon), PAF-1 after soxhlet extraction (orange) PAF-1 attempt 2 (yellow), PAF-1 attempt 3 (green))

The pore size distribution showed that the reactions are repeatable. It did not change after Soxhlet extraction (orange) and, hence, insignificant amounts of unreacted monomer or catalyst remained in the network after work up. In the previously discussed Sonogashira networks, one could see a definite shift in pore sizes to smaller pores before and after Soxhlet extraction,[19] showing that the pores were blocked by catalyst and / or monomer. The distribution also shows that a small amount of meso pores, pores with pore width larger than 20 Å, were present. This suggests that the reaction, no matter how many times it was repeated, did not go to completion and left unreacted end groups within the material, which increased pore sizes due to insufficient packing.[20] This was in agreement with the

CHN analysis for these networks (see Chapter 3 for discussion) which did not match the theoretical values entirely. As discussed before, this was most likely due to the reaction vessels not being 100 % airtight, i.e. the atmosphere in the reaction vessels cannot be kept 100 % oxygen free, which caused the catalyst to decompose and hence will have decreased the degree of completion of the reaction.

For the reaction where the iodo monomer instead of the bromo monomer was used, one can observe a Type I isotherm (Figure 75) with Type IV characteristics. The network is therefore predominantly microporous with some macropores present.

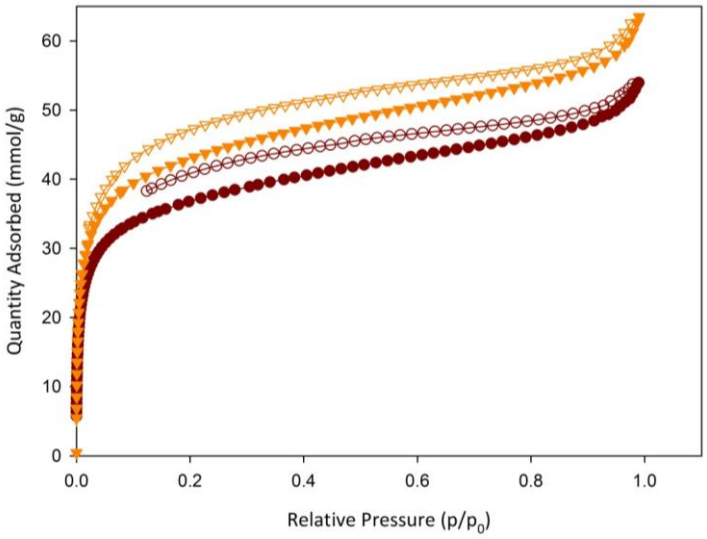

Figure 75: Nitrogen isotherms for PAF-1 type networks synthesised by Yamamoto coupling reaction from tetrakis(4-iodophenyl) methane before (orange triangles) and after (maroon circles) soxhlet extraction, filled symbols represent the adsorption and empty symbols the desorption

The nitrogen isotherm for this network was run before and after Soxhlet extraction. It was noticeable that the porosity was decreased after Soxhlet extraction. This was out of the ordinary. In general, one expects the porosity to increase or at least stay the same after soxhlet extraction, as the soxhlet extraction

is carried out to remove remaining monomer, solvent, base and / or catalyst from the material. In this case, it seemed that by extracting the material the pores collapsed by a small fraction. This might be due to trapped monomer, which was not blocking pores but actually stabilising pores, which have unreacted end groups within them. If this were true then the pore size distribution of the networks would show a decrease in pore volume. Figure 76 below shows the pore size distribution of this network before and after soxhlet extraction.

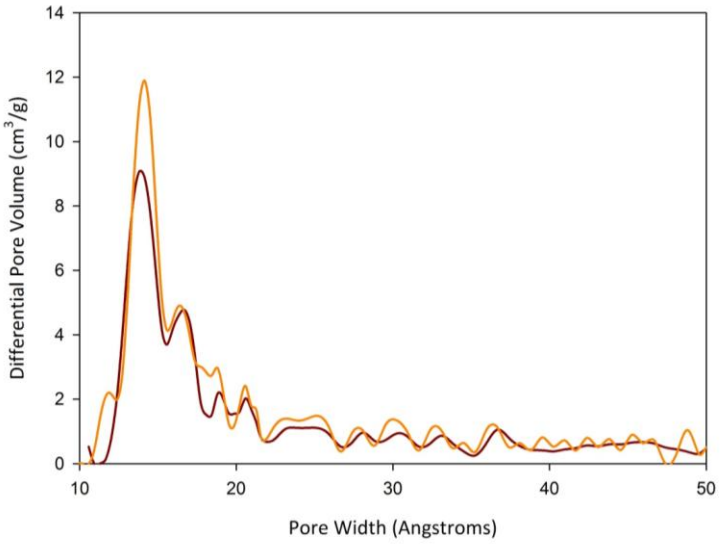

Figure 76: Pore Size Distributions of PAF-1 type networks synthesised by Yamamoto coupling reaction from tetrakis(4-iodophenyl) methane before (orange) and after (maroon) soxhlet extraction,

It was observed that the pore volume does indeed decrease after Soxhlet extraction of the material. The pore size was not changed after Soxhlet extraction, there was solely a decrease in volume of pores. This suggests that any trapped monomer did not actually block any pores but stabilised them and thus on removing of the 'trapped' monomer the volume of these pores decreased.

The same phenomenon can be observed for the PAF-1 type network synthesised by Yamamoto coupling reaction of 1,3,5,7-tetrakis(4-bromophenyl) adamantane. The nitrogen isotherm for this network (Figure 77, left) was more Type IV by IUPAC definition than the previous isotherms. It showed that a larger volume of meso pores was present than in the previous networks. Adamantane is a large central unit in the monomer, compared to a single carbon or silicon atom, perhaps rationalising this. The size of the adamantane centre caused the pore size to increase, compared to the carbon-centred networks, as was seen in the pore size distribution (Figure 77, right) of the network. The network was still mainly microporous with the majority of the pores having a pore width of 10 Å to 25 Å. However, a considerable amount of pores was larger than 25 Å therefore giving rise to hysteresis in the nitrogen sorption isotherm. This network therefore had microporous and mesoporous characteristics in terms of sorption measurements.

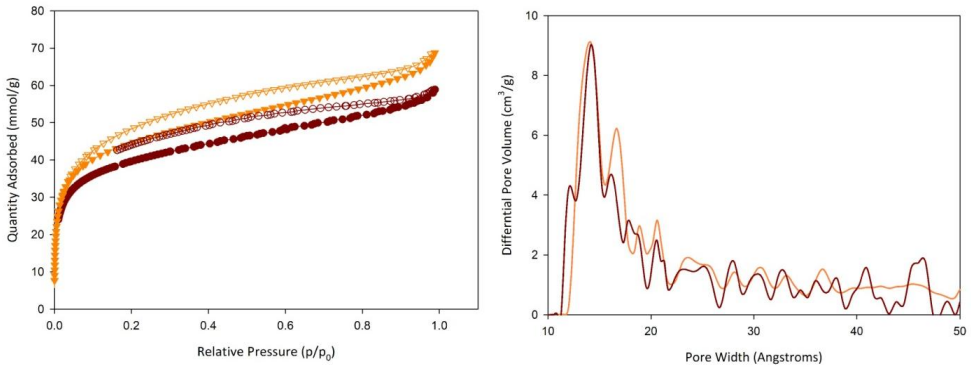

Figure 77: right: Nitrogen isotherms for PAF-1 type networks synthesised by Yamamoto coupling reaction from 1,3,5,7-tetrakis(4-bromodophenyl) adamantane before (maroon circles) and after (orange triangles) soxhlet extraction, filled symbols represent the adsorption and empty symbols the desorption; left: Pore Size Distributions of the same PAF-1 type networks before (maroon) and after (orange) soxhlet extraction

The nitrogen sorption isotherm (Figure 77, left) showed again that the porosity decreased after Soxhlet extraction. The pore size distribution (Figure 75, right) showed that after soxhlet extraction of the network the volume of pores smaller than 25 Å decreased and that the volume of pores larger than 25 Å increased slightly. This again suggest that some of the remaining monomer must stabilise and not block the smaller pores or that the materials are not fully stable towards Soxhlet extraction.

Figure 78 shows the nitrogen isotherm and the pore size distribution of the network synthesised by Yamamoto coupling reaction from tetrakis(4-bromophenyl) silane.

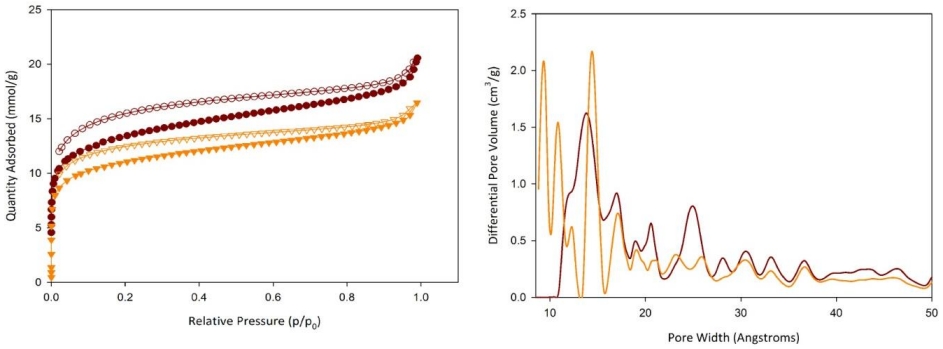

Figure 78: right: Nitrogen isotherms for PAF-1 type networks synthesised by Yamamoto coupling reaction from tetrakis(4-bromodophenyl) silane before (maroon circles) and after (orange triangles) soxhlet extraction, filled symbols represent the adsorption and empty symbols the desorption; left: Pore Size Distributions of the same PAF-1 type networks before (maroon) and after (orange) soxhlet extraction

Looking at the nitrogen isotherm (Figure 78, left) for this network, it was seen that the shape of this isotherm is similar to a Type I isotherm by IUPAC definition with some Type IV character. This showed that the network is mainly microporous, but had some macro pores present within it as well. The porosity of the network increased after Soxhlet extraction (maroon). This indicated that the

reaction had not gone to completion, leaving a significant amount of unreacted monomer in the material, which was removed upon Soxhlet extraction. The pore size distribution (Figure 78, right) confirmed this. Before Soxhlet extraction, large amounts of small pores were present which disappeared after Soxhlet extraction of the material. The unreacted monomer therefore partially blocked some pores, making them appear smaller than they actually were. The network, after Soxhlet extraction, consisted mainly of pores in the range of 10 to 20 Å, although as expected from the nitrogen isotherm some larger pores were present. This showed that some pores were partially blocked by either unreacted monomer or catalyst. The extraction step is therefore necessary for this material.

Figure 79 below shows a comparison of nitrogen isotherm between the networks discussed here, after Soxhlet extraction. The comparison shows that the silane centred network was the least porous compared to the rest of them. In comparison the isotherm for networks synthesised from tetrakis(4-bromophenyl) silane (TPS-Br) and tetrakis(4-bromphenyl) methane (TPM-Br) were more microporous than the other two networks, which showed some Type IV characteristics by IUPAC definition; that is the networks had some meso- or macropores.

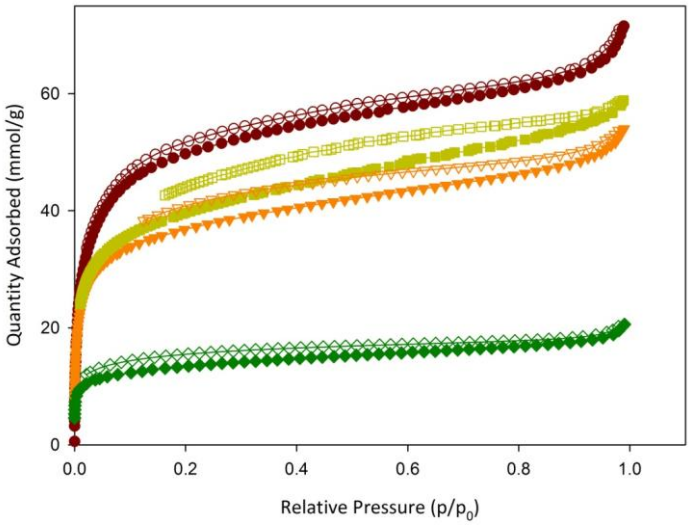

Figure 79: Nitrogen isotherms for all PAF-1 type networks synthesised by Yamamoto coupling reaction (TPM-Br network in maroon circles, TPM-I network in orange triangles, TPA-Br network in yellow squares, TPS-Br network in green diamonds), filled symbols represent the adsorption and empty symbols the desorption

Comparing the micropore and total pore volumes (Table 14), it was seen that most of the four homo-coupled networks had about 50 % of their total pore volume defined as micro pores at $p/p_0 = 0.1$. The total pore volume was recorded at $p/p_0 = 0.9$.

Table 14: (a) Surface area calculated from the N_2 adsorption isotherm using the BET method. (b) Micropore volume calculated using the t-plot method based on the Halsey thickness equation (c) Total pore volume at $p/p_0 = 0.99$

	S_{BET} (m^2/g)[a]	V_{micro} (cm^3/g)[b]	V_{total} (cm^3/g)[c]
TPM-Br	3990	1.42	2.12
TPM-I	3610	1.16	1.79
TPA-Br	3700	1.07	2
TPS-Br	1100	0.36	0.56

As was seen when looking at the micropore volumes of the networks discussed here, all networks are highly microporous but not exclusively so. This was

confirmed by the pore size distributions of the networks. Figure 80 below shows the comparison of all pore size distributions for the four homo-coupled networks. The majority of the pore sizes for the networks were present in the region of 10 Å to 20 Å. Comparing the pore size distributions, it was seen that some networks had a very similar pore size distribution. The networks with the highest surface area, synthesised from tetrakis(4-bromophenyl) methane (PAF-1 and TPM-Br), had the highest pore volume at 16 Å. These two networks were synthesised independently from another in two different laboratories, PAF-1 in Berlin by Arne Thomas' group and TPM-Br in our laboratories by myself. This shows that although the networks were synthesised in two different locations they are repeatable reactions, which gave rise to the same pore size distribution.

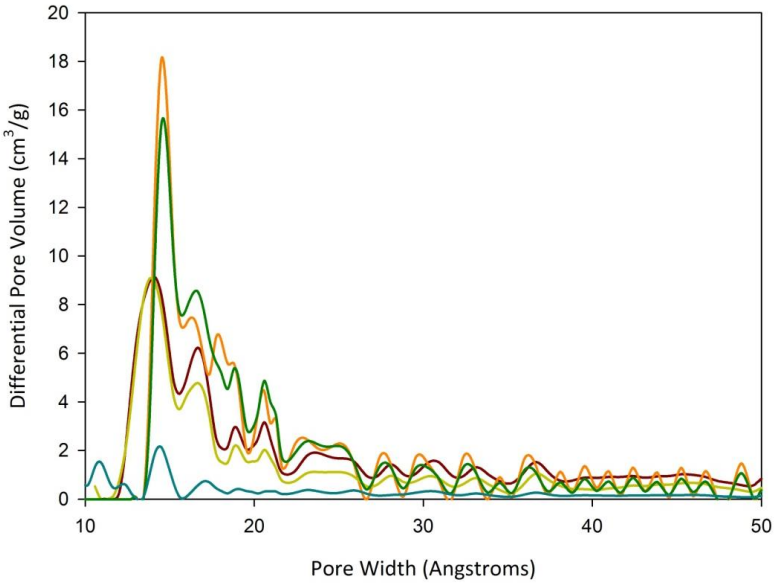

Figure 80: Pore Size Distributions of all PAF-1 type networks synthesised by Yamamoto coupling reaction (TPA-Br in maroon, TPM-Br in orange, TPM-I in yellow, PAF-1 (Berlin) in green, TPS-Br in turquoise)

Surprisingly, the pore size distributions for the networks synthesised from tetrakis(4-bromophenyl) adamantane and tetrakis(4-iodophenyl) methane (TPA-Br

and TPM-I, respectively) showed a very similar pore size distribution. It would have been expected that the TPA-Br network has a slightly larger pore size distribution, due to the size of the adamantane, than the carbon centred equivalent, TPM-I.

5.2.2.1 Gas Uptake in Yamamoto Coupled Networks

The focus in recent years was on hydrogen storage in MOFs, with numerous reviews published describing the recent progress.[21] Microporous organic materials have also been investigated and few reviews have been published.[22] COFs show significant amounts of adsorbed hydrogen when measured to saturation particularly the 3D COFs. COF-102 and 103 show 7.2 and 7.0 wt% respectively at 40bar and 77 K. Trip-PIM shows a hydrogen uptake of 1.63 wt% at 1 bar (77 K) and 2.71 wt% at 10 bar (77 K),[22b] while the PIM OFP-3 showed higher uptakes of 3.94 wt% at 10 bar (77 K).[23] Hypercrosslinked poly(vinylbenzyl chloride) showed a similar uptake to that of Trip-PIM at 10 bar of 2.75 wt%.[24] Hypercrosslinked DCX and BCMBP have shown some of the highest uptakes in HCPs of up to 1.69 wt% at 1 bar (77 K).[1] The highest surface area microporous organic polymer (PAF-1, 5600 m^2/g) has a reported absolute hydrogen uptake of 10.7 wt%[16] at 48 bar and 77 K which is the highest so far reported for any organic materials and exceeds that of many MOFs.[21a]

A number of groups have also investigated the storage of methane gas in microporous materials.[25, 11, 3] COFs have shown maximum uptakes of 10.9 mmol/g for COF-103 at a saturation pressure of 70 bar and 298 K.[11]

Carbon dioxide gas is one of the leading green house gasses and the burning of fossil fuels is its main source. The need for its capture is therefore apparent.[26] Amine containing materials have been used for the chemisorption of CO_2[27] while some of the best porous materials for CO_2 capture have been ZIFs which contain polar groups.[28] In COFs, maximum uptakes of CO_2 of 27.3 mmol/g at 35 bar and 298 K for COF-102.[11] PAF-1 reported a CO_2 uptake of 29.5 mmol/g at 40 bar and 298 K.[16]

The following figures show the hydrogen, carbon dioxide and methane gas uptakes for the four homo-coupled networks. The hydrogen uptake of the networks was shown in Figure 81. It showed that the adamantane network (TPA-Br) had the highest hydrogen uptake at 1 bar of 12 mmol/g. The network synthesised from tetrakis(4-iodophenyl) methane (TPM-I) had the next highest uptake of 11 mmol/g. This showed that the hydrogen uptake was not dependent on the surface area alone. A high surface area was desirable but a very narrow pore size distribution and high micropore volume, as was the case for these two networks, seems to be equally important.

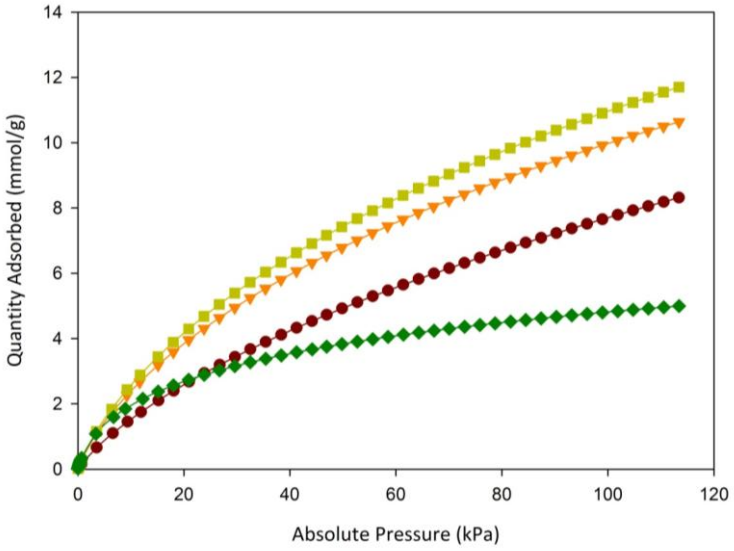

Figure 81: Hydrogen uptake (77 K) of all PAF-1 type networks (TPM-Br (maroon), TPM-I (orange), TPA-Br (yellow), TPS-Br (green))

The networks synthesised from tetrakis(4-bromophenyl) methane had a hydrogen uptake of 8.5 mmol/g and the network synthesised from tetrakis(4-bromophenyl) silane had a hydrogen uptake of 5.2 mmol/g. One would expect the hydrogen uptake for the TPM-Br network to be higher than it is when looking at the surface area of the network. This was the network with the highest surface area and it was expected that this network also would have had the highest hydrogen uptake. However, as Dawson et al.[29] have shown, the prediction of gas uptake at 1 bar from its surface area was not necessarily correct. All networks but the silane network (TPS-Br) showed that they have not reached maximum saturation; that is, the common 'plateau' in gas uptake was not reached and the gas uptake could therefore increase further at higher pressures. It was expected that the hydrogen uptake at higher pressures would increase compared to the measurements taken up to 1 bar. Measurements were only carried out to 1 bar initially to assess the gas

uptake ability of the networks, to give an initial idea if the particular material had a promising gas uptake.

Figure 82 below shows the carbon dioxide uptake of the homo-coupled networks discussed here. It was observed that all networks had not reached their maximum saturation at 1 bar. It was expected that the uptake will increase at higher pressures. The measurements at 1 bar give a good indication if the networks adsorb CO_2 and therefore if they are suitable as CO_2 capture materials. CMP type networks have shown higher CO_2 uptakes at higher pressures.

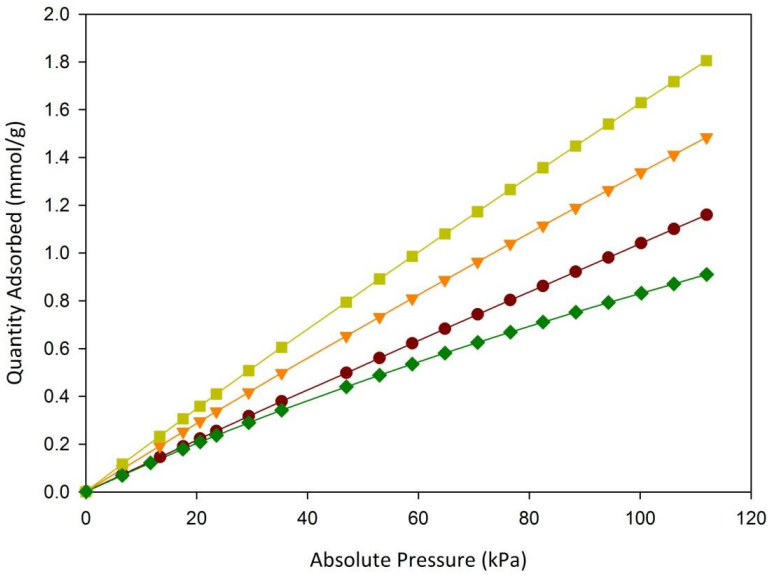

Figure 82: CO_2 uptake of all Yamamoto homo-coupled PAF-1 type materials at 1 bar, 300 K (TPM-Br in maroon (circles), TPM-I in orange (triangles down), TPA-Br in yellow (squares), TPS-Br in green (diamonds))

Considering the CO_2 uptake of all networks (Figure 82) it was seen that again the adamantane (TPA-Br) and the iodo network (TPM-I) had the highest uptake. The TPA-Br network had an uptake of 1.8 mmol/g and the TPM-I network had an uptake of 1.5 mmol/g. The higher surface area network, TPM-Br, had a lower CO_2 uptake, compared to the TPA-Br and TPM-I networks, of 1.15 mmol/g and the silane

network, TPS-Br, had an uptake of 0.9 mmol/g. The low gas uptake of the high surface area network (TPM-Br) was surprising. It showed that the gas uptake was not dependent on surface area alone.[29c] Comparing the gas uptake of TPM-Br and TPA-Br, it seemed as though the correct pore size[30] was more important than the surface area of a material. This was proven when considering that TPS-Br had only a quarter of the surface area of TPM-Br but had a similar gas uptake. The pore size of TPS-Br was comparable with TPA-Br, although with less volume. Therefore, the pore size[31] had an influence on the gas uptake ability of a material.

Figure 83 below shows the methane uptake of all PAF-1 type materials at 1 bar. The same trend as before was observed with TPA-Br having the highest uptake (0.6 mmol/g), TPM-I the next highest (0.55 mmol/g), TPM-Br with 0.45 mmol/g and TPS-Br with the lowest uptake (0.3 mmol/g). This again showed that the surface area was not the most important influence on the gas uptake.

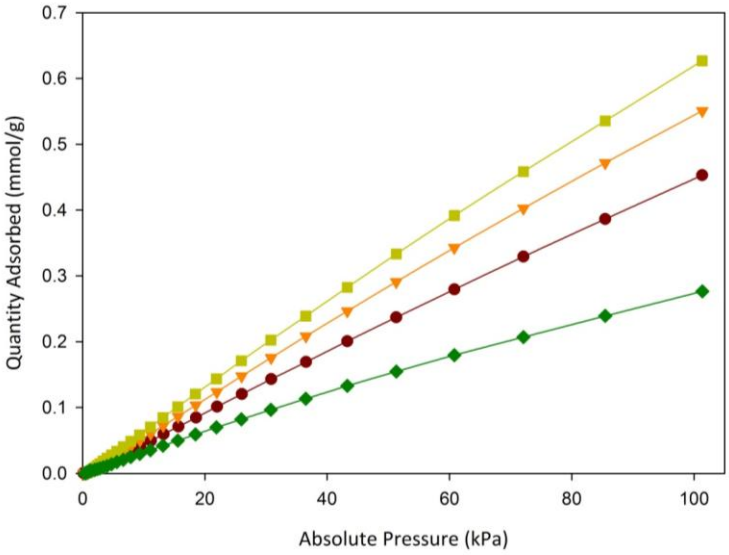

Figure 83: CH_4 uptake of all Yamamoto homo-coupled PAF-1 type materials at 1 bar, 300 K (TPM-Br in maroon (circles), TPM-I in orange (triangles down), TPA-Br in yellow (squares), TPS-Br in green (diamonds))

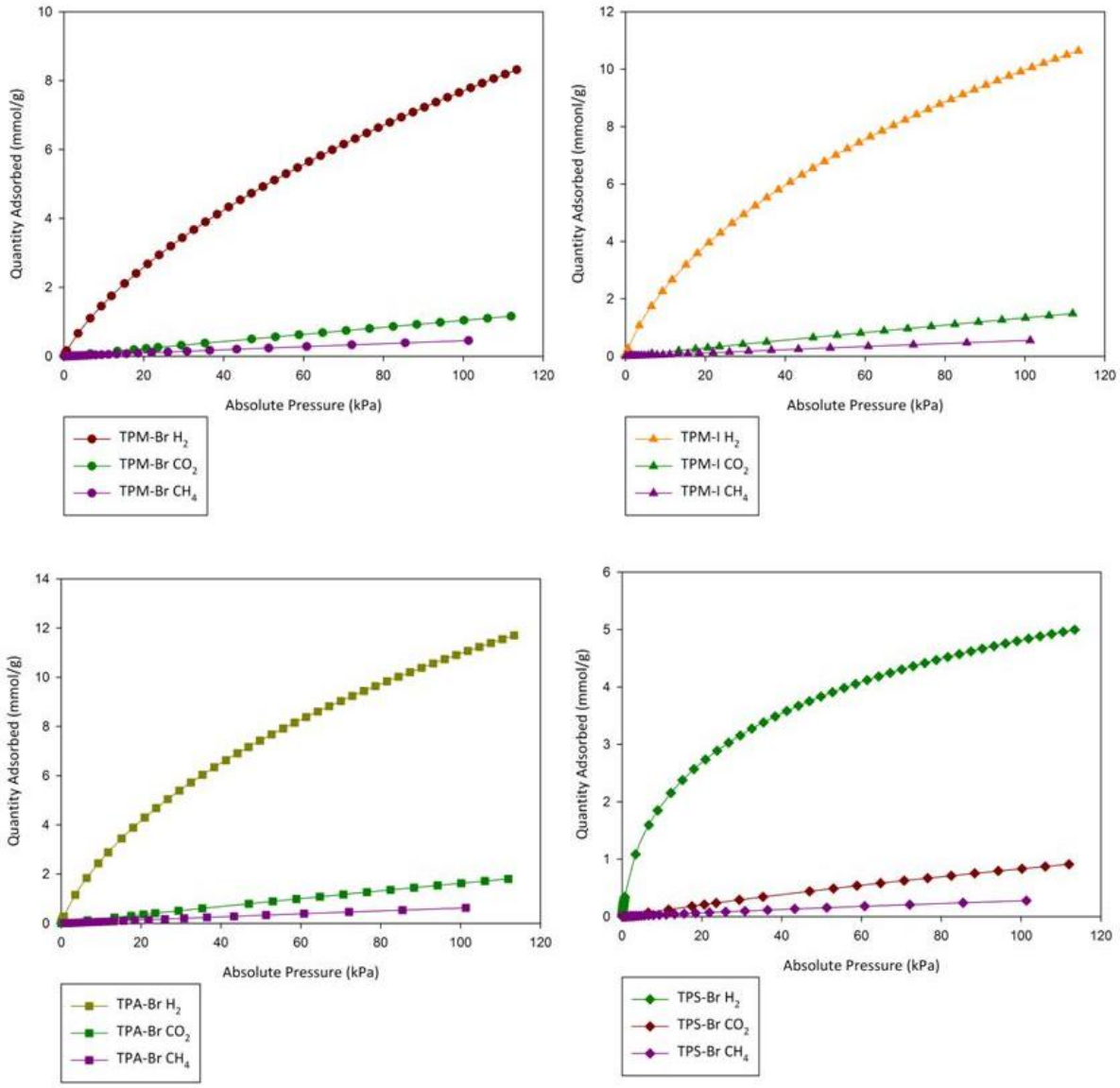

Figure 84: Comparison of all gas uptakes measured for all homo-coupled networks (top left TPM-Br network, top right TPM-I network, bottom left TPA-Br network, bottom right TPS-Br network), hydrogen collected at 77 K, carbon dioxide collected at 300 K, methane collected at 300 K

This showed that the high surface area materials synthesised from tetrakis(4-bromophenyl) methane, tetrakis(4-bromophenyl) adamantane, tetrakis(4-iodophenyl) methane and tetrakis(4-bromophenyl) silane were all promising hydrogen storage materials with hydrogen uptakes of up to 2.4 wt% (12 mmol/g, TPA-Br). Although this hydrogen uptake was not as high as anticipated by the DoE, it was a good result for an organic material.

5.2.3 Templating Effect (Chapter 4)

The following results are based on the gas sorption measurements for the reactions discussed in Chapter 4, where PEG300 and PEG550 were used as templating agents in an attempt to increase surface area and gas uptake.

Table 15 below shows the comparison of the BET surface areas and the pore volumes of the networks synthesised by Sonogashira cross-coupling reaction between 1,4-diethynylbenzene and tetrakis(4-iodophenyl) methane with PEG300 as templating agent. The original surface area of the E-1 network was 1213 m^2/g with a total pore volume of 0.65 cm^3/g at $p/p_0 = 0.9$.

Table 15: surface areas and pore volumes for E-1 networks templated with PEG300

	$SA\ (m^2/g)$	$V_{tot}\ (cm^3/g)$
original E1	1210	0.65
E1-DMF	1130	0.93
E1-DMF/PEG 300 (75/25)	1330	1.31
E1-DMF/PEG 300 (50/50)	1100	1.12
E1-DMF/PEG 300 (25/75)	820	0.55
E1-DMF/PEG 300 (10/90)	1050	0.51
E1-PEG 300	890	0.45

Comparing the pore volumes it was seen that by changing the solvent from toluene to DMF the pore volume increases from 0.65 cm^3/g to 0.93 cm^3/g, while the surface area decreased. This, most likely, means that an increase in macropores occurred as the increase in pore volume with a decreased surface area was only achieved if a larger amount of macropores was present. The pore size distribution

for the original E-1 network, synthesised in toluene was very narrow (Figure 83, black), with pores almost exclusively of approximately 10 Å being present.

Initially, one can observe an increase in pore volume when adding a templating agent. After initial addition of a low concentration, 25 %, of PEG300 the pore volume decreased again and when the reaction was run solely in PEG300 the pore volume was lowest. This showed that the network formation was hindered by the templating agent. The low solubility of the monomers is decreased further, when increasing the concentration of the template, and the network cannot be formed, resulting in a low surface area and a low pore volume.

The same trend can be observed when increasing the molecular weight of the template to PEG550 (Table 16). The surface areas are slightly increased but not significantly.

Table 16: surface areas and pore volumes for E-1 networks templated with PEG550

	SA (m^2/g)	*V_{tot} (cm^3/g)*
original E1	1210	0.65
E1-DMF/PEG 550 (90/10)	1330	1.41
E1-DMF/PEG 550 (75/25)	1350	1.59
E1-DMF/PEG 550 (50/50)	1310	0.63
E1-DMF/PEG 550 (25/75)	1300	0.62
E1-DMF/PEG 550 (10/90)	1115	0.59
E1-PEG 550	1210	0.54

By introducing a template to the reaction, PEG550 in this case, the pore volumes initially increased by a factor of 2.4 when reaching a concentration of 25 % of PEG550. After this initial increase the pore volumes decreased again, reaching the lowest value when the reaction was run solely in PEG550. This showed again that the network was not formed to the same degree of condensation as when synthesised without a template present.

Figure 85 below shows the comparison of the pore size distributions of original E-1 network and template E-1 network.

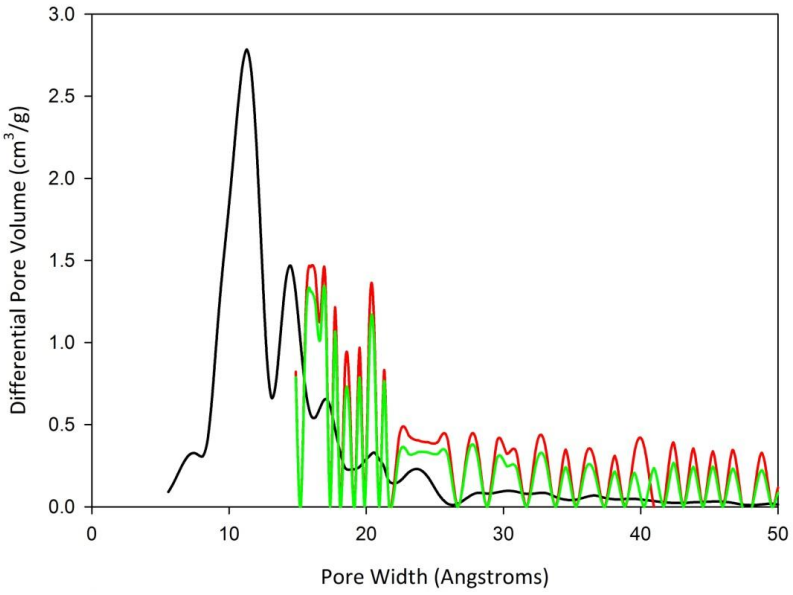

Figure 85: Pore size distribution of original E-1 network (black), E-1 in DMF templated with 50 % PEG 300 (red, E-1 synthesised in 100 % PEG550 (green)

As was seen from the pore size distributions the amount of meso pores was increased significantly. The pore size distribution for E-1 synthesised in DMF[29b] was very similar to the distribution of the original E-1 network synthesised in toluene. The difference in distribution therefore arose from the template and not from the change in solvent.

Table 17 below shows a summary of the surface areas for the E-1 network, with changing the concentration of the reaction and adding 50 % template into the solvent system. The surface areas were all lower than the original surface of 1213 m^2/g.

Table 17: Summary of surface areas for E-1 network with varying amounts of PEG550 and with varying concentration (a) BET surface area

	Volume DMF (ml)	Volume PEG550 (ml)	Surface Area (m^2/g)[a]
1	25	0	1130
2	50	0	1205
3	100	0	1020
4	12.5	12.5	855
5	25	25	970
6	50	50	1000

The dilution of the reaction was initially increased from the original 5 ml to 25 ml. The surface area decreased slightly from the original 1200 m^2/g to 1130 m^2/g. Decreasing the concentration further to 50 ml, the surface area rose to 1200 m^2/g and then decreased again to 1000 m^2/g when decreasing the concentration further to a 100 ml scale. This showed that the dilution of the reaction did not influence the surface area. The idea of decreasing the concentration arose from the synthesis of the PAF-1 networks, which was done at a lower dilution of 120 ml than the original E-1 network, with an increased surface area.

Figure 86 shows a selection of CO_2 sorption measurements. The selection of the networks was based on their surface areas. The highest surface areas were selected from the networks synthesised with varying amounts of templating agent (Table 4) and from the dilution study (Table 5). It is noticeable that all CO_2 uptakes,

carried out at 300 K, are very similar no matter what the dilution or the amount of template in the reaction. The networks take up about 7.5 wt% (38 cm^3/g) of CO_2 at 1 bar. When decreasing the temperature to 273 K (blue circles) for the network synthesised in DMF only, an uptake of 10.8 wt% (55 cm^3/g) can be measured. This shows that the gas uptake of CO_2 is dependent on the temperature the measurement was taken at. The difference of running the measurements around freezing or at room temperature makes a large difference to the uptake of CO_2 in the network.

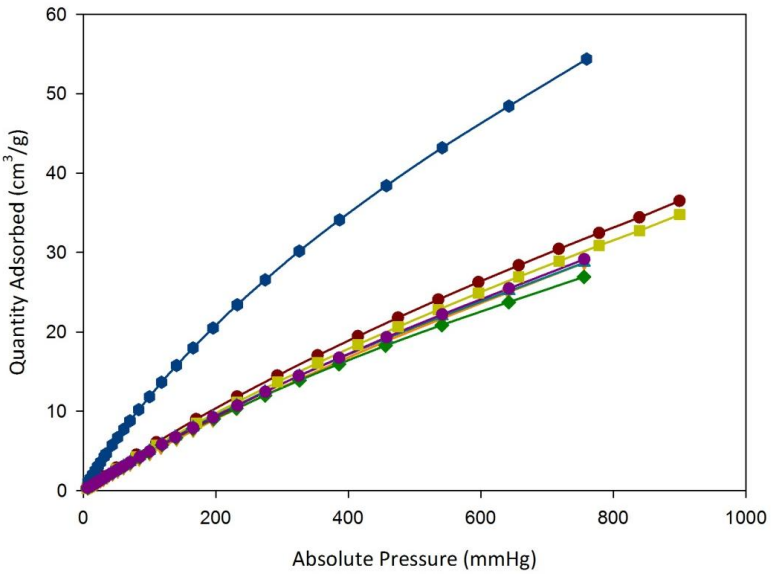

Figure 86: CO_2 adsorption of the E-1 network at different dilutions, all measurements carried out at 300 K unless otherwise stated, (50 ml DMF (red circles), 5 ml DMF/PEG300 (75/25) (orange triangles down), 5 ml PEG550 (yellow squares), 50 ml PEG300 (green diamonds), 5 ml DMF (300 K) (turquoise triangle up), 5 ml DMF (273 K) (blue circles), 5 ml DMF/PEG500 (75/25) (purple circles))

The adsorption of 7.5 wt% (1.7 mmol/g) of CO_2 for these networks compares very well to other microporous organic polymers.[29b] Dawson et al. compared different microporous polymers and the only polymer that performs better than these networks is a triazine network (C, blue squares)[29b] with an uptake of 2.2 mmol/g.

Figure 87 shows a comparison of CH_4 uptake of the E-1 networks synthesised at different concentrations and in combination with templating agents. Again, the highest surface area materials were chosen. The highest methane uptake was reached with the network synthesised in 5 ml DMF/PEG300 (75/25) (turquoise triangles up) of 2.1 wt% (30 cm^3/g, 1.3 mmol/g). The next highest uptake was reached by the network synthesised in 5 ml DMF (yellow squares) of 1.8 wt% (25 cm^3/g, 1.1 mmol/g). This shows that the template has a small influence on the gas uptake. By using PEG300 as the template, the methane uptake was increased by 0.3 wt% compared to the same reaction carried out in DMF without templating agent. The type of template also seems to play a role in the methane uptake of the network. When using PEG300 instead of PEG550 (green diamonds) as the template a decrease in methane uptake of 0.5 wt% can be observed. The solvent system of the reaction - that is, solvent plus template - plays an important role in the gas uptake of the network.

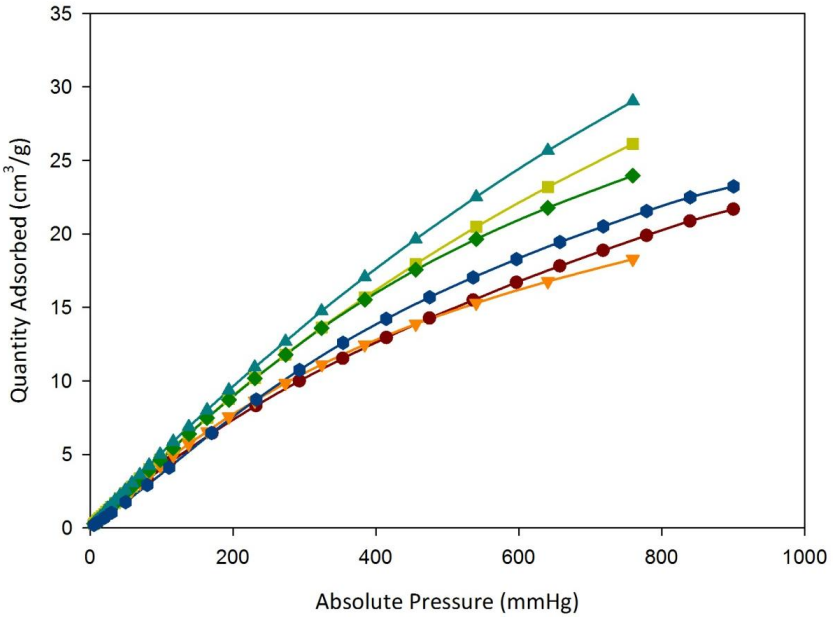

Figure 87: CH_4 adsorption of the E-1 network at different dilutions, all measurements carried out at 300 K, (50 ml DMF (blue circles), 5 ml DMF/PEG300 (75/25) (turquoise triangles up), 5 ml PEG550 (red circles), 5 ml PEG300 (orange triangles down), 5 ml DMF (yellow squares), 5 ml DMF/PEG550 (75/25) (green diamonds))

Increasing the amount of solvent used in the reaction decreased the methane adsorption. By increasing the dilution by a factor of ten (blue circles) compared to the original reaction mixture (yellow squares) the methane uptake was decreased by 0.3 wt% from 1.8 wt% (25 cm^3/g, 1.1 mmol/g, yellow squares) to 1.5 wt% (15 cm^3/g, 0.9 mmol/g). This shows that a lower concentration of the reaction did not positively influence the methane uptake of the network. The least amount of methane was adsorbed by the networks synthesised in PEG550 (red circles) and PEG300 (orange triangles down). Both networks adsorbed around 1.3 wt% of methane at 1 bar.

Table 15 below shows a summary of the surface areas of the E-2 type networks synthesised with varying amounts of template and varying concentrations. The increase in dilution of the reaction arose from the previous reactions to form PAF-1 type polymers, which are carried out at a dilution of 120 ml and increases and results in a material with a very high surface area.[16]

The original surface area of the E-2 network was 500 m^2/g.[32] By increasing the dilution of the reaction system, the surface area was almost quadrupled to 1900 m^2/g. This shows that the concentration of the reaction system can have an influence on the surface area.

Table 18: Summary of surface areas for E-2 network with varying amounts of PEG550 and with varying concentration (a) BET surface area

	Volume DMF (ml)	Volume PEG550 (ml)	Surface Area (m^2/g)[a]
1	25	0	1900
2	50	0	1750
3	100	0	1810
4	12.5	12.5	1325
5	25	25	1300
6	50	50	1350

By introducing a templating agent, PEG550 in this case, the surface area was decreased again but it is still higher than the original surface area. Based on these results it was decided to measure the gas uptake ability of all six networks (Figure 88).

Firstly, comparing the pore size distribution of the networks (Figure 88 top left), shows that all networks have the same distribution of pore sizes. The highest volume of pores is shown at the highest and lowest dilution without added templating agent (blue and orange). When introducing a templating agent into the reaction the pore size distributions are the same up to 40 Å (turquoise, red, yellow) and are only marginally different after that. Again, the lowest dilution had the highest volume in pores and the highest dilution the lowest volume of pores. This showed that the concentration of the reaction was highly important for the surface area and for the pore size distribution. The dilution did not alter the distribution of pores but influenced the volume of pores present.

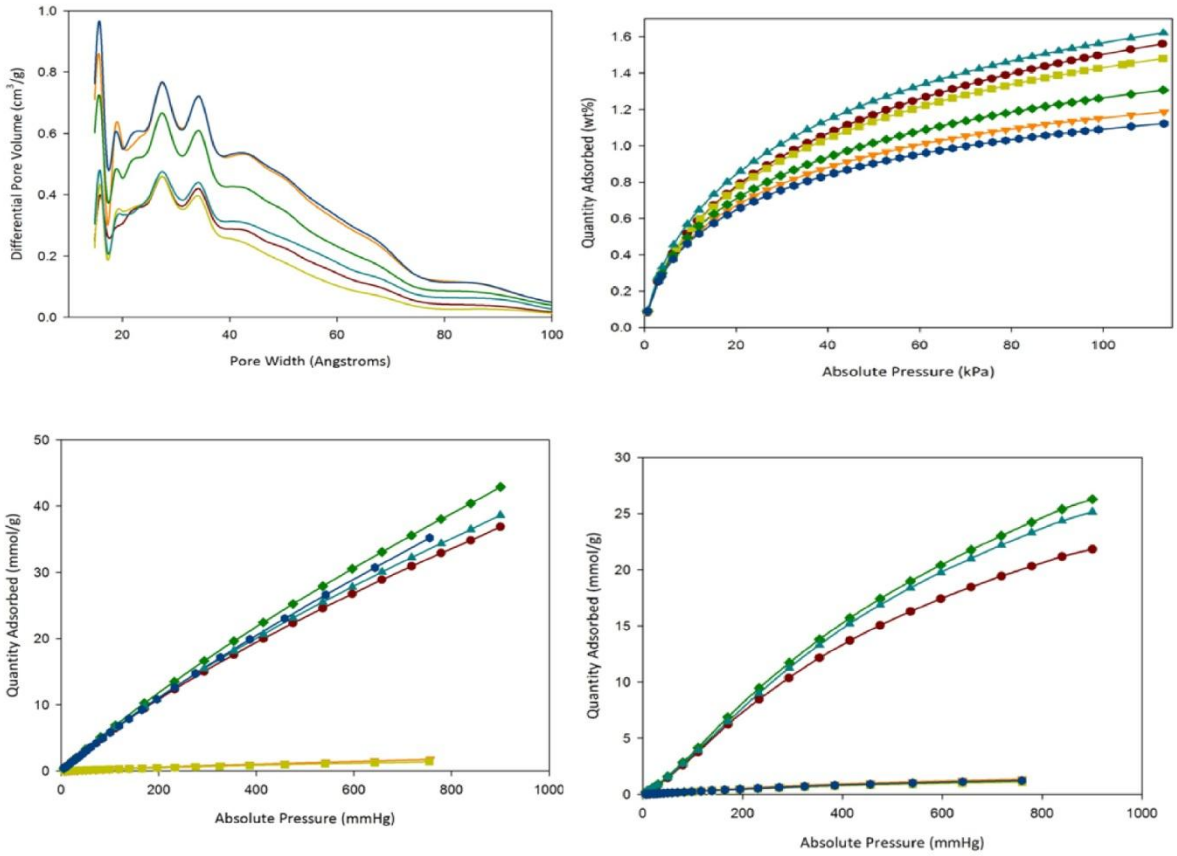

Figure 88: top left pore size distribution, top right hydrogen uptake, bottom left carbon dioxide uptake, bottom right methane uptake

Looking at the hydrogen uptake (Figure 88, top right), it can be seen that the highest dilution (100 ml, turquoise triangles up) without added template, also had the highest hydrogen uptake of 1.6 wt%. The network synthesised in 25 ml DMF (red circles) had a hydrogen uptake of 1.5 wt% and the medium dilution reaction (50 ml DMF, yellow squares) adsorbed 1.4 wt% of hydrogen. The differences between these uptakes did not correlate with the trend in surface area. The highest surface area material (25 ml DMF) did not have the highest hydrogen uptake. When introducing a template into the reaction the hydrogen uptake was decreased like the surface area. This showed that the template, PEG550 in this case, did not

increase the hydrogen uptake for these types of networks. The concentration of the reaction was more important than the addition of a templating agent.

Regarding the CO_2 uptake of these networks (Figure 88, bottom left), it was seen that two of the six networks, the network synthesised in 50 ml DMF/PEG550 and in 100 ml DMF, were not porous to CO_2. The remaining four networks had a CO_2 uptake between 35 cm^3/g and 40 cm^3/g (6.9 wt% to 7.8 wt%) with the network synthesised in 50 ml DMF having the highest uptake. This network did not have the highest surface area and thus this showed that the surface area was not directly related to the CO_2 uptake. These networks again compared very well to other microporous organic networks discussed by Dawson et al.[29b] Again as discussed by Dawson et al. this uptake was slightly smaller than the CO_2 uptake of a triazine network (C, blue squares).[29b]

Looking at the CH_4 uptake (Figure 88, bottom right) of these six networks it was observed that three of the six networks were not porous to CH_4. The three networks porous to methane were the networks synthesised in 50 ml DMF, in 25 ml DMF/PEG550 and in 100 ml DMF/PEG550. The networks had uptakes of 1.8 wt%, 1.7 wt% and 1.6 wt% respectively.

5.3 Conclusion

In conclusion, the amount of catalyst has relatively little influence on the porosity of the networks discussed here and previously in Chapter 2. The base has a greater influence, increasing the surface area of some networks significantly.

Although the surface areas for the Yamamoto homo-coupled networks are not the same or higher as the reported surface area for PAF-1, it can be seen that the networks are selectively porous to hydrogen. The carbon dioxide and methane uptake was also measured and found to be very low compared to the hydrogen uptake. This shows that the networks are good storage materials for hydrogen.

By using a templating agent, PEG300 or PEG550, the surface area for one of the two networks discussed here was increased by a factor of 4. The pore volume of the networks was initially increased with a small amount of template present, up to 25 %, but when adding more template the pore volume was decreased.

5.4 References

[1] Wood, C. D. *et al., Chem. Mat*., **2007**, *19*, 2034-2048

[2] Martín, C. F., *et al., J. Mater. Chem.,* **2011**, *21*, 5475-5483

[3] Wood, C. D., *et al., Adv. Mater*., **2008**, *20*, 1916-21

[4] http://web.mac.com/jeremytitman/Solid-state_NMR_Group/Lectures_files/Lecture7.pdf (accessed 9/08/11)

[5] Laws, D. D., *et al., Angew*. *Chem*. *Int*. *Ed*., **2002**, 41, 3096 - 3129

[6] http://mutuslab.cs.uwindsor.ca/schurko/ssnmr/ssnmr_schurko.pdf (accessed 22/08/11)

[7] (a) Morris, R. E., *Angew. Chem. Int. Ed.***, 2008,** 47 (27), 4966–4981 (b) Menon, V. C., Komarneni S., *Journal of Porous Materials,* **1998**, 5 (1), 43-58

[8] http://www.ak-tremel.chemie.uni-mainz.de/literature/10.1038_35104634.pdf

[9] Linga, P., *et al., Journal of Hazardous Materials*, **2007,** 149 (3), 625-629

[10] Favre, E., *Journal of Membrane Science***, 2007**, 294 (1-2), 50-59

[11] Furuka, H., Yaghi, O., M., *J. Am. Chem. Soc.,* **2009**, 131, 8875

[12] (a) Eddaoudi, *et al., Science,* **2002***,* 295 (5554), 469-472 (b) Furukawa, H. *et al., J. Am. Chem. Soc.*, **2009**, 131 (25), 8875–8883

[13] http://www.sigmaaldrich.com/catalog/ProductDetail.do?lang=en&N4=02391|FLUKA&N5=SEARCH_CONCAT_PNO|BRAND_KEY&F=SPEC (accessed 09/08/11)

[14] Jiang, J., *et al., Angew. Chem. Int. Ed*., **2007**, *46*, 8574-8578

[15] Dawson, R., *et al., Macromolecules*, **2010**, *43*, 8524-8530

[16] Ben, T., *et al.*, *Angew. Chem. Int. Ed.*, **2009**, *48*, 9457 –9460

[17] Yuan, D., *et al.,Advanced Materials***, 2011**, 23 (12), 3723–3725

[19] Coutinho, D., *et al., Microporous and Mesoporous Materials,* **2005**, 81 (1-3), 321-332

[20] Trewin, A., Cooper, A. I., *Angew. Chem. Int. Ed.,* **2010**, 49, 1533-1535

[21] (a) Murray, L. J., *et al.*, *Chem. Soc. Rev.*, **2009**, 38, 1294 ; (b) Morris, R. E., *et al.*, *Angew. Chem. Int. Ed.*, **2008**, 47, 4966; (c) Xiao, B., *et al.*, *Particuology*,

2009, 7, 129; (d) Dinca, M., *et al.*, *Angew. Chem. Int. Ed.*, **2008**, 47, 6766 ; (e) Han, S. S., *et al.*, *Chem. Soc. Rev.*, **2009**, 38, 1460 ; (f) Hirscher, M., *et al.*, *Scripta Materialia*, **2007,** 56, 809; (g) Collins, D. J., *et al.*, *J. Mater. Chem.*, **2007**, 17, 3154; (h) Hirscher, M., *et al., Microporous Mesoporous Mater.*, 129, 335

[22] (a) Svec, F., *et al., Small*, **2009**, 5, 1098; (b) McKeown, N. B., *et al., Macro. Rap. Comm.*, **2007**, 28, 995; (c) Budd, P. M., *et al., Phys. Chem. Chem. Phys.*, **2007**, 9, 1802

[23] Makhseed, S., *et al., Chem. Comm.*, **2008**, 4342

[24] Lee, J. Y., *et al.*, *Chem. Comm.*, **2006**, 2670

[25] Duren, T., *et al.*, *Langmuir*, **2004**, 20, 2683

[26] (a) Arenillas, A., *et al.*, *Fuel*, **2005**, 84, 2204; (b) Holloway, S., *Energy*, 30, 2318

[27] Figueroa, J. D., *et al., International Journal of Greenhouse Gas Control*, **2008**, 2, 9

[28] (a) Banerjee, R., *et al., Science*, **2008**, 319, 939; (b) Banerjee, R., *et al., J. Am. Chem. Soc.*, **2009**, 131, 3875

[29] (a) Dawson, R., *et al., Macromolecules*, **2010**, *43*, 8524-8530, (b) Dawson, R., *et al., Energy Environ. Sci.,* **2011** DOI: 10.1039/C1EE01971F, (c) Dawson, R., *et al.,* ***Chem. Sci.***, 2011, **2**, 1173-1177

[30] Lowell, S., *et al., Characterization of porous solids and powders: surface area, pore size, and density*, **2004,** Kluwer Academic Publishers

[31] Lozano-Castelló, D., *et al., Carbon*, **2002**, 40 (7), 989-1002

[32] Stöckel, E., *et al., Chem. Commun*., **2009**, 212-214

Chapter 6

Experimental Section

6.1 Chemicals

The following reactions were carried out on a Radleys 6 or 12 place carousel unless otherwise stated. The external temperature was measured. All reactions were carried under N_2 atmosphere using standard schlenk techniques. All glassware was dried in an oven at approx. 100°C for 12 hours prior to the reaction. Bis[(trifluoroacetoxy)iodo] benzene (97 %), carbon tetrachloride (anhydrous ≥ 99.5 %), chloroform (anhydrous ≥ 99.5 %), 1-bromoadamantane (99 %), benzene (99 %), *tert*-butyl bromide (98 %), 1,4-diethynylbenzene (96 %) , bis(triphenylphosphine) palladium(II) dichloride (99 %), tetrakis(triphenylphosphine) palladium(0) (99%), copper iodide (99 %), toluene (anhydrous 99.8 %), *N,N*-dimethylformamide (anhydrous 99.8 %), PEG300 (M_n 285-315), PEG550 (average mol wt 550; 50:50 blend of m.w. 300 Da and 1,450 Da), triethylamine (anhydrous 99 %), diisopropylamine (purified by redistillation, 99.95 %), *cis,cis*-1,5-cyclooctadiene (98 %), 2,2′-bipyridyl (98 %), 1,3,5-tribromobenzene (98 %), 1,2,4,5-tetrabromobenzene (97 %) and 1,4-dibromobenzene (98 %) were purchased from Sigma Aldrich and used as received. Tetraphenylmethane (99 %) was purchased from Alfa Aesar and used as received. 1,3,5-Triethynylbenzene (99 %) and bis(1,5-cyclooctadiene)nickel(0) (98 %) were purchased from ABCR and used as received. Iodine (99 %), tetrahydrofuran (HPLC grade), sodium hydroxide (99 %), bromine (98 %), ethanol (analytical grade), sodium bisulfite (99 %), chloroform (HPLC grade), $AlCl_3$ (99 %), methanol (AR), acetone (AR) and concentrated HCl (11.3 M) were purchased from Fisher Scientific and used as received.

6.2 Gas Sorption Analysis

Surface areas were measured by nitrogen adsorption and desorption at 77.3 K using either a Micromeritics ASAP 2420 or a Micromeritics ASAP 2050 volumetric adsorption analyzer. Samples were degassed 120 °C for 15 h under vacuum (10^{-5} bar) before analysis. The BET surface areas were calculated over 0.01 to 0.2 bar. Pore size distributions and pore volumes were derived from the adsorption branches of the isotherms using the nonlocal density functional theory model (NL-DFT) for pillared clay with cylindrical pore geometries found within the Micromeritics ASAP software.

Hydrogen, carbon dioxide and methane isotherms up to 1 bar were measured at 77.3 K, 300 K and 300 K respectively using a Micromeritics ASAP 2420 and 2020 volumetric adsorption analyzer.

6.2.1 BET Theory

The BET theory is an explanation of the adsorption of gas molecules on a solid surface. It is the basis for the analysis of the materials, such as microporous polymeric materials discussed in this thesis, by surface area measurements. The theory was first published in JACS by Stephen Brunnauer, Paul H. Emmett and Edward Teller in 1938.[1] The theory is an extension of the Langmuir theory. As discussed previously the Langmuir theory only considers monolayer molecular adsorption. In the BET theory, the monolayer adsorption is further developed to take multilayer adsorption into consideration. In the BET theory, the following assumptions are made:

(a) gas molecules are physically adsorbed on a solid in infinite layers,

(b) there is no interaction between each adsorption layer,

(c) the Langmuir theory can be applied to each layer.

The BET equation can be expressed by (1)

$$\frac{1}{v\,[(P_0 / P) - 1]} = \frac{c - 1}{v_m c}\left(\frac{P}{P_0}\right) + \frac{1}{v_m c} \quad \textbf{(1)}$$

where, p and p_0 are the pressures where equilibrium and saturation, respectively, of the adsorbate at the temperature of adsorption is reached. υ is the quantity of gas adsorbed and υ_m is the quantity adsorbed onto the monolayer. C is the BET constant, which is expressed by (2)

$$c = \exp\left(\frac{E_1 - E_L}{RT}\right) \quad \textbf{(2)}$$

where, E_1 is the heat of adsorption for the first layer of adsorbate and E_L is the heat of adsorption for all following layers. Equation (1) is an adsorption isotherm and can be plotted as a straight line with $1/v[(p/p_0)-1]$ on the y-axis and $\phi = p/p_0$ on the x-axis (Figure 11).

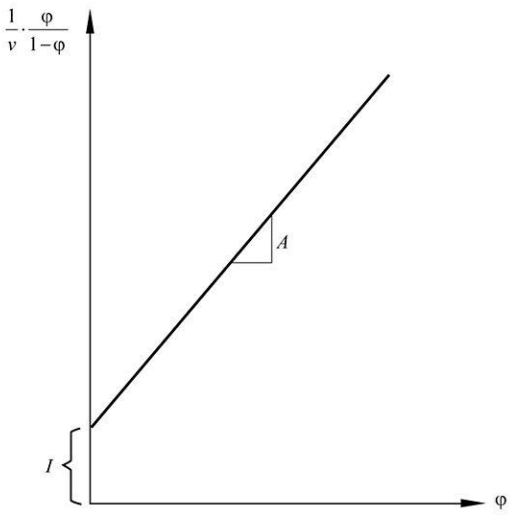

The linear relationship can only be maintained in the region of $0.05 < p/p_0 < 0.35$. The slope *A* and the y-intercept *I* are used to calculate v_m and *c*. The following equations can be applied:

$$v_m = \frac{1}{A + 1} \quad (3)$$

$$c = 1 + \frac{A}{I} \quad (4)$$

By application of the BET theory the surface area of solids through physisorption of gas molecules can be calculated by the following equation:

$$S_{BET,\ total} = \frac{(v_m N s)}{V} \quad (5)$$

where, *N* is Avogadro's number, *s* is the adsorption cross section of the adsorbing species and *V* is the molar volume of adsorbate gas. The total surface area S_{total} divided by the amount of adsorbent *a* in grams gives the specific or BET surface area, S_{BET}.

$$S_{BET} = \frac{S_{total}}{a} \quad (6)$$

6.3 Infra-red Spectroscopy

IR spectra were collected in reflectance mode using a Bruker Tensor 27 fitted with HT-XTS and cooled with liquid N_2.

6.4 Solution Nuclear Magnetic Resonance

^{1}H NMR spectra were recorded at 400.13 MHz using a Bruker Avance 400 NMR spectrometer. ^{13}C NMR spectra were recorded at 100.6 MHz. Deutereated solvents as specified were obtained from Sigma Aldrich and used as received. Spectra were referenced to TMS.

6.5 Thermogravimetric Analysis

TGA analysis was carried out using a Q5000IR analyzer (TA instruments) with an automated vertical overhead thermobalance. The samples were heated at a rate of 5 °C/min under a flow of nitrogen to 1000 °C. Air was supplied from a gas cylinder obtained from BOC and streamed across the sample at 5 °C/min.

6.6 Monomer Synthesis

6.6.1 Iodination of tetraphenylmethane[6]

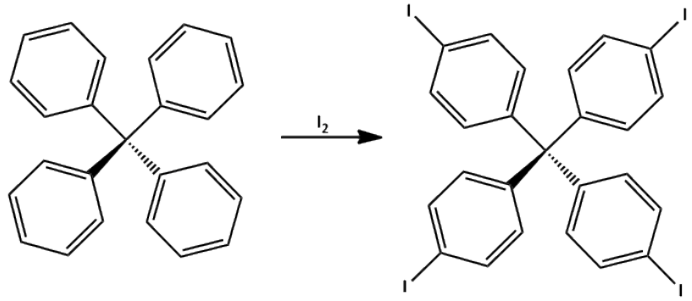

Tetraphenylmethane (7.53g, 23.5 mmol), bis[(trifluoroacetoxy)iodo] benzene (23.48g, 54.6 mmol) and iodine (12.64g, 49.8 mmol) were dissolved in 150 mL of carbon tetrachloride (alternatively chloroform can also be used). The reaction was heated to 60°C until the iodine colouration disappeared. This generally took 3 - 12 hours depending on the scale. The solvent was removed under reduced pressure

and the residue was washed excessively with methanol, and acetone until the filtrate ran clear. The purity of the tetrakis(4-iodophenyl) methane was checked, after drying overnight in a vacuum oven, by NMR and if necessary recrystallised from THF to give the pure product as a white to lightly pink coloured solid. Average of 60% yield; ^{1}H-NMR ($CDCl_3$, 400 MHz) δ 7.6 (J = 8.79 Hz; 8H, d), δ 6.9 (J = 8.8 Hz; 8H, d); ^{13}C-NMR ($CDCl_3$, 100 MHz) δ 64.3, δ 77 ($CDCl_3$), δ 92.1, δ 129.9, δ 138.3; Anal. calcd for $C_{25}H_{16}I_4$: C, 36.44; H, 1.96; I, 61.60. Found: C, 36.41; H, 1.96.

6.6.2 Bromination of tetraphenyl methane[7]

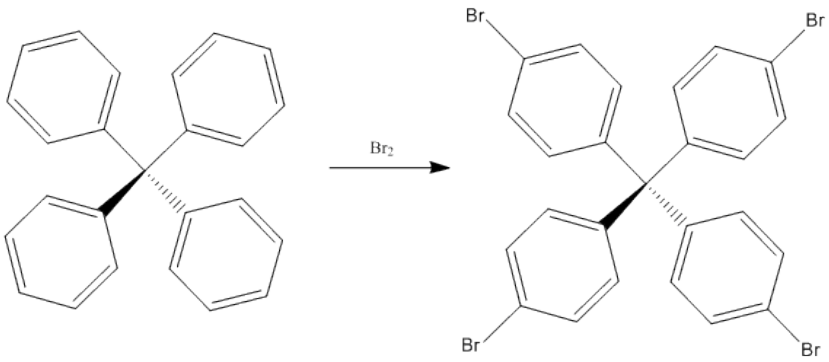

A 250 mL round-bottomed flask was equipped with a stirrer bar. An outlet adaptor was connected via rubber tubing to a pipette, which was immersed in an aqueous sodium hydroxide solution. Tetraphenylmethane (18 g, 0.056 mol) was added. Bromine (20 mL) was added slowly over the next 5 minutes via a dropping funnel, while the reaction mixture was stirred. The gaseous hydrobromic acid developed was guided via the rubber tubing in to the solution of sodium hydroxide to neutralise it. The slurry was stirred for a further 20 minutes and then poured into ethanol (250mL), cooled on a dry-ice/acetone bath. The precipitate was filtered and washed with aqueous sodium bisulfite solution and recrystallised from chloroform/ethanol to give the product as an off-whit solid. 93% yield; ^{1}H-NMR

($CDCl_3$, 400 MHz) δ 7.4 (J = 8.7 Hz; 8H, d), δ 7.0 (J = 8.7 Hz; 8H, d); ^{13}C-NMR ($CDCl_3$, 100 MHz) δ 144.5, δ 132.4, δ 130.8, δ 120.7, δ 77 ($CDCl_3$), δ 63.6; Anal. calcd for $C_{25}H_{16}Br_4$: C, 47.21; H, 2.54; Br, 50.25. Found: C, 46.68; H, 2.47.

6.6.3 Synthesis of tetraphenyladamantane[8]

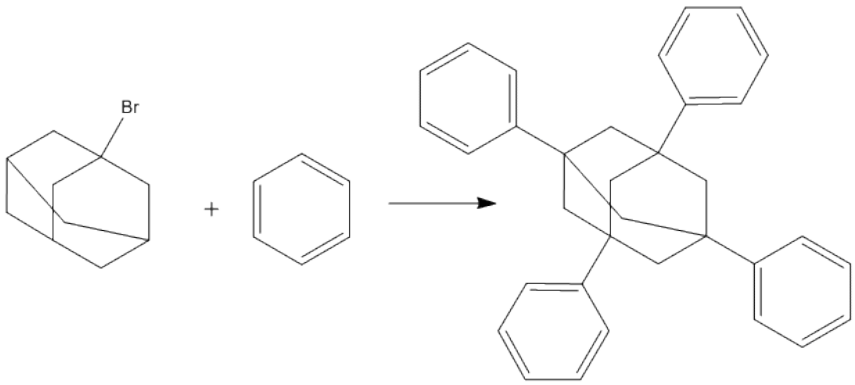

This reaction was not carried out on a Radleys carousel. A dry 1 L 3-neck-round-bottomed flask was equipped with 2 condensers, 2 outlets leading to a 30% NaOH solution, a N_2 inlet and a stirrer bar. The flask was placed in an ice-bath and cooled for several minutes. 1-Bromoadamantane (30g, 0.14mol), benzene (300mL) and *tert*-butyl bromide (38.37g, 0.28mol) were added to the flask. $AlCl_3$ (1.6g, 0.012mol) was added in four portions of approximately 0.4 g over 30 minutes. The flask was removed from the ice-bath and lowered in to an oil-bath. The reaction mixture was allowed to warm to room temperature first and then heated to reflux for an hour. The mixture was allowed to cool to room temperature again and was poured on to acidic ice. Benzene (300 mL) was added and the mixture was stirred for an additional hour. The solution was decanted into a separating funnel, leaving as much of the solid behind as possible. The mixture was separated and the precipitate in the organic layer filtered off. The combined solids were soxhlet

extracted overnight from chloroform. The desired product was insoluble in chloroform. 64 % yield; ^{1}H-NMR (DMSO, 400 MHz) δ 7.2 - 7.5 (20H, m), δ 1.7 – 2.0 (12H, m);^{13}C-NMR (DMSO, 100 MHz) δ 28.4, δ 49.5, δ 125.6 – 128.7, δ 149.7; Anal. calcd for $C_{34}H_{28}$: C, 93.54; H, 6.46. Found: C, 93.28; H, 6.44.

6.6.4 Bromination of tetraphenyladamantane[7]

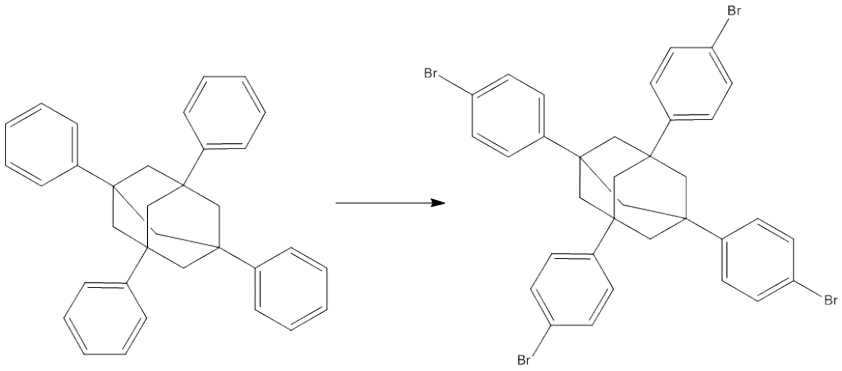

A 250mL round-bottomed flask was equipped with a stirrer bar. An outlet adaptor was connected via rubber tubing to a pipette, which was immersed in an aqueous sodium hydroxide solution. 1,3,5,7-Tetraphenyl adamantane (24.6 g, 0.056 mol) was added. Bromine (20 mL) was added slowly over the next 5 minutes via a dropping funnel, while the reaction mixture was stirred. The gaseous hydrobromic acid developed was guided via the rubber tubing in to the solution of sodium hydroxide to neutralise it. The slurry was stirred for a further 20 minutes and then poured into ethanol (250 mL), cooled on a dry-ice/acetone bath. The precipitate was filtered and washed with aqueous sodium bisulfite solution and recrystallised from chloroform/ethanol to give an off-white solid. 91 % yield; ^{1}H-NMR ($CDCl_3$, 400 MHz) δ 7.89 (2H, d), δ 7.3 (2H, d), δ 2.0 - 1.8 (12H, dd); ^{13}C-NMR ($CDCl_3$, 400 MHz) δ 148.0, δ 131.5, δ 126.9, δ 120.3, δ 77 ($CDCl_3$), δ 49.8, δ 28.6; Anal. calcd for $C_{34}H_{28}Br_4$: C, 54.00; H, 3.73; Br, 42.27. Found: C, 54.38; H, 3.62.

6.6.5 Synthesis of Tetrakis(4-bromophenyl) silane

Tetrakis(4-bromophenyl) silane was prepared by Dr. Xiaofeng Wu via the method described in *Canadian Journal of Chemistry*, **2003**, 81 (5), 376 – 380.

6.7 CMPs by Sonogashira Coupling

6.7.1 General Procedure for Network Synthesis –Catalyst Study 1, 2, 3, 4 and 5

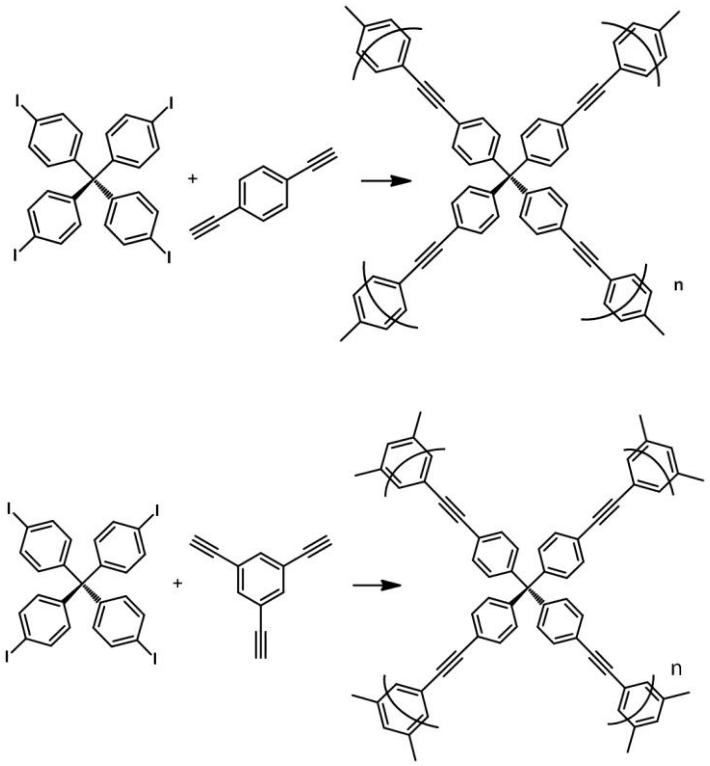

To 50 mL round-bottomed flask, 1,4-diethynylbenzene (6 mmol) or 1,3,5-triethynylbenzene (4 mmmol), tetrakis(4-iodophenyl) methane (2 mmol), bis(triphenylphosphine) palladium(II) dichloride or tetrakis(triphenylphosphine) palladium(0) and CuI (masses according to Tables 1 – 5, Chapter 2) were added and dissolved in toluene (5 mL). Diisopropylamine (2.5 mL) or triethylamine (2.5 mL) was added to the stirred reaction mixture. The reaction was stirred at 80°C for 24 hours. After cooling to room temperature, the reaction was filtered and washed

excessively with MeOH and acetone until the filtrate ran clear. The insoluble polymer was extracted using soxhlet extraction for 24 hours from MeOH to remove unreacted monomers as well as remaining catalyst. The insoluble polymer was dried under vacuum at 70°C for 24 hours. Yields 70 – 95 %.

6.7.2 Templating with PEG300 and PEG550

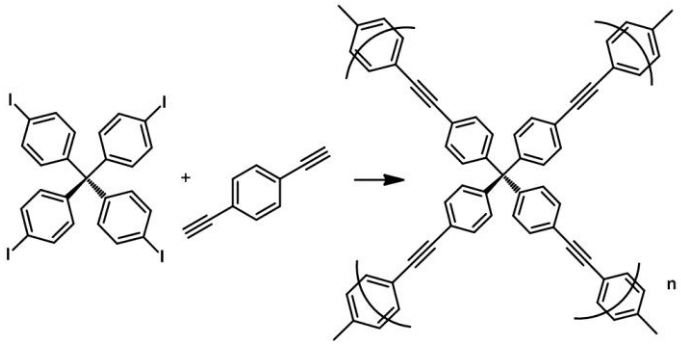

To a 50 mL round-bottomed flask, 1,4-diethynylbenzene (6 mmol), tetrakis(4-iodophenyl) methane (2 mmol), bis(triphenylphosphine) palladium(II) dichloride (60 mg) and CuI (18 mg) were added and dissolved in DMF and PEG300 or PEG550 (volumes according to Tables 1 and 2, Chapter 4). Diisopropylamine (2.5 mL) was added to the stirred reaction mixture. The reaction was stirred at 80°C for 24 hours. After cooling to room temperature, the reaction was filtered and washed excessively with MeOH and acetone until the filtrate ran clear. The insoluble polymer was extracted using soxhlet extraction for 24 hours from MeOH to remove unreacted monomers as well as remaining catalyst. The insoluble polymer was dried under vacuum at 60°C for 24 hours. Yields 85 – 95 %.

6.7.3 Templating with PEG550 – Concentration Study

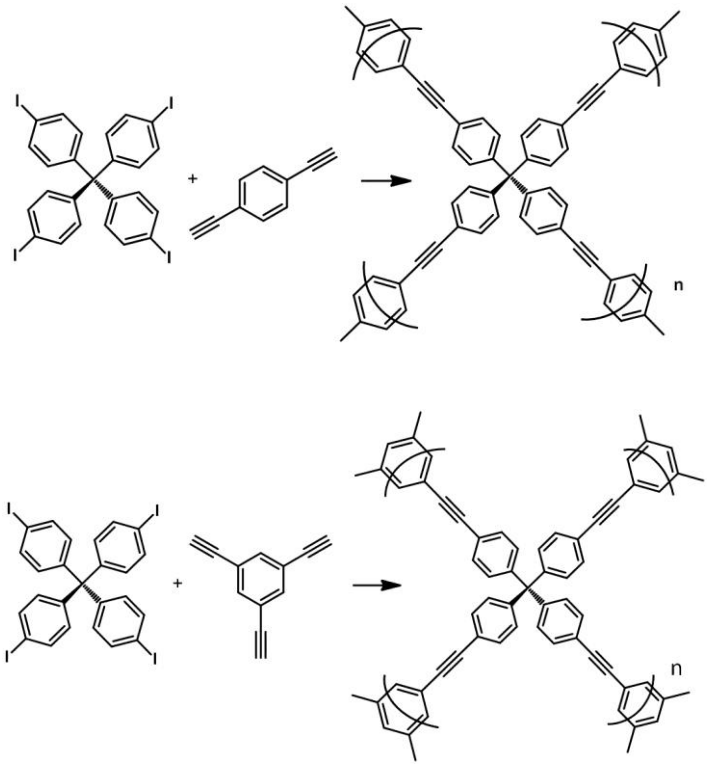

To a 100 mL round-bottomed flask, 1,4-diethynylbenzene (6 mmol) or 1,3,5-triethynylbenzene (4 mmmol), tetrakis(4-iodophenyl) methane (2 mmol), bis(triphenylphosphine) palladium(II) dichloride (60 mg) and CuI (18 mg) were added and dissolved in DMF and PEG550 (volumes according to Tables 3 and 4, Chapter 4). Diisopropylamine (2.5 mL) was added to the stirred reaction mixture. The reaction was stirred at 80°C for 24 hours. After cooling to room temperature, the reaction was filtered and washed excessively with MeOH and acetone until the filtrate ran clear. The insoluble polymer was extracted using soxhlet extraction for 24 hours from MeOH to remove unreacted monomers as well as remaining catalyst. The insoluble polymer was dried under vacuum at 70°C for 24 hours. Yields of 90 %.

6.8 CMPs by Yamamoto cross coupling

6.8.1 Homo-coupling of Tetrahedral Monomers

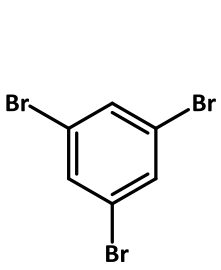

1,3,5-tribromobenzene

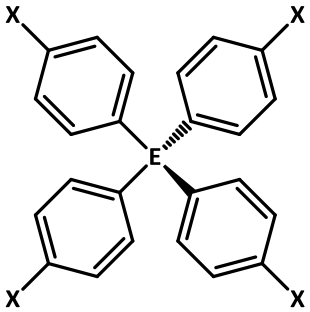

E = C, Si, adamantane
X = I, Br

3D-monomers

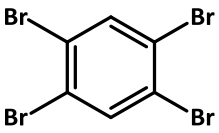

1,2,4,5-tetrabromobenzene

cis,cis-1,5-Cyclooctadiene (1.05 ml, 8.32 mmol) was added to solution of bis(1,5-cyclooctadiene)nickel(0) (2.25 g, 8.18 mmol) and 2,2′-bipyridyl (1.28g 8.18 mmol) in anhydrous DMF (120 ml). The mixture was heated to 80 °C for 1 hour, giving a deep purple solution. Tetrakis(4-bromophenyl)methane (1 mmol) or 1,3,5,7-tetrakis(4-bromopehnyl) adamantane (1 mmol) or tetrakis(4-bromophenyl) silane (1 mmol) or tetrakis(4-iodophenyl)methane (1 mmol) or 1,3,5-tribromobenzene (1 mmol) or 1,2,4,5-tetrabromobenzene (1 mmol) was added to the reaction and the mixture, which was stirred at 80 °C overnight. The deep purple suspension was allowed to cool to room temperature. Concentrated HCl was slowly added to the suspension and stirred for a further two hours. The mixture was filtered and washed with chloroform, tetrahydrofuran and water (5 x 30 ml each). After drying under vacuo the insoluble polymer was extracted from MeOH over night. Yields 85 – 95 %.

6.8.2 Cross-Coupling of Tetrahedral Monomers

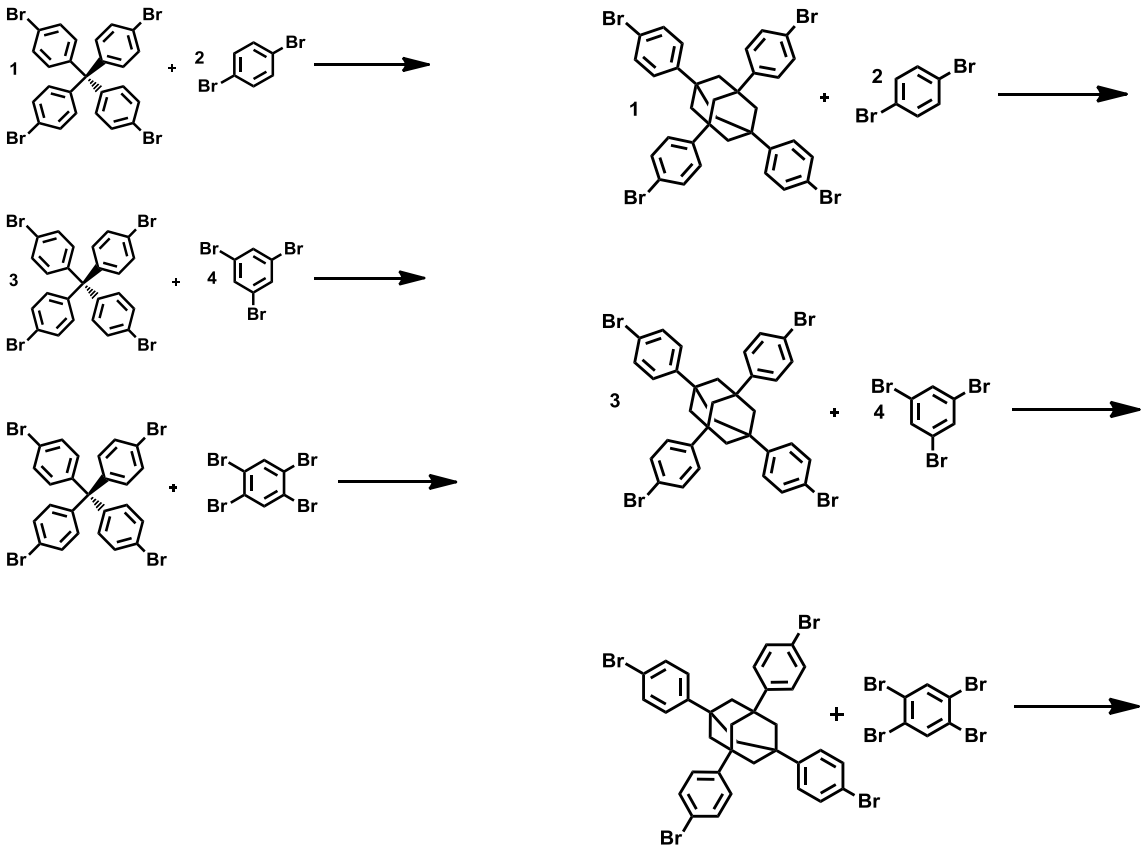

cis,cis-1,5-Cyclooctadiene (1.05 ml, 8.32 mmol) was added to solution of bis(1,5-cyclooctadiene)nickel(0) (2.25 g, 8.18 mmol) and 2,2′-bipyridyl (1.28g 8.18 mmol) in anhydrous DMF (120 ml). The mixture was heated to 80 °C for 1 hour, giving a deep purple solution. Tetrakis(4-bromophenyl)methane (0.33 mmol) and 1,4-dibromobenzene (0.66 mmol); or tetrakis(4-bromophenyl)methane (0.4 mmol) and 1,3,5-tribromobenzene (0.6 mmol); or tetrakis(4-bromophenyl)methane (0.5 mmol) and 1,2,4,5-tetrabromobenzene (0.5 mmol); or 1,3,5,7-tetrakis(4-bromopehnyl) adamantane (0.33 mmol) and 1,4-dibromobenzene (0.66mmol); or 1,3,5,7-tetrakis(4-bromopehnyl) adamantane (0.4 mmol) and 1,3,5-tribromobenzene (0.6 mmol); or 1,3,5,7-tetrakis(4-bromopehnyl) adamantane (0.5

mmol) and 1,2,4,5-tetrabromobenzene (0.5 mmol) was added to the reaction and was stirred at 80 °C overnight. The deep purple suspension was allowed to cool to room temperature. Concentrated HCl was slowly added to the suspension and stirred for a further two hours. The mixture was filtered and washed with chloroform, tetrahydrofuran and water (5 x 30 mL each). After drying under vacuo the insoluble polymer was extracted from MeOH over night. Yields 75 – 95 %.

6.9 References

[1] Brunauer, S. *et al., J. Am. Chem. Soc.*, **1938**, 60 (2), pp 309–319

[2] Captain Abney, Major-General Festing, *Proc. R. Soc.,* **1886**, 40, 378-380

[3] W. De.W.Abney, Major-General Festing, *Proc. R. Soc.,* **1891**, 50, 369-372

[4] Coblentz, W. W., *Phys. Rev. (Series I)* **1903,** 16, 35-50

[5] http://www.cis.rit.edu/htbooks/nmr/inside.htm (accessed 17/06/2011)

[6] Su, D., *Tetrahderon Letters*, **1997**, *38 (9)*, 1485-1488

[7] Rathore, R., *et.al.*, *J.Org.Chem.*, **2004**, *69*, 1524-1530

[8] Reichert, V. R., Mathias, L. J., *Macromolecules*, **1994**, *27*, 7015-7023

Chapter 7

General Conclusion and Future Work

7.1 Conclusion

The aim of this project was to design, synthesise and characterise new conjugated microporous polymers (CMPs), which have good gas storage characteristics. In the course of this work, I have synthesised some of the most porous organic polymers prepared by any research group. Networks synthesised from tetrakis(4-bromophenyl) adamantane and tetrakis(4-iodo) methane for example have BET surface areas of 3180 and 3160 m^2/g, respectively,[1] which is more than three times higher than the first generation of CMPs prepared in our group, and higher than all other microporous polymer networks with the exception of two recent publications, both of which appeared during the course of this work.

A number of synthetic points have been made clear by my studies. It was shown in Chapter 2 that the amount of catalyst and the type of base can influence the surface area and pore volume in conjugated microporous polymers. More importantly the surface area can be increased by introducing a three-dimensional monomer and by decreasing the amount of catalyst originally used by Jiang et al.[2] A maximum increase in surface area of 700 m^2/g was achieved compared to the original CMP networks[2] which had initial surface areas of 800 m^2/g. The characterisation of these networks showed that the amount of catalyst used, as well as the type of base used in the reactions influenced not only the surface area but also the degree of polycondensation in the networks. It was also shown that the oxidation state of the catalyst does not affect the surface area significantly, apart from a few cases. The materials synthesised were robust and stable and had some of the highest surface areas at the time.

By changing the chemistry from Sonogashira coupling chemistry to Yamamoto coupling chemistry as described in Chapter 3, the surface area was increased further and a range of interesting networks was synthesised with very high surface areas and high thermal stabilities. The cross-coupling reactions in particular were interesting as they form novel networks with high surface areas of up to 3300 m^2/g. The networks synthesised expanded on the PAF-1 network, giving the first novel networks with very high surface areas similar to PAF-1. Since this work was carried out, it has been shown that the same networks can have higher surface areas than reported here by changing the reaction conditions.

It was shown in Chapter 4 that the introduction of a templating agent could increase surface areas significantly for low surface area materials. Due to the change in solvent and templating agent the surface area of the E-2 network could be quadrupled, giving a surface area that is almost 2.5 times higher than the comparable surface area of CMP-1. However, the introduction of templating agents in the synthesis of high surface area materials had no significant influence. The porosity for all these templated networks was characterised by nitrogen gas sorption from which BET surface areas of over 1200 m^2/g can be achieved.

7.2 Future Work

Now that it has been shown that conjugated microporous polymers can have high surface areas and high gas uptake abilities, there is now an opportunity to explore the gas sorption properties of these networks further, by introducing different functionalities for example.[3] The introduction of nitrogen into the porous network is thought to increase the carbon dioxide uptake of these types of materials. Nitrogen could be introduced by using pyridine analogous monomers and amine functionalities. First investigations into amine containing monomers for the synthesis of microporous polymers were started but were unsuccessful for now.

The application of the materials in different ways, such as hydrogen fuel cells, carbon dioxide scrubbers and as methane storage materials needs to be further investigated.

7.3 References

[1] J.R. Holst, E. Stöckel, D.J. Adams and A.I. Cooper, *Macromolecules*, **2010**, *43*, 8531-8538

[2] J.X. Jiang, F. Su, A. Trewin, C.D. Wood, N.L. Campbell, H. Niu, C. Dickinson, A.Y. Ganin, M.J. Rosseinsky, Y.Z. Khimyak and A.I. Cooper, *Angew. Chem. Int. Ed*., **2007**, *46*, 8574-8578

[3] R. Dawson, A. Laybourn, R. Clowes, Y.Z. Khimyak, D.J. Adams and A.I. Cooper, *Macromolecules*, **2009**, *42*, 8809-8816

Appendix

Supporting Publications